General Disclaimer

One or more of the Following Statements may affect this Document

- This document has been reproduced from the best copy furnished by the organizational source. It is being released in the interest of making available as much information as possible.

- This document may contain data, which exceeds the sheet parameters. It was furnished in this condition by the organizational source and is the best copy available.

- This document may contain tone-on-tone or color graphs, charts and/or pictures, which have been reproduced in black and white.

- This document is paginated as submitted by the original source.

- Portions of this document are not fully legible due to the historical nature of some of the material. However, it is the best reproduction available from the original submission.

Produced by the NASA Center for Aerospace Information (CASI)

OGRAM: LEAKAGE TESTS FOR
LICALLY-GROOVED SEALS Progress Report
exas A&M Univ.) 95 p HC A05/MF A01 Unclas
CSCL 11A G3/37 44524

NOV 8 1983

SSME SEAL TEST PROGRAM: LEAKAGE TESTS FOR HELICALLY-GROOVED SEALS

PROGRESS REPORT

NASA CONTRACT NAS8-33716

Prepared by

Dara W. Childs, Ph.D., P.E.
Professor of Mechanical Engineering

TURBOMACHINERY LABORATORIES REPORT

November 1, 1983

NOV 1983
RECEIVED
NASA STI FACILITY
ACCESS DEPT.

SSME SEAL TEST PROGRAM:
LEAKAGE TESTS FOR HELICALLY-GROOVED SEALS

Table of Contents

	page
ABSTRACT	
LIST OF FIGURES	1
LIST OF TABLES	3
NOMENCLATURE	
INTRODUCTION	4
TEST APPARATUS	
Test Section	5
Instrumentation	7
Test Fluid	9
Mechanical-System Layout	9
Control System	11
Data Acquisition Procedure	12
TEST SERIES	
Test Objectives	13
Test-Seal Geometrics	13
Test Results	17
CONCLUSIONS	91

SSME SEAL TEST PROGRAM:
LEAKAGE TESTS FOR HELICALLY-GROOVED SEALS

Table of Contents

	page
ABSTRACT	
LIST OF FIGURES	1
LIST OF TABLES	3
NOMENCLATURE	
INTRODUCTION	4
TEST APPARATUS	
Test Section	5
Instrumentation	7
Test Fluid	9
Mechanical-System Layout	9
Control System	11
Data Acquisition Procedure	12
TEST SERIES	
Test Objectives	13
Test-Seal Geometrics	13
Test Results	17
CONCLUSIONS	91

LIST OF FIGURES

		page
1.	Test-rig assembly.	6
2.	Test facility layout.	10
3.	Helically-grooved seal configuration.	15
4.	Static pressure distributions for seal 1 of rotor 8.	20
5.	Static pressure distributions for seal 2 of rotor 8.	22
6.	Static pressure distributions for seal 1 of rotor 9.	25
7.	Static pressure distributions for seal 2 of rotor 9.	27
8.	Static pressure distributions for seal 1 of rotor 10.	29
9.	Static pressure distributions for seal 2 of rotor 10.	31
10.	Static pressrue distributions for seal 1 of rotor 11.	34
11.	Static pressure distributions for seal 2 of rotor 11.	37
12.	Static pressure distributions for seal 1 of rotor 12.	40
13.	Static pressure distributions for seal 2 of rotor 12.	42
14.	Static pressure distributions for seal 1 of rotor 13.	45
15.	Static pressure distributions for seal 2 of rotor 13.	47
16.	Static pressure distributions for seal 1 of rotor 14.	50
17.	Static pressure distributions for seal 2 of rotor 14.	52
18.	Static pressure distributions for seal 1 of rotor 15.	55
19.	Static pressure distributions for seal 2 of rotor 15.	58
20.	Static pressure distributions for seal 1 of rotor 16.	61
21.	Static pressure distributions for seal 2 of rotor 16.	64
22.	Pressure gradient coefficients for seals 1 and 2 of rotor 8.	67
23.	Pressure gradient coefficients for seals 1 and 2 of rotor 11.	68
24.	Pressure gradient coefficients for seals 1 and 2 of rotor 14.	69
25.	Pressure gradient coefficients for seals 1 and 2 of rotor 9.	70
26.	Pressure gradient coefficients for seals 1 and 2 of rotor 12.	71
27.	Pressure gradient coefficients for seals 1 and 2 of rotor 15.	72
28.	Pressure gradient coefficients for seals 1 and 2 of rotor 10.	73
29.	Pressure gradient coefficients for seals 1 and 2 of rotor 13.	74
30.	Pressure gradient coefficients for seals 1 and 2 of rotor 16.	75
31.	Leakage coefficients for seals 1 and 2 of rotor 8.	79
32.	Leakage coefficients for seals 1 and 2 of rotor 11.	80
33.	Leakage coefficients for seals 1 and 2 of rotor 14.	81

34. Leakage coefficients for seals 1 and 2 of rotor 9. 82
35. Leakage coefficients for seals 1 and 2 of rotor 12. 83
36. Leakage coefficients for seals 1 and 2 of rotor 15. 84
37. Leakage coefficients for seals 1 and 2 of rotor 10. 85
38. Leakage coefficients for seals 1 and 2 of rotor 13. 86
39. Leakage coefficients for seals 1 and 2 of rotor 16. 87
40. $P\omega r/I^3$ (Normalized amperage consumption) for rotor 8. 89
41. $P\omega r/I^3$ (Normalized amperage consumption) for rotor 11. 89
42. $P\omega r/I^3$ (Normalized amperage consumption) for rotor 14. 90
43. $P\omega r/I^3$ (Normalized amperage consumption) for a smooth rotor. 90

LIST OF TABLES

		page
1.	Helically-grooved seal dimensions.	16
2.	Relative "pumping" effectiveness of seal configurations for zero pump flow.	18
3.	Leakage coefficients $C_L = (C/R)\ C_d^{-\frac{1}{2}C}$ for plain seals with various surface-roughness treatments.	78

INTRODUCTION

This report presents the results of leakage tests for a range of helically-grooved annular seal configurations in highly turbulent flow. The helical groove geometry has been used for bearings [1] and viscoseals [2] for some time. Unfortunately, no analysis exists for predicting either the leakage performance or the rotordynamic coefficients of helically-grooved seals in the turbulent regime. However, results which are available suggest that a helically grooved seal should both reduce leakage and enhance stability. Both of these proposed beneficial consequences would result from the "pumping" action of the seal which provides increased resistance to the leakage flow while retarding the development of circumferential flow in the direction of shaft rotation. Stability is enhanced by reducing the net circumferential flow in a seal, since this reduces the "cross-coupled" stiffness coefficient k.

The leakage results presented here were initially planned as a first step towards the development of a comprehensive understanding and prediction capability for helically-grooved seals. The tests reported here were to be followed by dynamic tests for measurement of force coefficients and the development of a statisfactory model for helically-grooved seals in the turbulent regime. The development of a model and analysis approaches are presently underway; however, changes in SSME program priorities have resulted in an indefinite postponement of the dynamic test efforts until more definite analytical predictions become available.

TEST APPARATUS

Test Sections

The basic test section is illustrated in figure 1. As illustrated, the test section is set up to test stepped and convergent-tapered seal configurations which have been used as interstage seals for the SSME HPFTP. For the present test program, the seal stators were bored out to a constant diameter of approximately 11.1 cm, and the seal rotors were sleeved with appropriate helically-grooved elements. Fluid enters the center of the test section and discharges axially across the two test seals. The test-section rotor is supported in Torrington hollow-roller bearings [3] which are extremely precise, radially preloaded, and have a predictable and repeatable radial stiffness. Axially-spaced Kulite strain-gauge pressure transducers are used to measure the pressure field. Inlet and discharge measurements are made of temperature and pressure for use in defining the density and viscosity of the test fluid.

The mechanical seals for the test section are from John Crane Co., Type EAB assembly. A carbon seat is used with a Tungsten Carbide washer. Leakage through these seals has been a continuing problem at all operating conditions. Wear of the mechanical elements has also been a problem, necessitating frequent resurfacing and replacement.

A ten hp. variable-speed electric motor has been used to drive the test section from five to 5300 rpm. In some cases, this unit had insufficient power to drive the helically-grooved seal configurations and a 50 hp, 3600 rpm unit was used instead. A motion transducer, actuated by a ten-toothed rotating wheel, provides a signal for a counter which defines the rotation rate for the test section.

ORIGINAL PAGE IS
OF POOR QUALITY

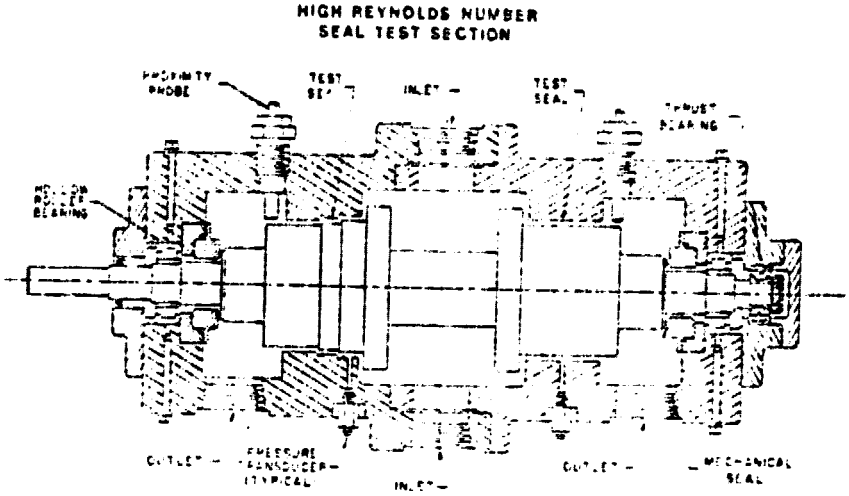

1. Test-rig assembly.

Instrumentation

Specifications for the instrumentation are given below:

(a) *Thermocouples.* Type J thermocouples from Honeywell were employed for temperature measurements. These units had a 1°F resolution, and were calibrated with a precision thermometer using an ice bath and boiling water. Rosemont transmitters were used to amplify the thermocouple output for transmission to the Data General Nova computer A/D circuits. Calibration of the thermocouples was based on the final readout of temperature-proportional voltage readings by the computer. Calibration results showed a repeatable resolution of temperature to within 1°F.

(b) *Flowmeters.* Fischer & Porter Type 10LV2 Liquid Vortex Flowmeters were used. According to the manufacturer, these units have a linear scale from 10 to 150 gpm with an accuracy of ±1.89 gpm. An additional loss of accuracy amounting to ±.14 gpm per 15°F change is possible; however, most of the testing in this project was conducted in the 80-85° temperature range.

The vortex flowmeter design is sensitive to vibration levels of the pipe to which it is mounted. Occasional problems were encountered due to high vibration levels in the piping. In addition, over some intermediate flow ranges, the flowmeters become unstable, oscillating widely and grossly overestimating the flow rate. When installed at the same location, an ultrasonic flowmeter behaved similarly; hence, either a flow instability or a resonance condition exists in the system. Additional pressure instrumentation has been added to the system for diagnosis of the problem when testing resumes.

(c) *Pressure Transducers.* Kulite ETM-375-1000 strain-gauge pressure transducers were used for static and dynamic pressure measurements.

These units had rated and maximum pressures of 1000 and 2000 psi, respectively. The manufacturer's specifications stated that the errors due to nonlinearity and hysteresis would be less than ±1% of full scale (±10 psi) with repeatability of ±0.25% of full scale (±2.5 psi). However, measured results for these units with a dead-weight load tester have generally shown errors to be less than 1 psi over a 600 to 1000 psi calibration range. The diaphragm natural frequency of the strain-gauge sensor element is 275 KHz. The Kulite units tend to be delicate and are relatively easy to damage; however, their performance has been quite satisfactory. The pressure transducers are calibrated by removing one of the units from the system before and after testing, calibrating it at 600 and 1000 psi, and then rechecking the output at the endpoints and an intermediate pressure condition. The repeatability and linearity of these tests has been within 1 psi. The reference unit is then reinstalled in the system and used to calibrate the remaining pressure transducers over the 600 to 1000 range. Calibration for the pressure transducers is based on voltage levels read through the Data General computer A/D boards.

(c) *Electronic Filters*. The high-frequency noise levels developed by the pressure transducers proved to be excessive, and necessitated the use of filters for attenuation. Fourth-order bessel-function filters were fabricated with the transfer function

$$V_2/V_1 = G_2 = \frac{105\omega_0^4}{s^4 + 1\omega_0^2 s + 105\omega_0^3 s + 105\omega_0^4}$$

where ω_0 = 1131 rad/sec = 180 Hz. Separate filters were used for all transient pressure measurements.

Test-Fluid

The test fluid is bromotrifluromethane, $CBrF_3$, which is manufactured as a fire extinguisher fluid (Dupont FE 1301 or Halon) and refrigerant (Freon 13B1). Its fluid properties at 25°C are:

$$\mu = 1.54 \times 10^{-4}\ Ns/m^2,\ \rho = 1570\ kg/m^3,$$

$$\nu = 1.0 \times 10^{-7}\ m^2/s.$$

This liquid actually has a lower kinematic viscosity than liquid hydrogen and has the additional advantage of being nonflammable and nontoxic. A disadvantage of Halon is that the vapor pressure is approximately 200 psi at room temperature; hence, the test flow loop must be held at an elevated pressure to keep the Halon liquid.

The density and viscosity properties of Halon as defined in [4,5] have been curve-fitted as a function of temperature and pressure, and are used to define average axial and circumferential Reynolds numbers for test seals.

Mechanical System Layout

Figure 2 illustrates the flow loop used to provide specified flowrates through the test-section seals. A six-stage Goulds pump provides the flowrate required. Loop flow rate discharges from the pump, and then may split with part of the flow going through the test section, and the remainder proceeding through control valves 1 and 3. Two control valves in series are required to absorb the full output pressure of the pump without cavitation. The bypass-flow mode is used for total test-section flowrate less than 100 gpm, which represents the lowest flowrate operating point for the pump. Valve 4 is closed in the bypass mode. As the required flowrate increases above 100 gpm, valve 1 is closed and valves 2 and 3 are progressively opened. Valve 4, which has a larger capacity than the remaining valves, is opened in parallel with valves 2 and 3 to achieve maximum-flow conditions. Flowrates through the test section seals are measured by Fischer-Porter vortex flowmeters.

ORIGINAL PAGE IS
OF POOR QUALITY

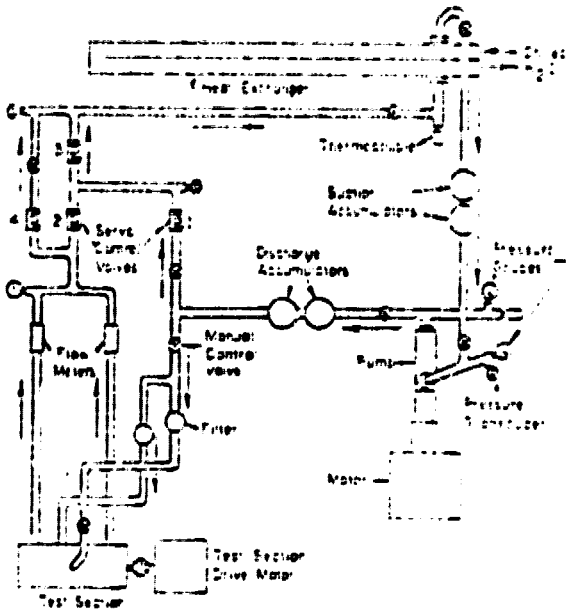

2. Test facility layout.

The test-section fluid is circulated through a heat exchanger, which is supplied chilled water by the Tran chiller. The chiller capacity is augmented by a 2000 gallon water tank which is buried outside the test facility.

The ambient system pressure is maintained by the accumulators illustrated in figure 2, which keep the pump suction pressure at approximately 350 psi. This yields a peak pump discharge pressure of approximately 1000 psi. The accumulators are also used to remove liquid Halon from the test section for replacement of rotors and transfer fluid back and forth from the 2000 lb Dupont delivery tank. In fact, all of the Halon can be pumped back into the delivery tank using the accumulators.

The filters illustrated in Figure 2 have a ten micron limit for particles. The complete flow system is stainless steel except for the pump body and the heat exchanger to minimize particle contamination in the test fluid.

Control System

The axial and circumferential Reynolds numbers are the quantities to be controlled in the seals. These variables are determined by the pressure and temperature measurements within the seal (which define ρ and μ), the seal rotational speed ω, and the flowrates through the seals. Flowrate control is supplied by means of a Data General Nova computer. Control signals are generated, based upon the difference between a measured R_{ao} and a specified $\overline{R}_{ao}$, and cause a change is the Masoniellan control valve settings. Active control is not entirely closed-loop. The operator specifies the number of control cycles to be executed by the computer. The computer calculates the running speed that is required to achieve a specified $\overline{R}_{co}$, and the specified test section speed is set man v.

Data Acquisition Procedure

The following data is required to evaluate the leakage performance of annular seals:

(a) leakage rate

(b) inlet and exit temperatures

(c) pressure measurements at the seal's inlet and exit and along its length.

The instrumentation for making these measurements was discussed at the beginning of this chapter. The data was captured via the A/D boards of the Data General Nova computer. Only static data is desired; hence, each variable is sampled 200 times and averaged before it is transferred to disk storage on the D. G. machine.

TEST SERIES

Test Objectives

Figure 3 illustrates the helically-grooved seal designs tested in this study. The tests reported here were carried out to provide answers for the following questions:

(a) How does the leakage performance of helically-grooved seal configuration compare to plain annular seals?

(b) How does the leakage performance depend on the ridge clearance C_r, the pitch angle α, the groove-depth d_g, and the rotational speed ω?

(c) What are the amperage requirements for driving test rotors which mount helically-grooved seals?

Test-Seal Geometries

To provide answers to question (b), three separate rotors were manufactured. Two helically-grooved seals having the same pitch angle α were mounted on each rotor, with pitch angles of 20°, 30°, and 40°. Each helically-grooved seal was formed from sixteen separate grooves with appromixately equal groove and ridge widths. The nominal ridge clearance C_r for the seals in a given rotor are .508 and .380mm, respectively. As original machined, the rotors are identified by numbers 8, 9, and 10, and their dimensions are given in table 1. The following nomenclature is used in this table:

C_r:	Ridge clearance illustrated in figure 3.
C_g:	Groove clearance.
$d_g = C_g - C_r$:	Groove depth.
w_r:	Minimum ridge width.
w_g:	Minimum groove width.

Following tests of the seals on rotors 8, 9, and 10, the groove depths were

increased yielding the rotors identified as rotors 11, 12, and 13, respectively, with the groove depths cited in table 1. Increasing the groove depths again yielded rotors 14, 15, and 16, whose dimensions are also specified in table 1.

The groove depth to clearance ratios, d_g/C_r, of table 1 compare to values of 2.7 and 3 developed by Chow and Vohr [2] for optimum stiffness bearings with circumferential Reynolds numbers (R_c=RWC/υ) of 1000 and 9000, respectively.

ORIGINAL PAGE IS
OF POOR QUALITY

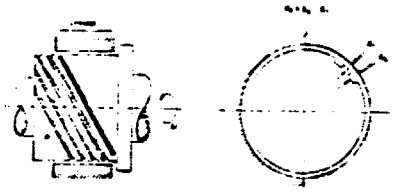

3. Helically-grooved seal configuration.

ORIGINAL PAGE IS
OF POOR QUALITY

A. Pitch Angle $\alpha = 20°$; $w_r = 3.89$ mm; $w_g = 3.53$ mm

Seal 1: $C_r = .368$ mm, D = 11.04 cm, L = 5.08 cm
Seal 2: $C_r = .521$ mm, D = 11.01 cm, L = 5.08 cm

	Seal 1		Seal 2	
Rotor	dg (mm)	dg/C_r	dg (mm)	dg/C_r
8	.406	1.10	.584	1.12
11	1.168	3.17	1.016	1.95
14	1.549	4.21	1.549	2.97

B. Pitch Angle $\alpha = 30°$; $w_r = 5.58$ mm; $w_g = 5.51$ mm

Seal 1: $C_r = .381$ mm, D = 11.04 cm, L = 5.08 cm
Seal 2: $C_r = .495$ mm, D = 11.01 cm, L = 5.08 cm

	Seal 1		Seal 2	
Rotor	dg (mm)	dg/C_r	dg (mm)	dg/C_r
9	.381	1.00	.559	1.13
12	1.168	3.07	1.016	2.05
15	1.549	4.07	1.549	3.13

C. Pitch Angle $\alpha = 40°$; $w_r = 7.04$ mm; $w_g = 7.19$ mm

Seal 1: $C_r = .381$ mm, D = 11.04 cm, L = 5.08 cm
Seal 2: $C_r = .508$ mm, D = 11.01 cm, L = 5.08 cm

	Seal 1		Seal 2	
Rotor	dg (mm)	dg/C_r	dg (mm)	dg/C_r
10	.330	.866	.508	1.00
13	1.168	3.07	1.016	2.00
16	1.549	4.07	1.549	3.05

Table 1. Helically-grooved seal dimensions.

Test Results

Static Pressure Distribution

Figures 4 through 21 contain the pressure profiles which were measured for the helically-grooved seals. The data points indicated are from pressure measurements made at the inlet and exit chambers and throughout the seal length. The first two data points on the left are seal supply pressure. The data points to the right are downstream pressure. Pressure measurements are made at nine and five axial locations, respectively, within the seal 2 and seal 1 configurations of table 1.

Figure 4 (a) shows the static pressure distribution which results from shaft pressure distribution which results from shaft rotation only, i.e., no pump flow. Without the helical grooves, there would be no axial pressure gradient. An understanding of this figure is facilitated by noting that the various pressure distributions have all been shifted by addition or subtraction of a constant to yield the same average supply pressure. This modification is helpful when comparing pressure gradients due to leakage flow, but can be confusing when looking at pressure gradients due to shaft rotation. Generally speaking the zero-pump-flow curves show an increase in seal pressure differential as the running speed increases. The pressure rises from the normal seal discharge to the normal seal inlet due to seal rotation. A relative measure of "pumping" effectiveness of a seal can be obtained by taking the difference between the seal discharge pressures at different running speeds and dividing by the running speed differences. For figures 4 (a) this gives:

$$\frac{\Delta P}{\Delta \omega} = \frac{24.82 - 24.33}{4996 - 1005} = 1.23 \times 10^{-4} \qquad \text{Bar}\cdot\text{Sec/Rev.}$$

Although zero-pump-flow data were not taken for all seals, the available results are summarized in table 2 below. The results of table 2 support the following general conclusions with respect to "pumping" capacity:

ORIGINAL PAGE IS
OF POOR QUALITY

Rotor	$\alpha°$	C_r (mm)	d_g (mm)	$(\Delta P/\Delta\omega)X10^4$ (BAR/RPM)
8	20	.368	.406	1.23
14		.368	1.549	3.05
8		.521	.584	1.74
11		.521	1.016	2.24
14		.521	1.549	2.75
9	30	.381	.381	3.40
15		.381	1.549	5.22
15		.495	1.549	2.99
10	40	.381	.330	1.62
16		.381	1.549	2.30
16		.508	1.549	2.73

Table 2. Relative "pumping" effectiveness of seal configuration for zero pump flow.

(a) The 30° pitch angle configuration is better than the 20° or 40° configuration.

(b) Pumping performance increases as the groove-depth increases.

The results with respect to changes in ridge clearance is inconclusive. For the 20° and 30° cases, increasing C_r while holding d_g constant reduces pumping effectiveness. However, the opposite situation holds for the 40° cases. The leakage results of the next section demonstrate that pumping performance is a very poor predictor of leakage performance.

Figure 8 (b) and 8 (c) illustrate the types of pressure profiles which are obtained with seal leakage. The initial pressure drops in the seal arise from the abrupt acceleration of the fluid. The pressure gradients are seen to

increase with running speed ω; i.e., for the same flowrate, the resistance increases with increasing ω. However, as the flowrate increases, the dependency decreases as illustrated in the frames of figure 5.

The power requirements to rotate the helically-grooved seals proved to be larger than those previously experienced with smooth or surface-roughened seals. The load on the drive motor generally increased with flowrate and running speed. The breaker system on the 10 hp motor would simply "cut-out" when called upon to exceed its capacity. After rotors 8, 9, and 10 were tested, provision was made for a 50 hp constant-speed 3600 rpm motor which had the capacity to drive the rotors at all flow conditions. The motor controller eventually failed and had to be repaired during testing rotors 14, 15, and 16. Following the repair, considerably higher amperage readings were possible with the motor. The maximum possible amount of data was taken for each seal; however, because of these problems, there is a considerable disparity between the amounts of data available for the separate seals. Amperage measurement results are reported in a subsequent section.

A comparison of the results of figures 4 through 21 illustrates that some of the seals have considerably higher entrance pressure losses than others. Generally speaking, seals which absorb relatively more of the applied differential pressure in entrance losses and less in the axial pressure gradients have much poorer leakage performance than seals with relatively steep pressure gradients and smaller inlet pressure drops. A comparison of leakage performance in terms of discharge coefficients is provided in the following section.

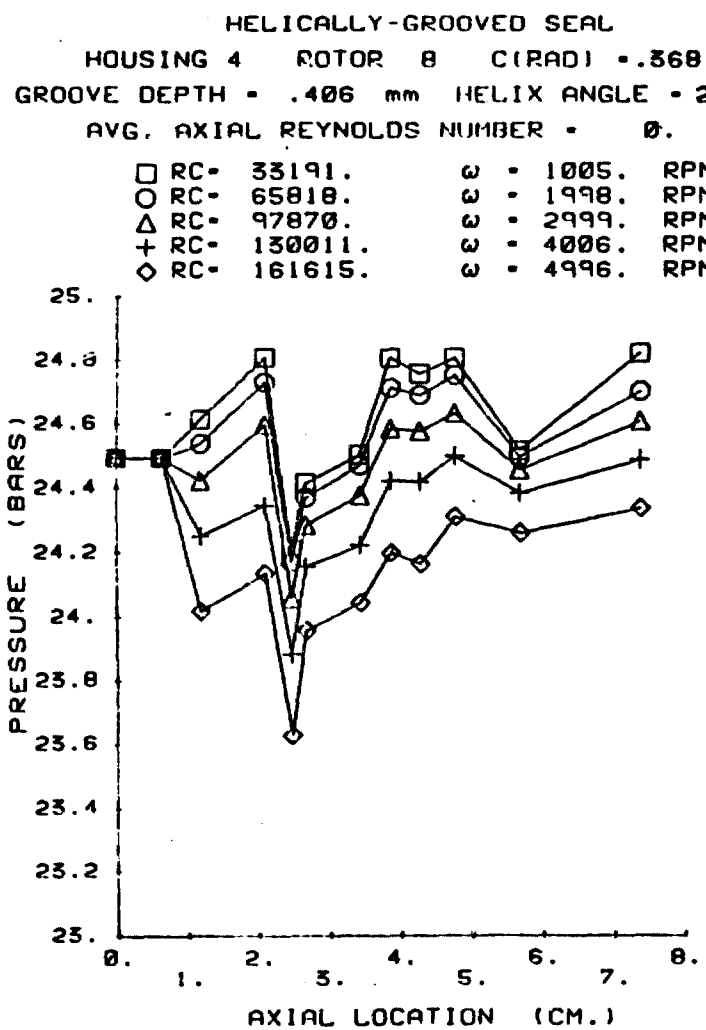

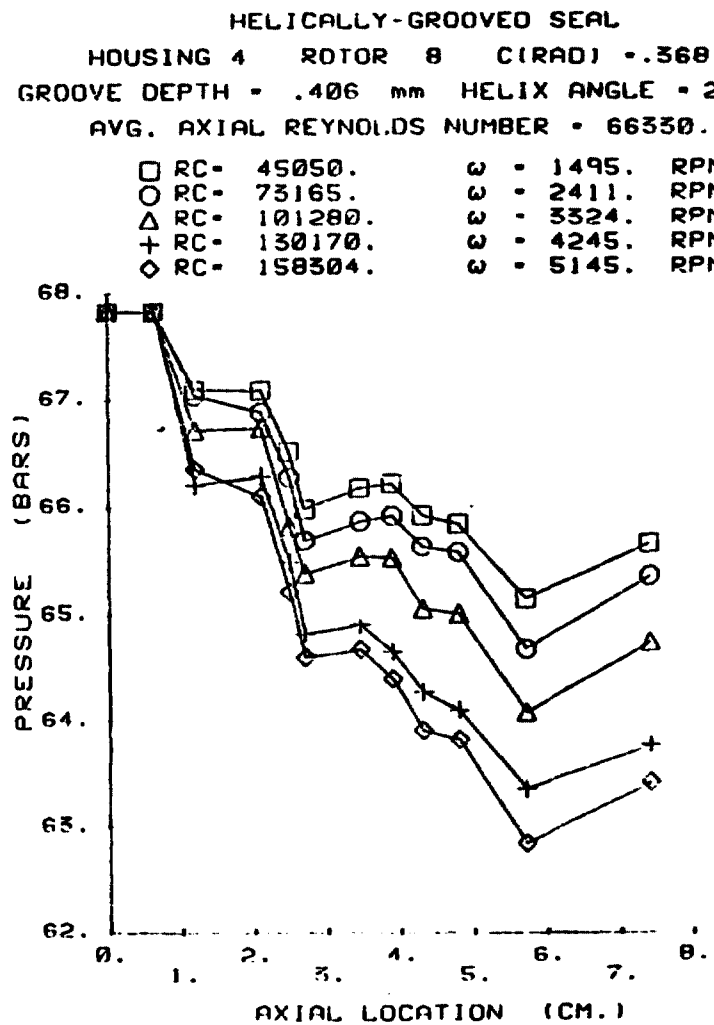

ORIGINAL PAGE IS OF POOR QUALITY

4. Static pressure distributions for seal 1 of rotor 8.

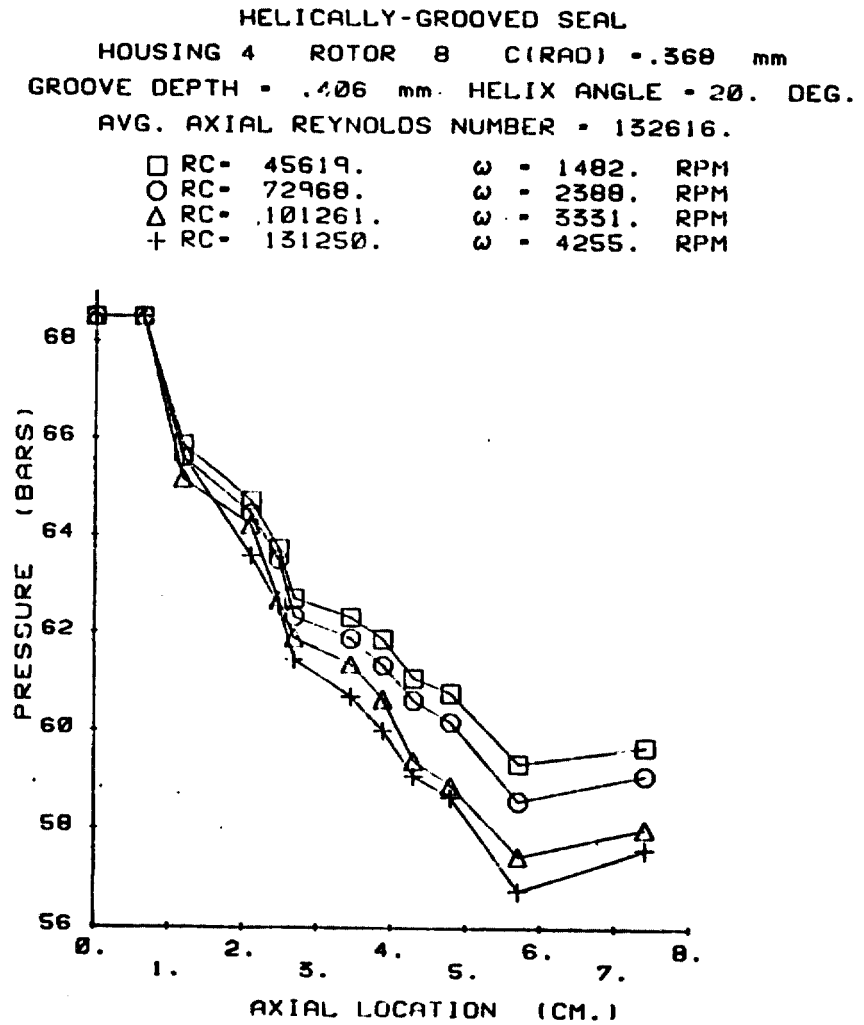

4. Static pressure distributions for seal 1 of rotor 8.

ORIGINAL PAGE IS
OF POOR QUALITY

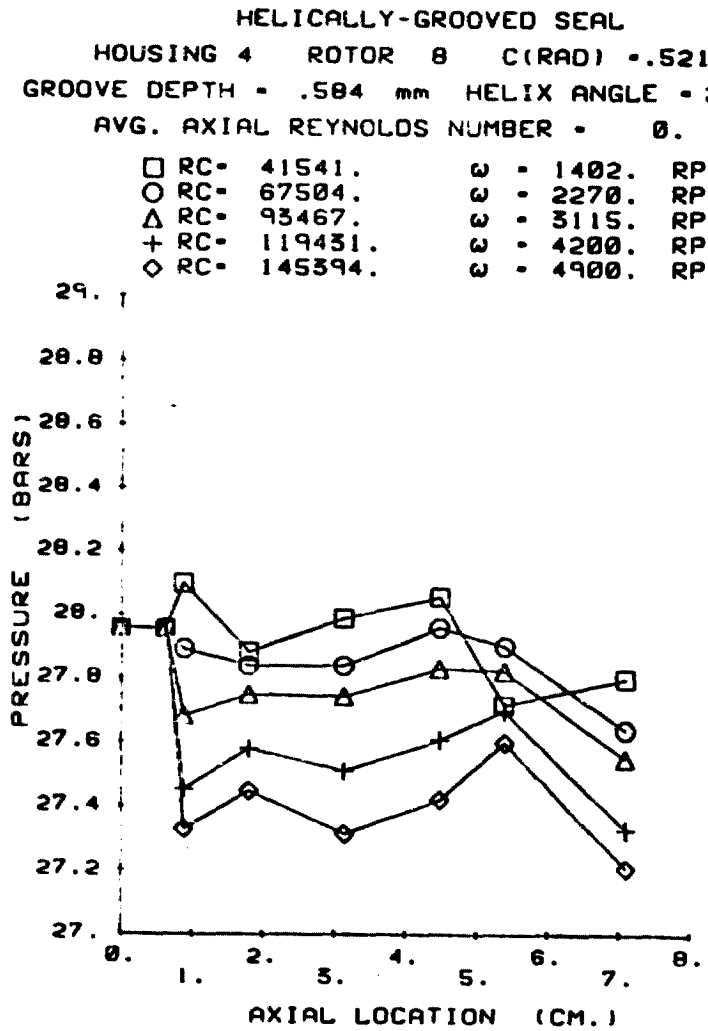

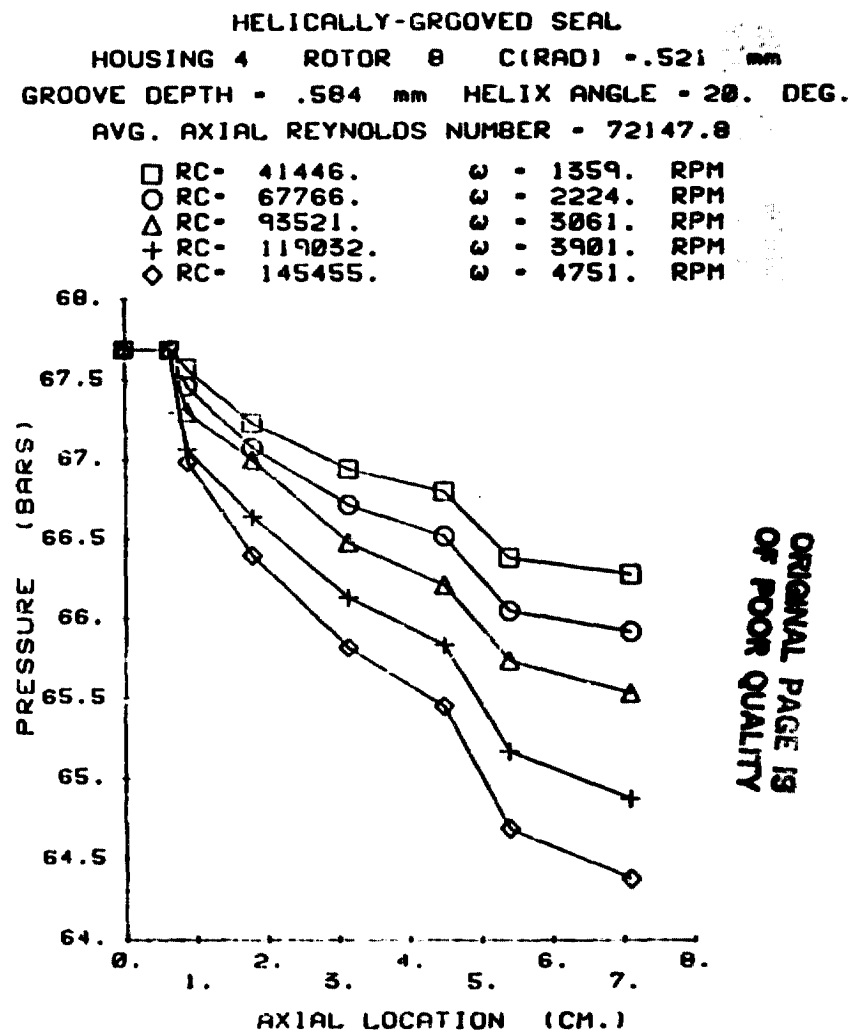

ORIGINAL PAGE IS OF POOR QUALITY

5. Static pressure distributions for seal 2 of rotor 8.

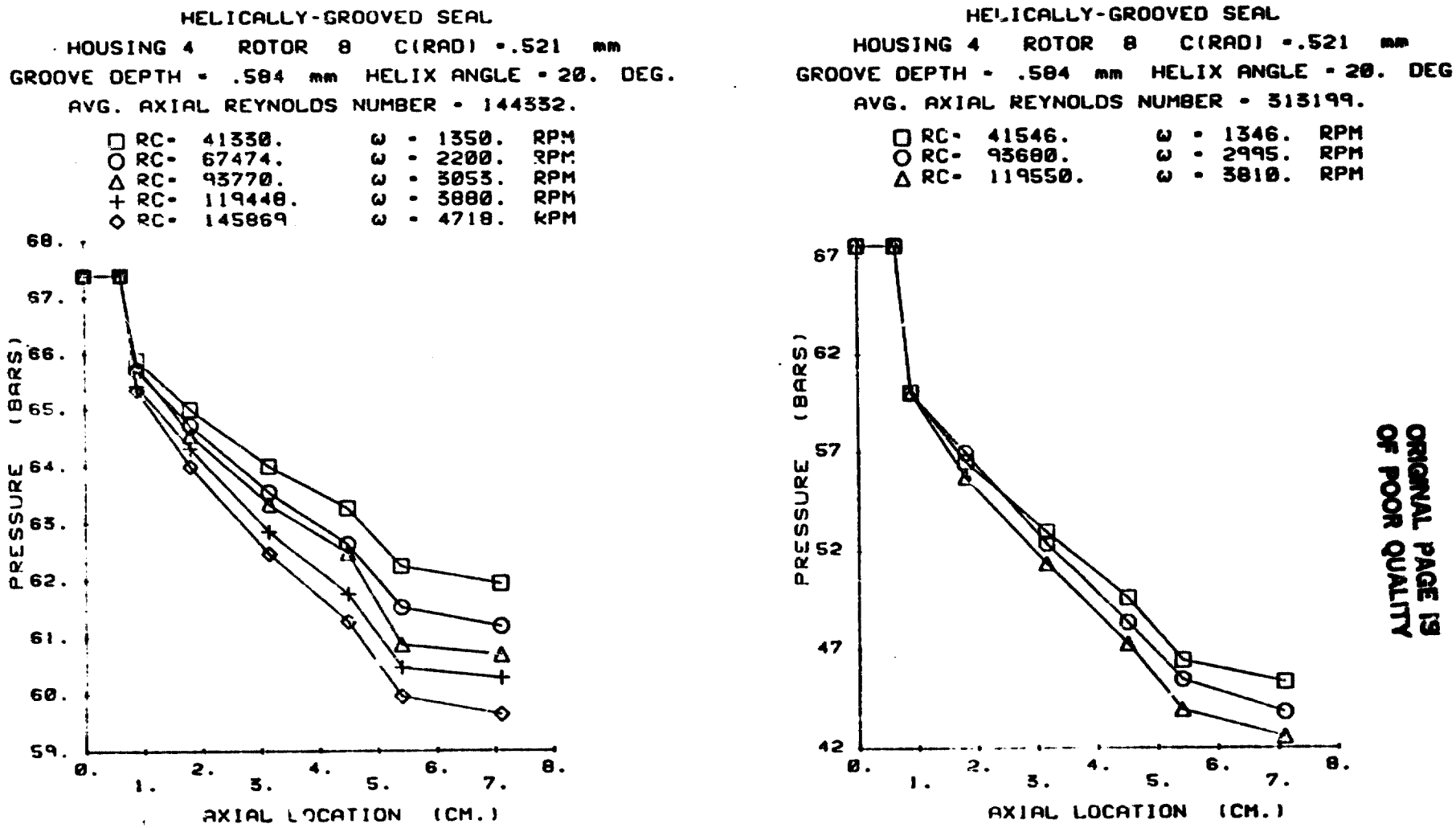

5. Static pressure distributions for seal 2 of rotor 8.

ORIGINAL PAGE IS OF POOR QUALITY

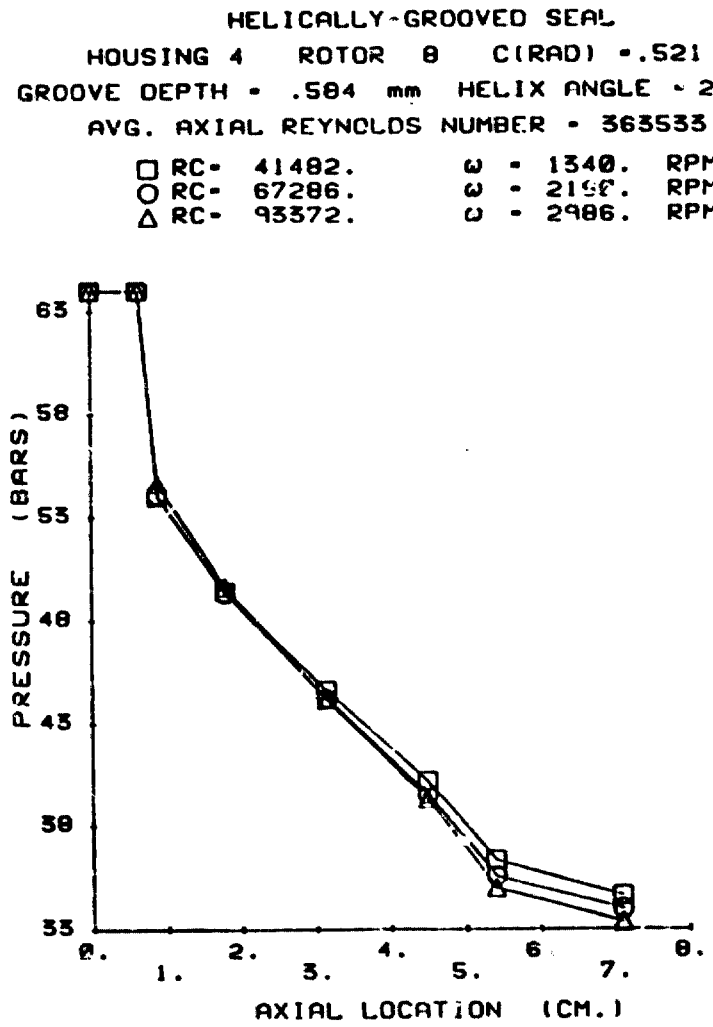

5. Static pressure distributions for seal 2 of rotor 8.

ORIGINAL PAGE IS
OF POOR QUALITY

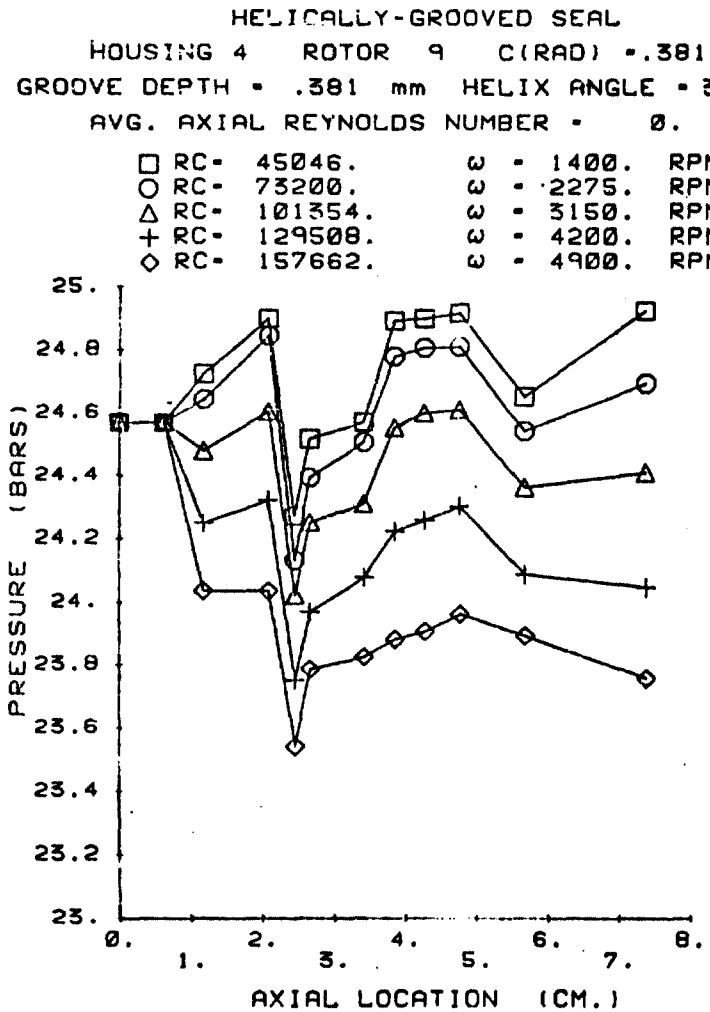

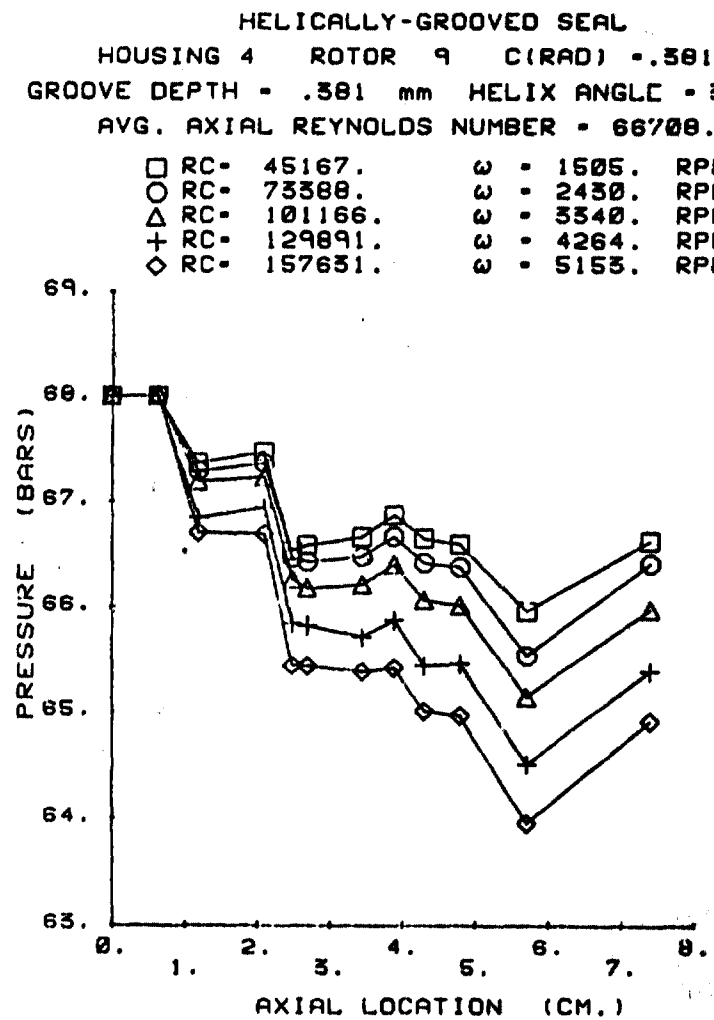

6. Static pressure distributions for seal 1 of rotor 9.

ORIGINAL PAGE IS OF POOR QUALITY

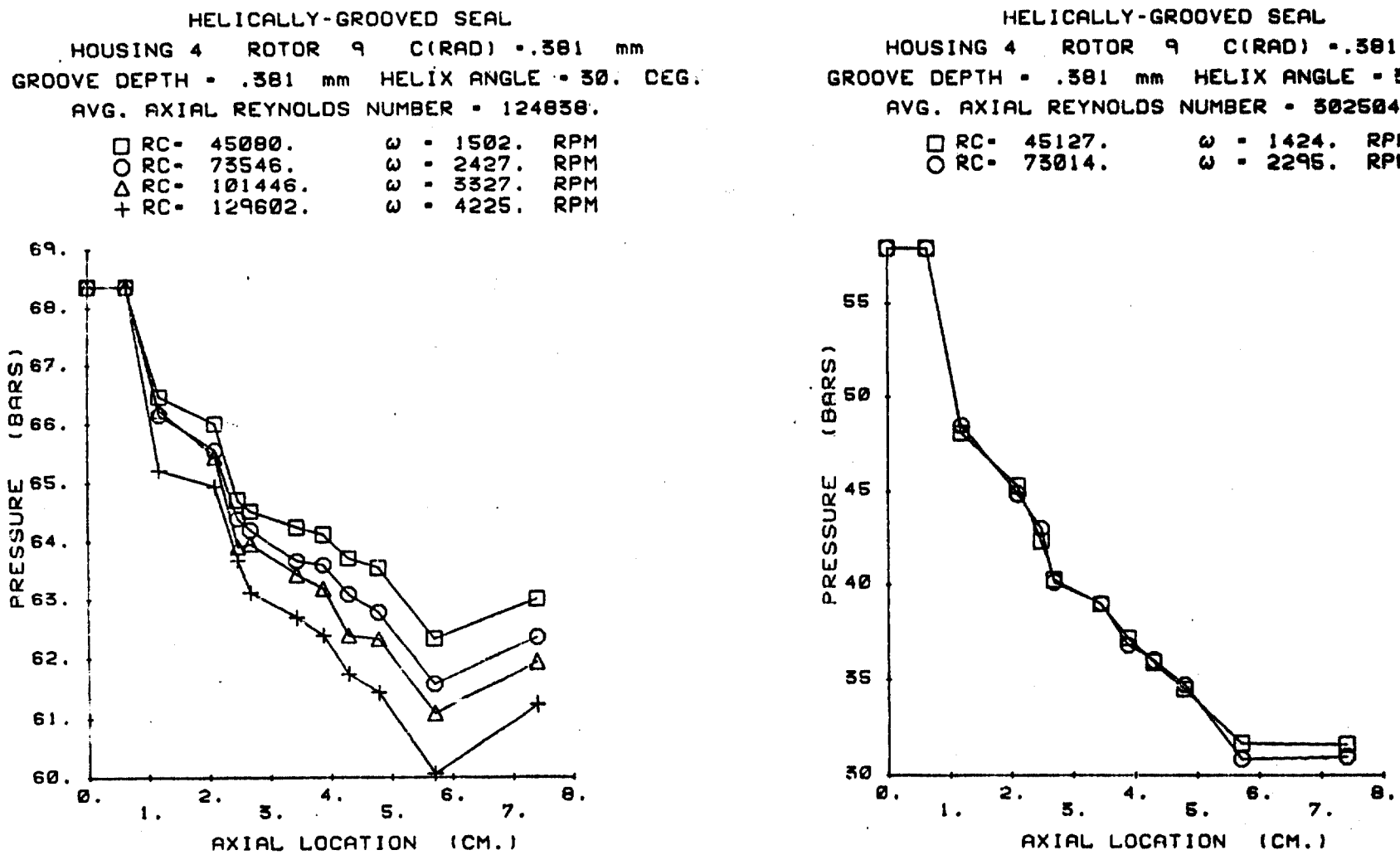

6. Static pressure distributions for seal 1 of rotor 9.

ORIGINAL PAGE IS OF POOR QUALITY

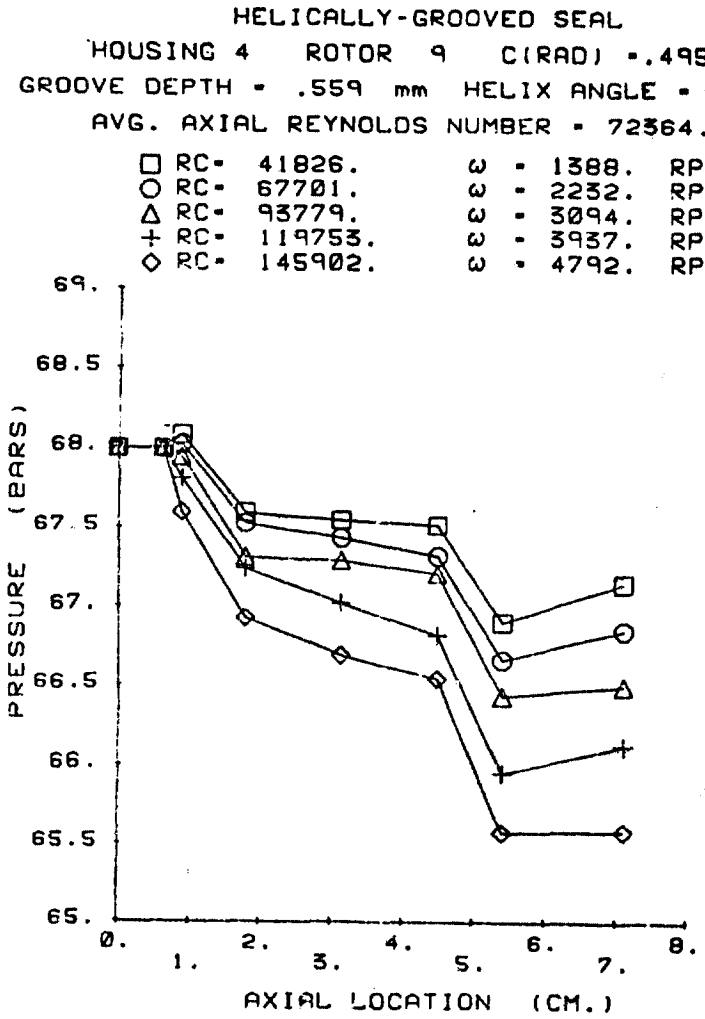

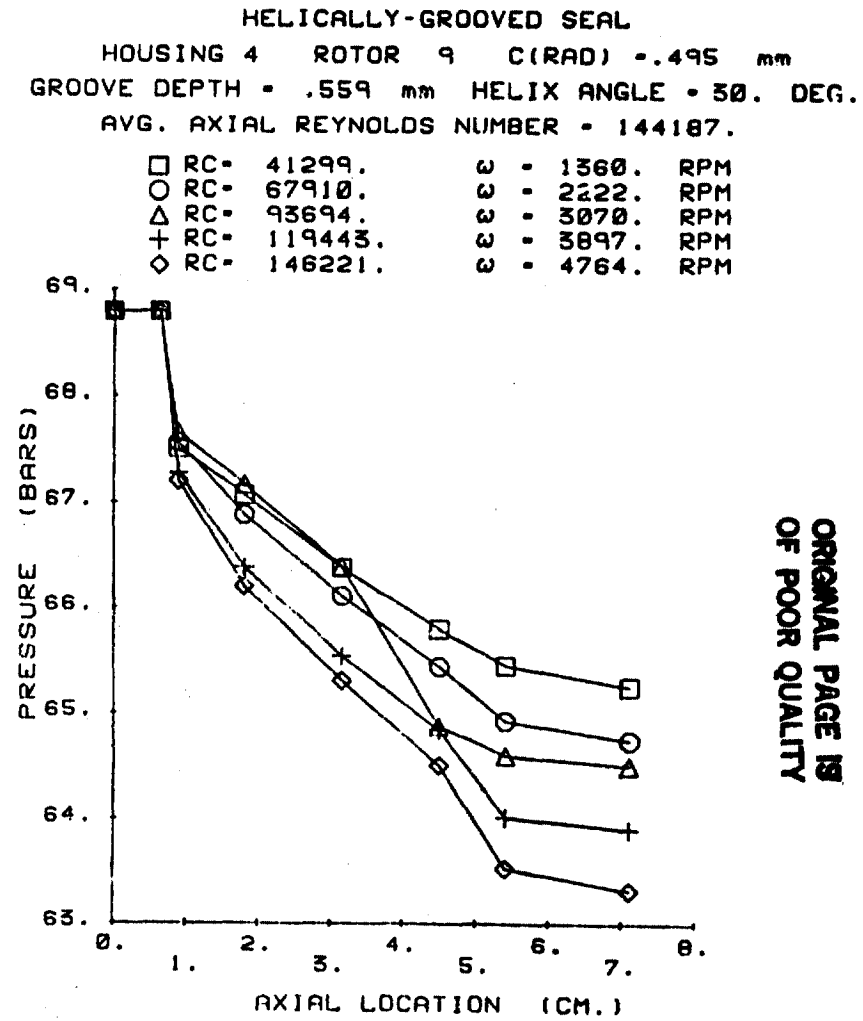

ORIGINAL PAGE IS OF POOR QUALITY

7. Static pressure distributions for seal 2 of rotor 9.

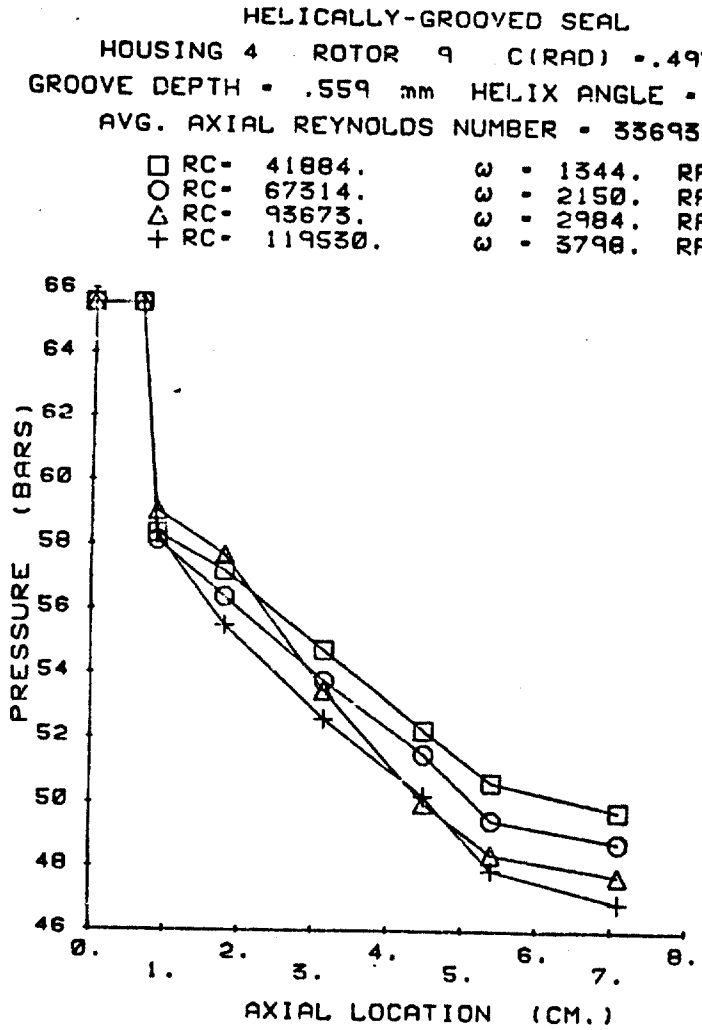

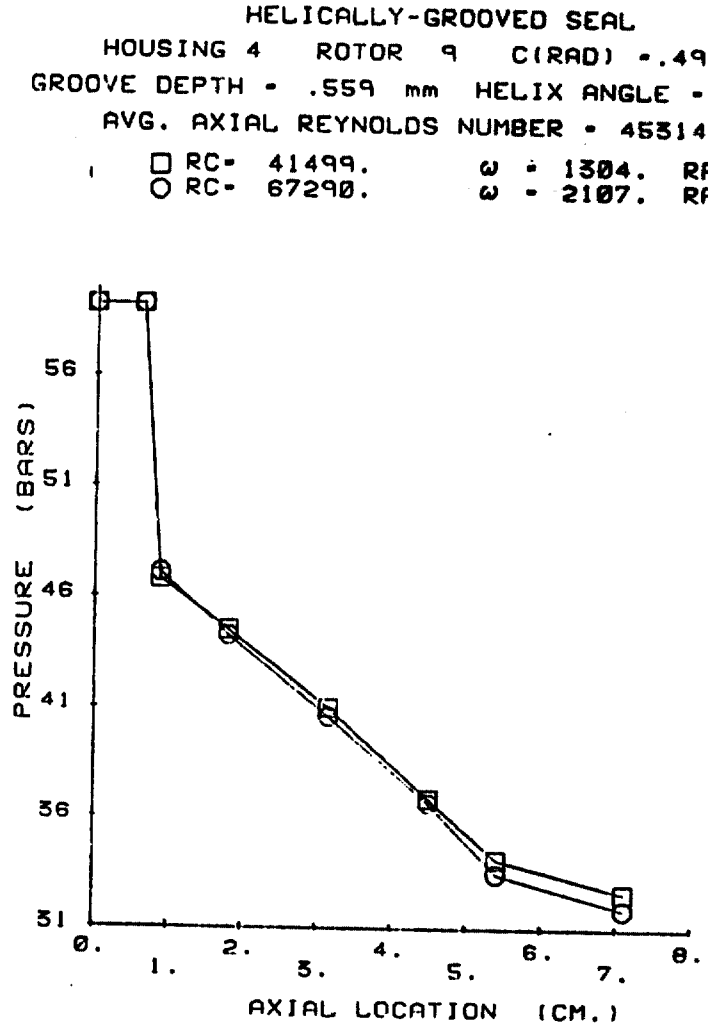

7. Static pressure distributions for seal 2 of rotor 9.

ORIGINAL PAGE IS
OF POOR QUALITY

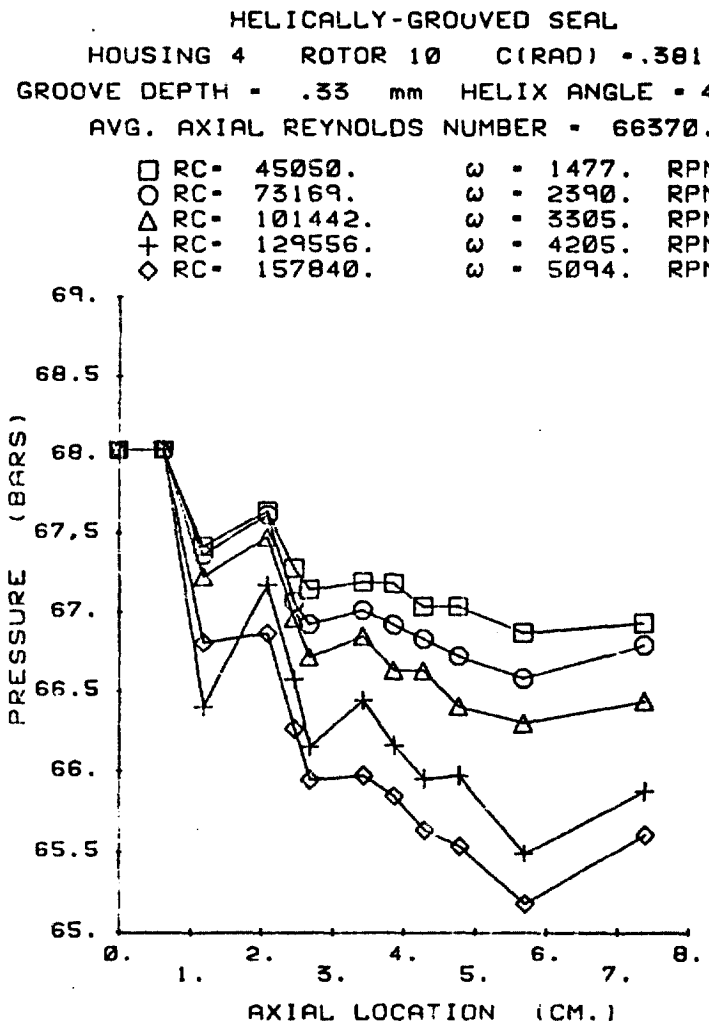

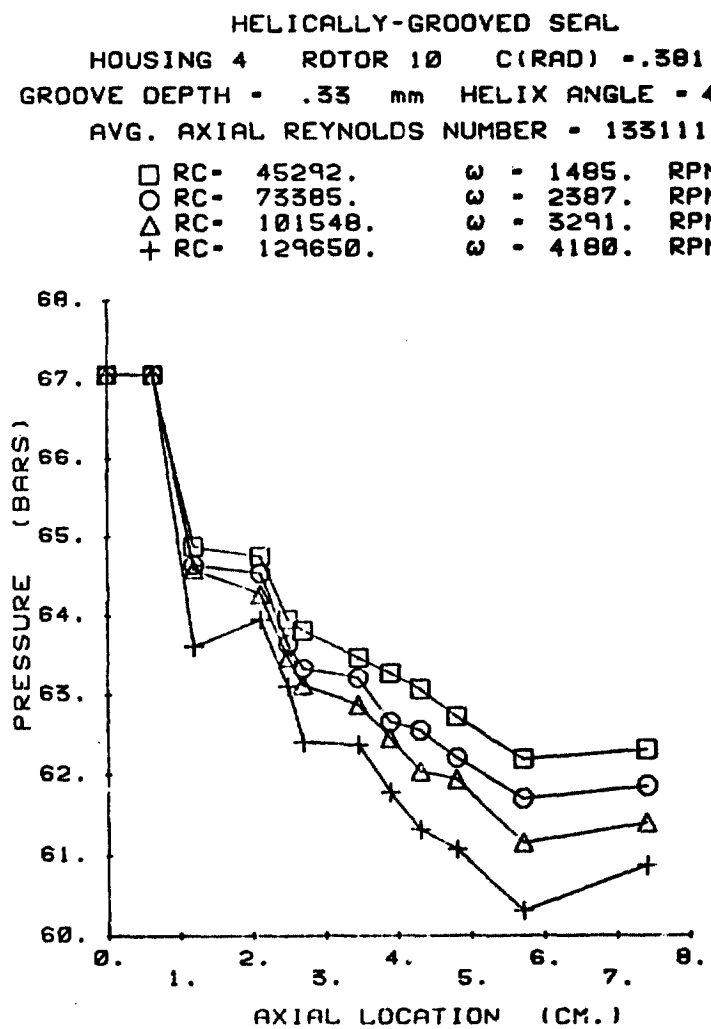

8. Static pressure distributions for seal 1 of rotor 10.

ORIGINAL PAGE IS OF POOR QUALITY

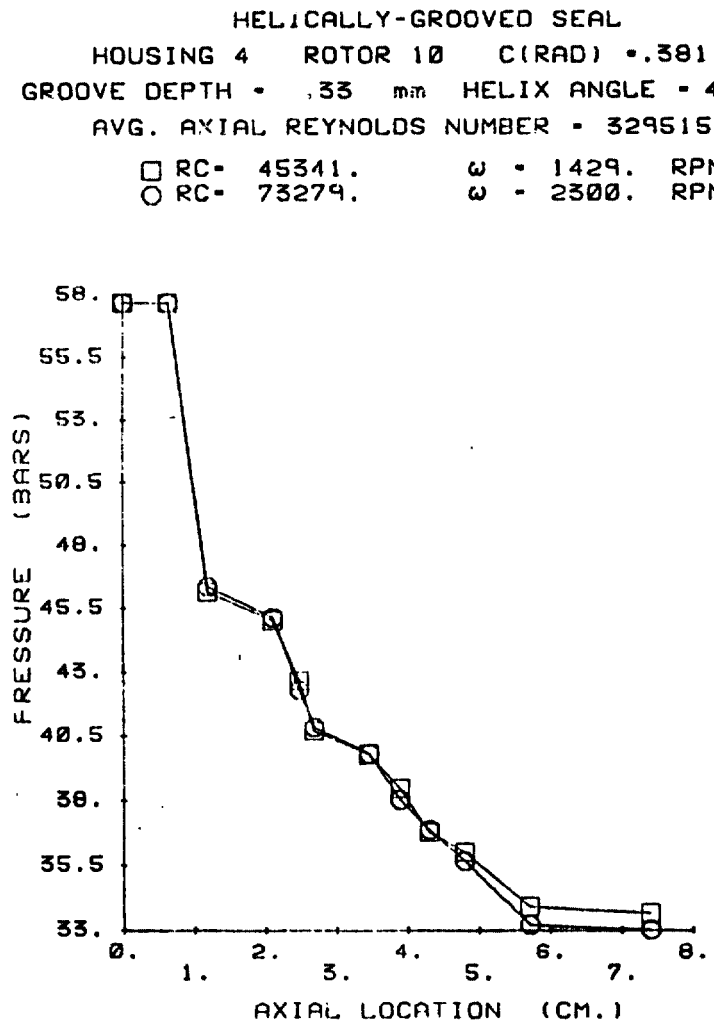

8. Static pressure distributions for seal 1 of rotor 10.

ORIGINAL PAGE IS
OF POOR QUALITY

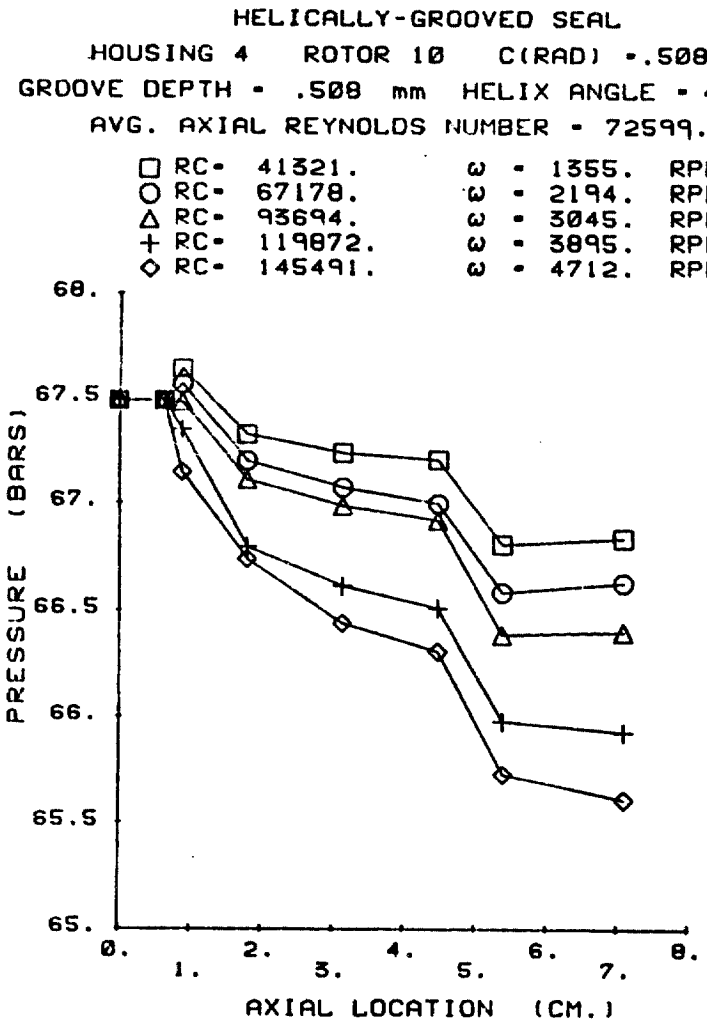

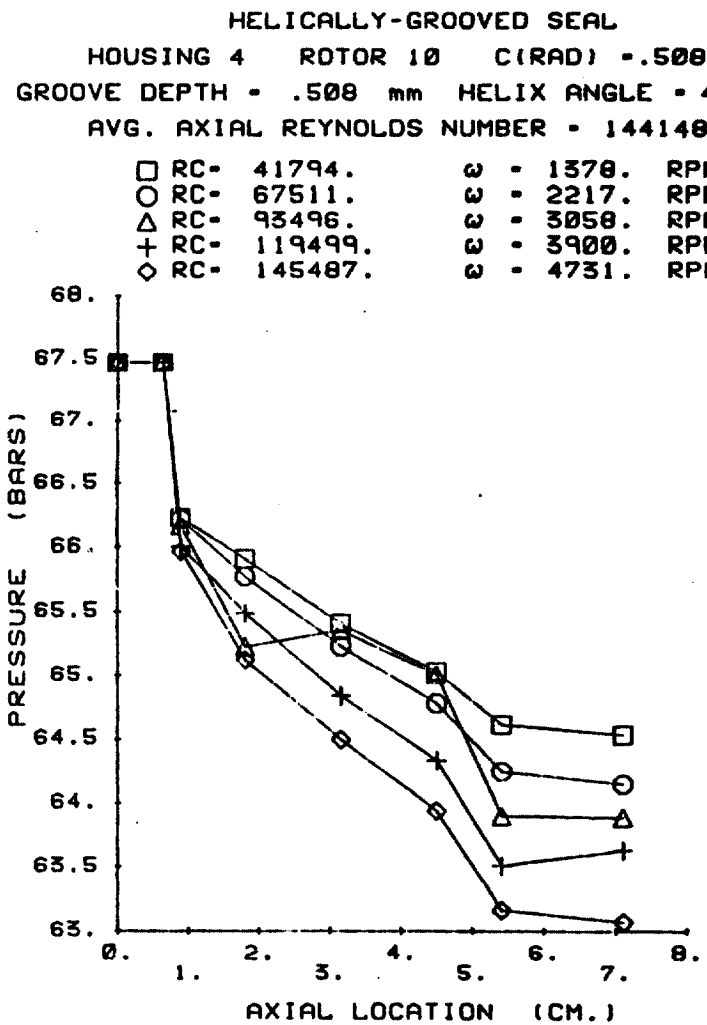

ORIGINAL PAGE IS OF POOR QUALITY

9. Static pressure distributions for seal 2 of rotor 10.

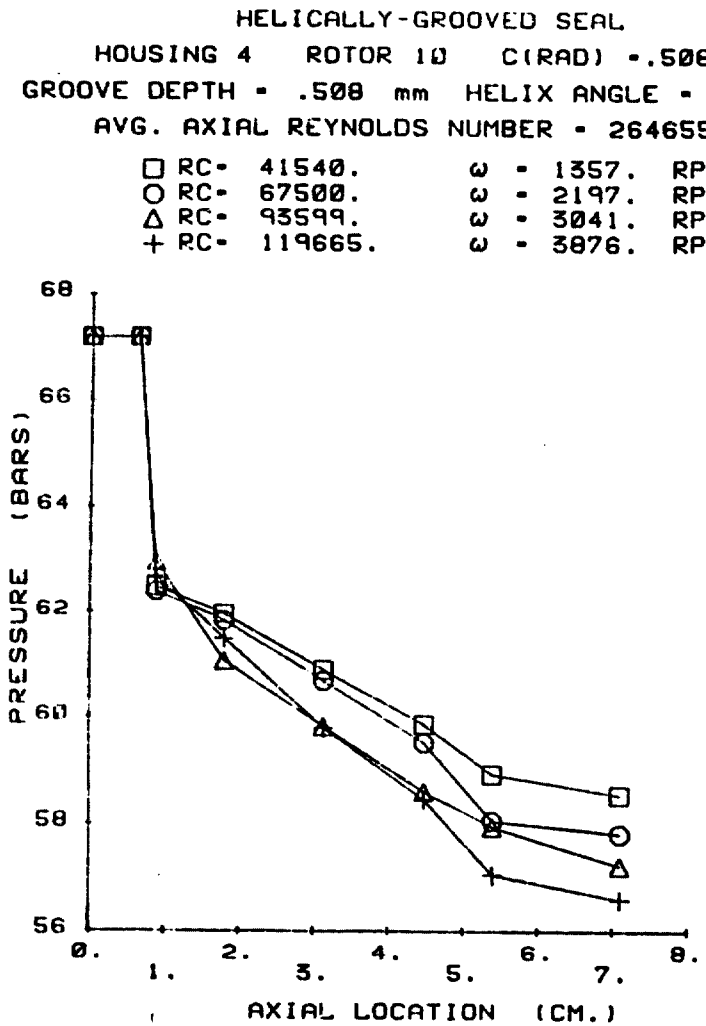

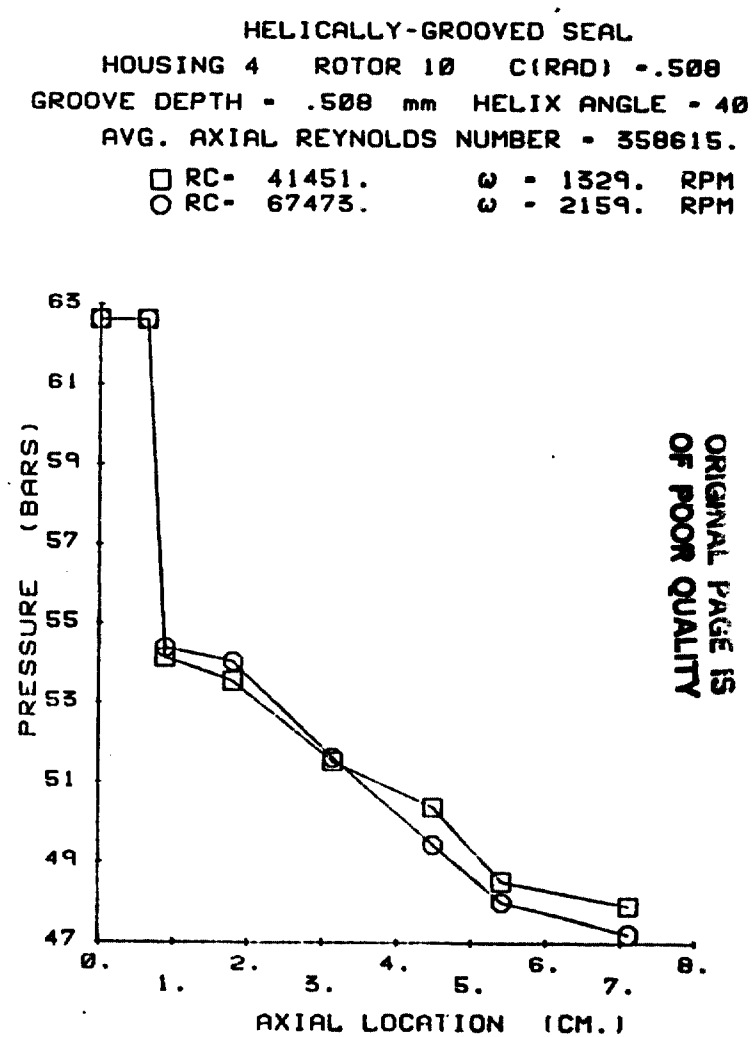

ORIGINAL PAGE IS
OF POOR QUALITY

9. Static pressure distributions for seal 2 of rotor 10.

ORIGINAL PAGE IS
OF POOR QUALITY

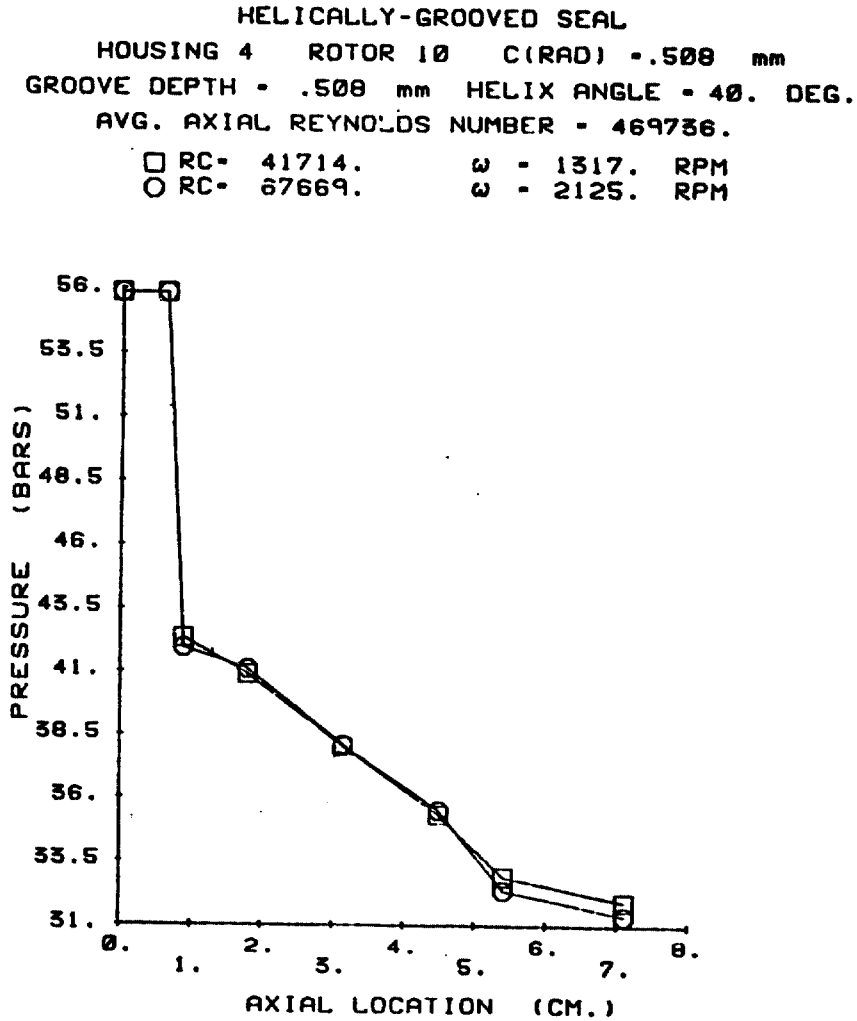

9. Static pressure distributions for seal 2 of rotor 10.

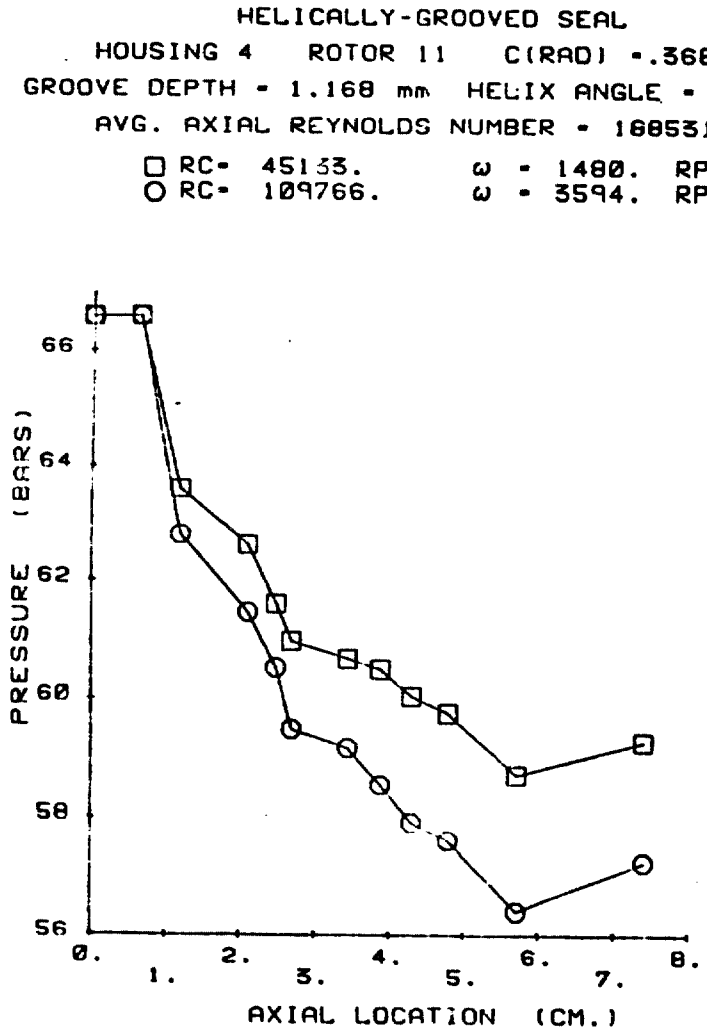

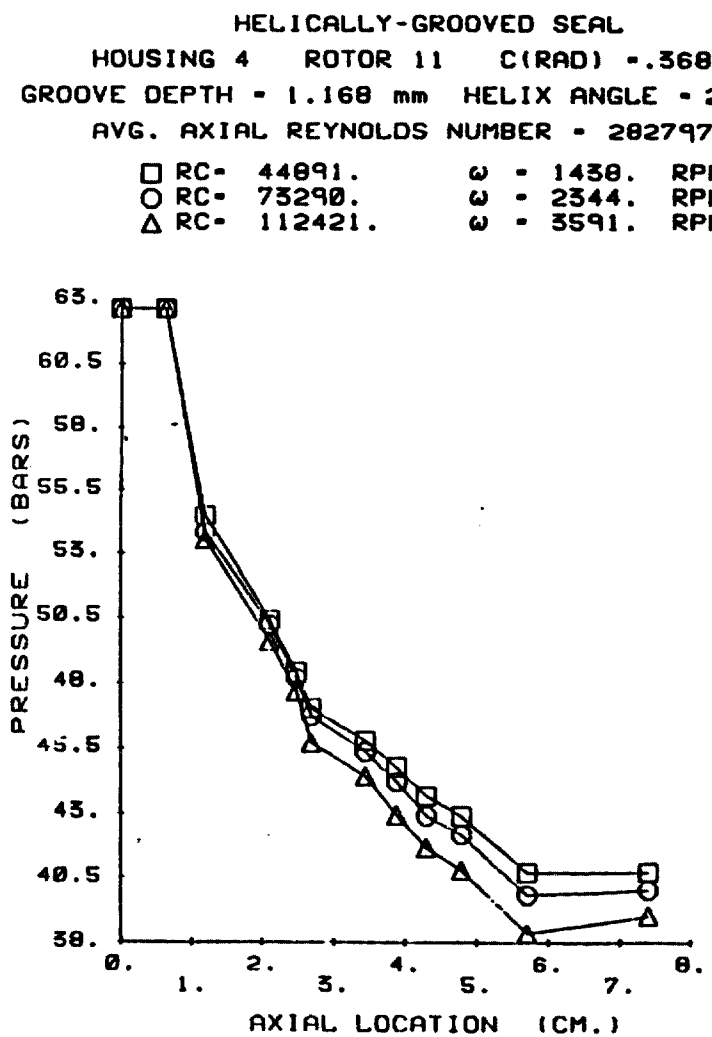

ORIGINAL PAGE IS
OF POOR QUALITY

10. Static pressure distributions for seal 1 of rotor 11.

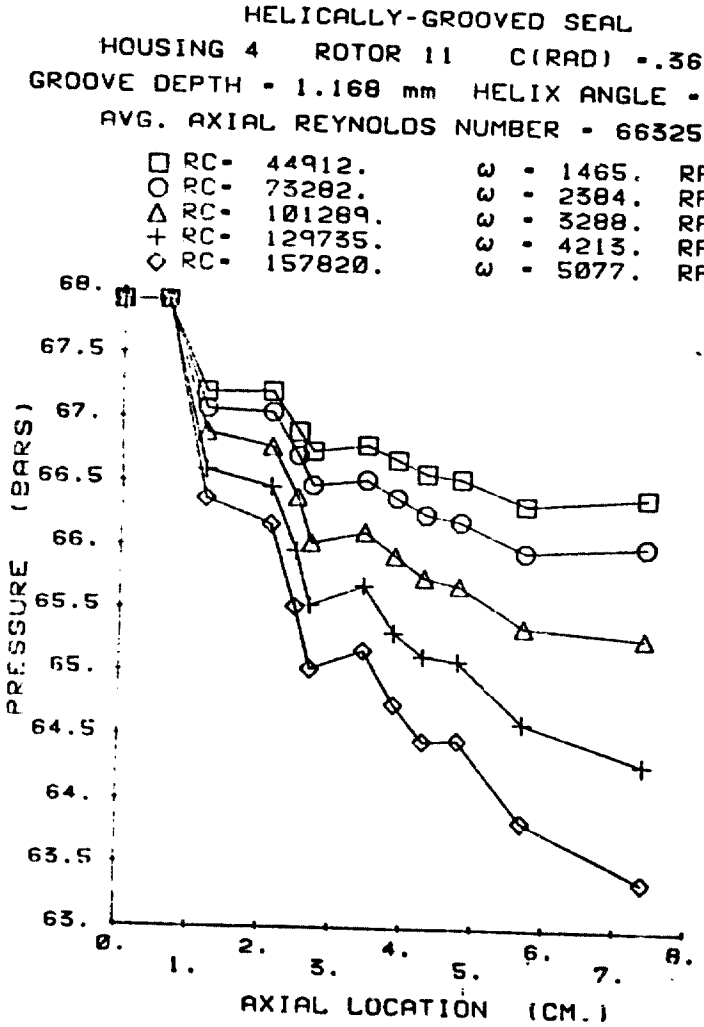

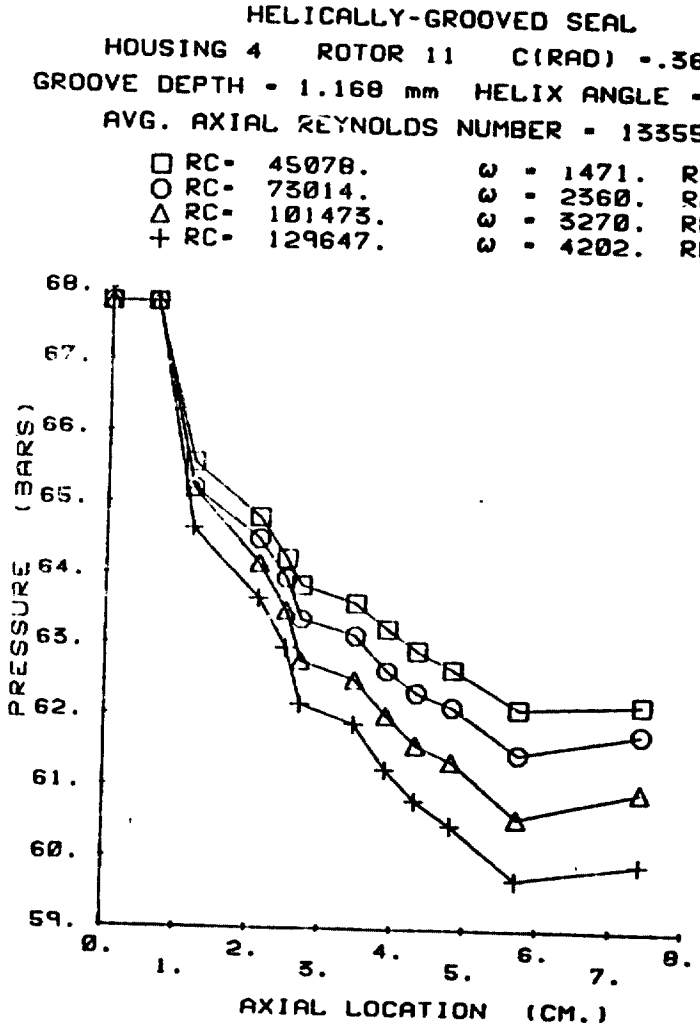

10. Static pressure distributions for seal 1 of rotor 11.

ORIGINAL PAGE IS
OF POOR QUALITY

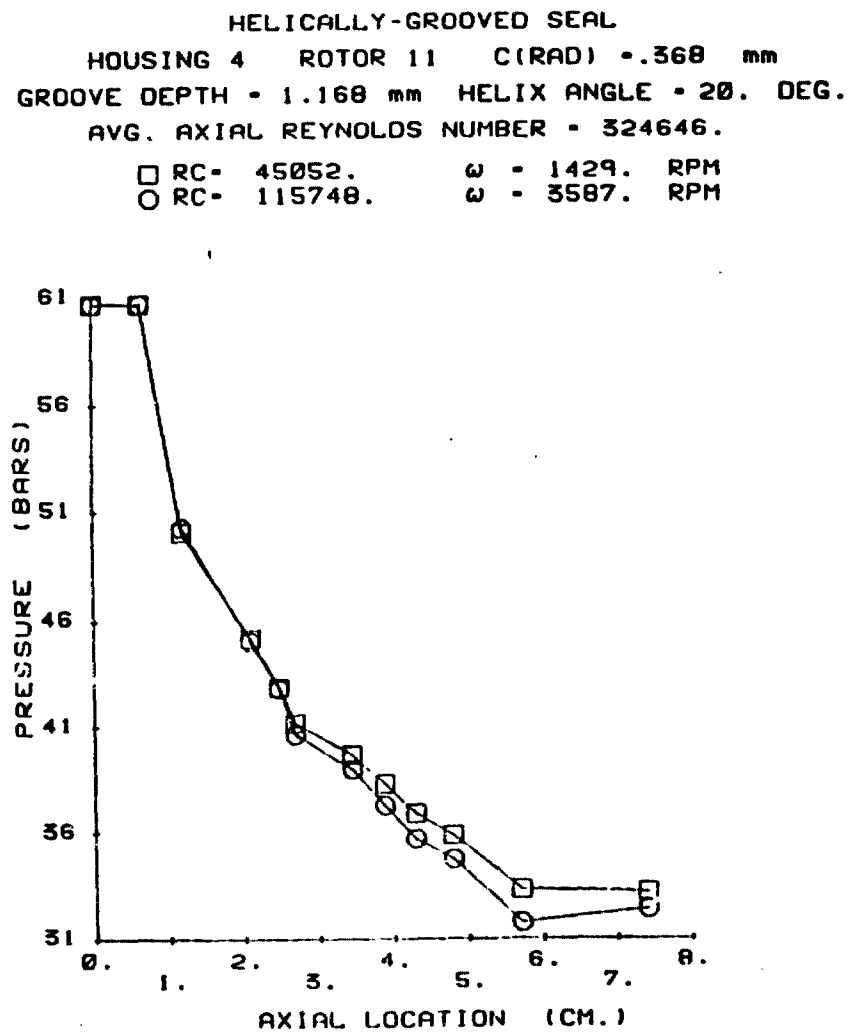

10. Static pressure distributions for seal 1 of rotor 11.

ORIGINAL PAGE IS
OF POOR QUALITY

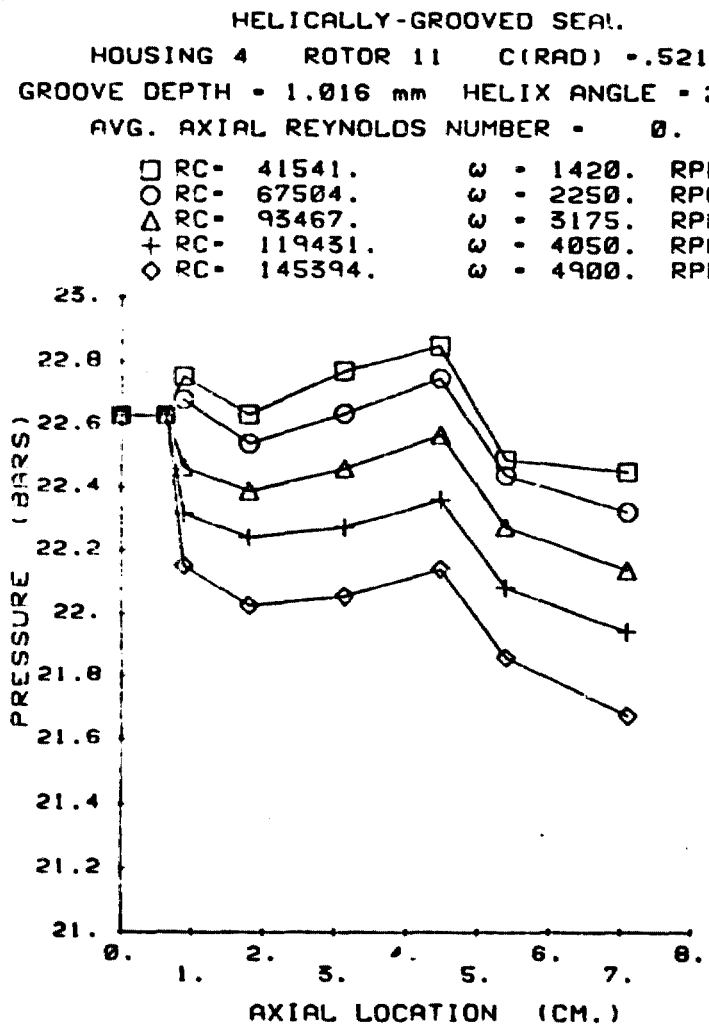

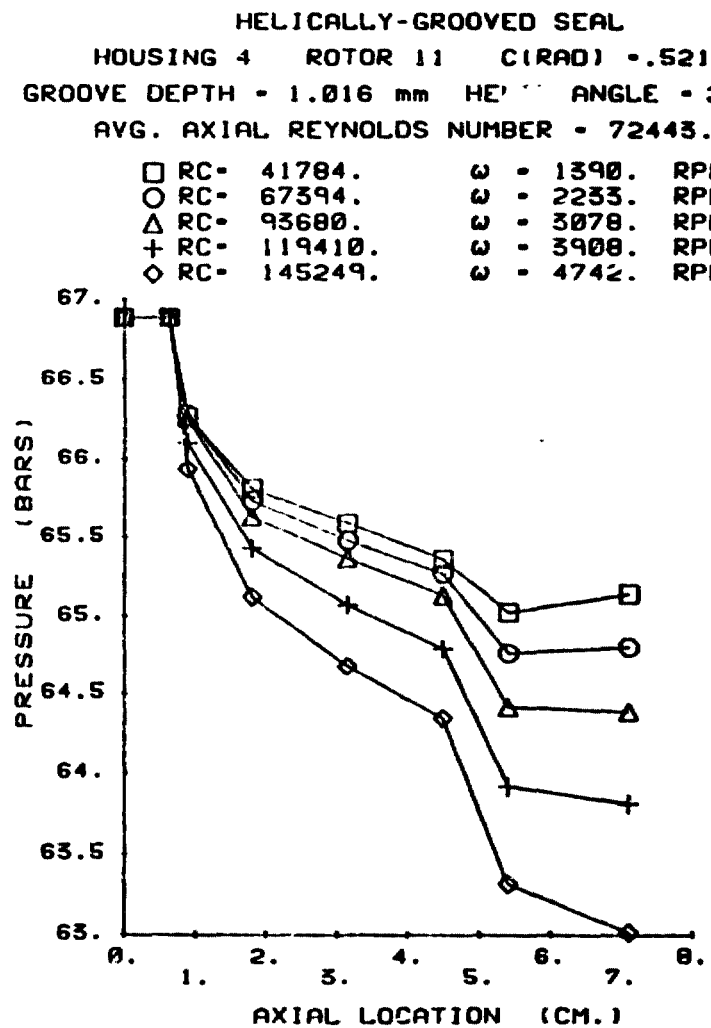

ORIGINAL PAGE IS
OF POOR QUALITY

11. Static pressure distributions for seal 2 of rotor 11.

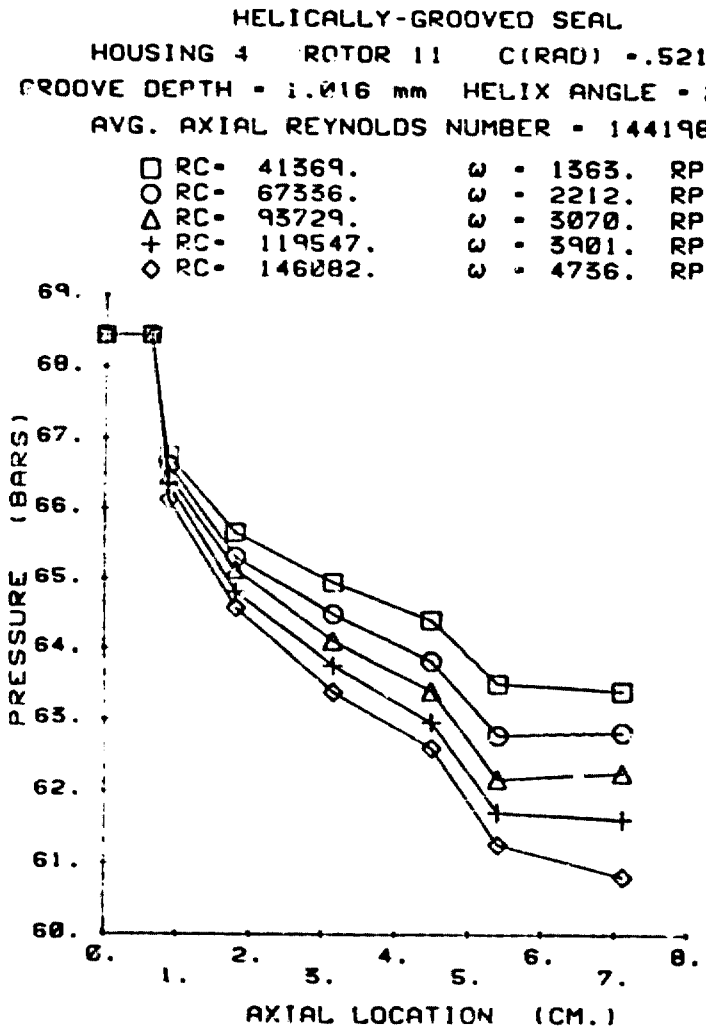

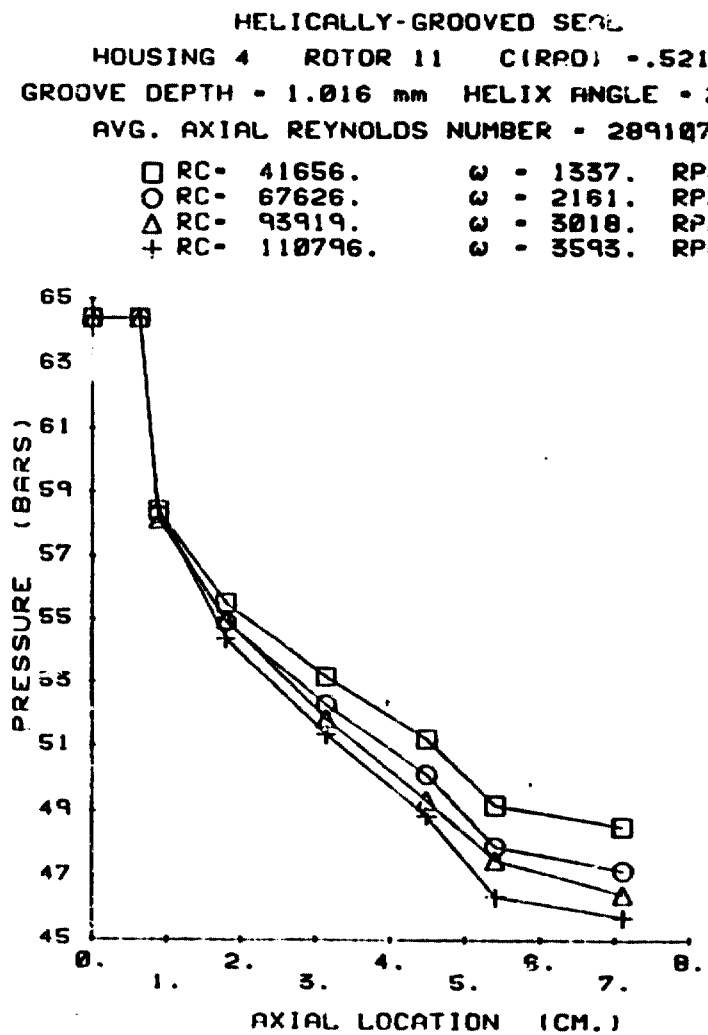

11. Static pressure distributions for seal 2 of rotor 11.

ORIGINAL PAGE IS
OF POOR QUALITY

ORIGINAL PAGE IS
OF POOR QUALITY

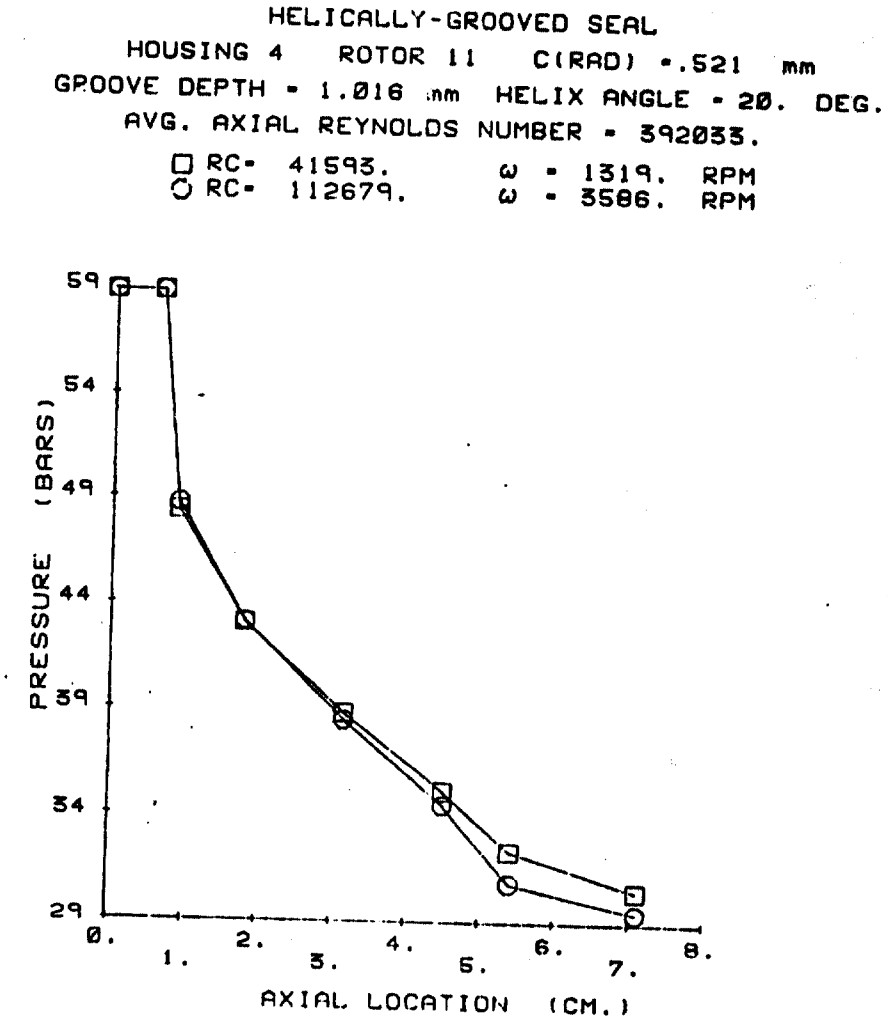

11. Static pressure distributions for seal 2 of rotor 11.

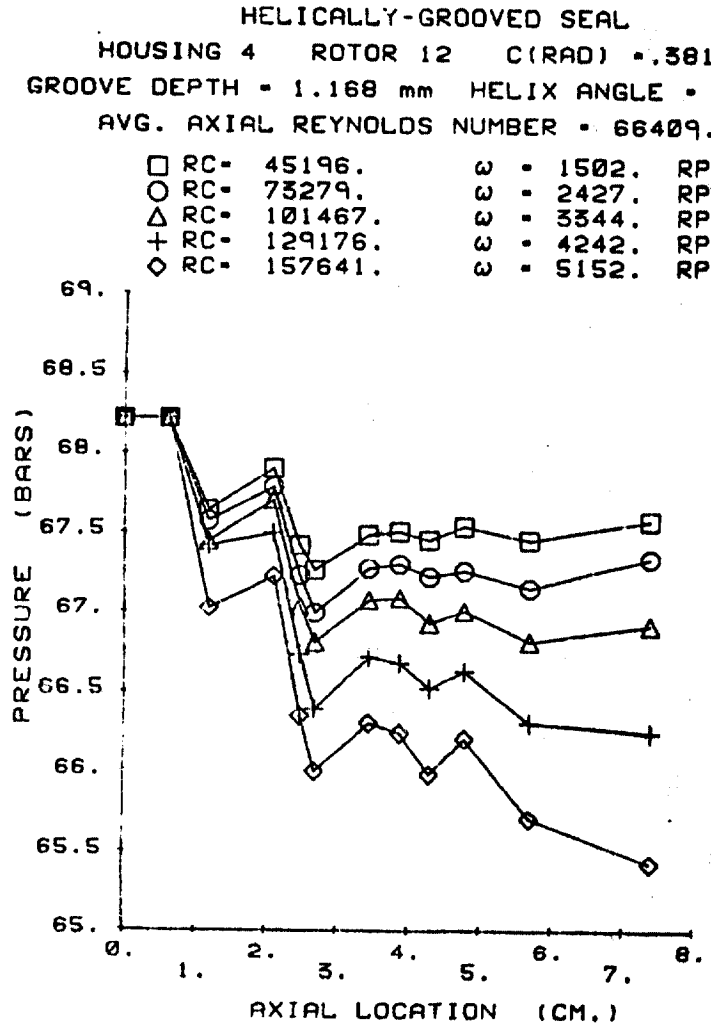

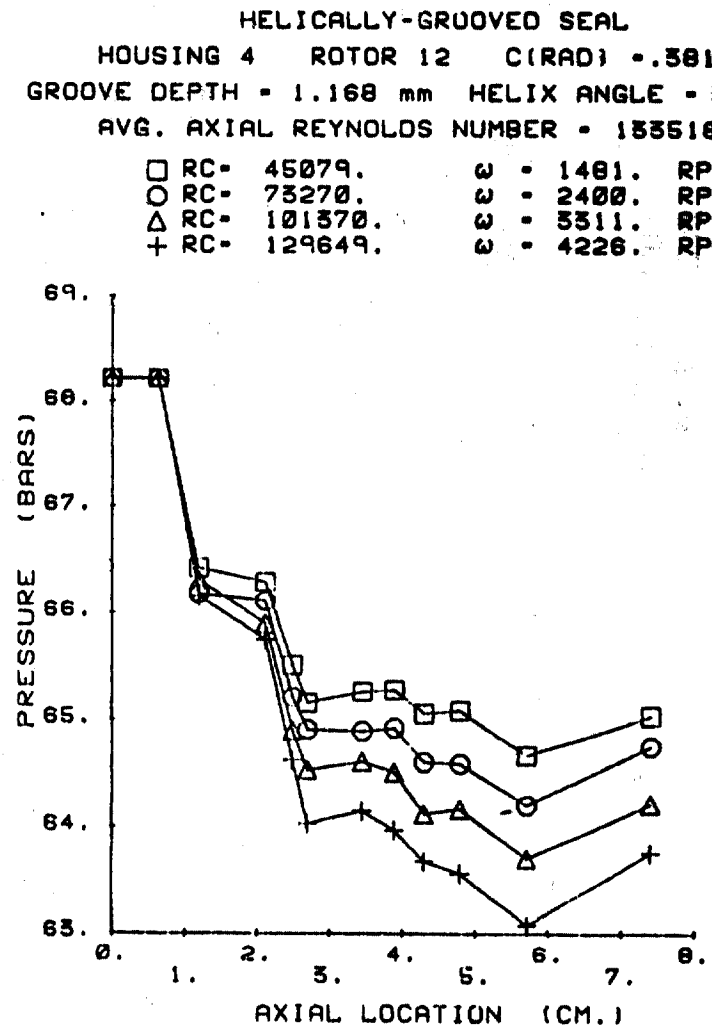

12. Static pressure distributions for seal 1 of rotor 12.

ORIGINAL PAGE IS OF POOR QUALITY

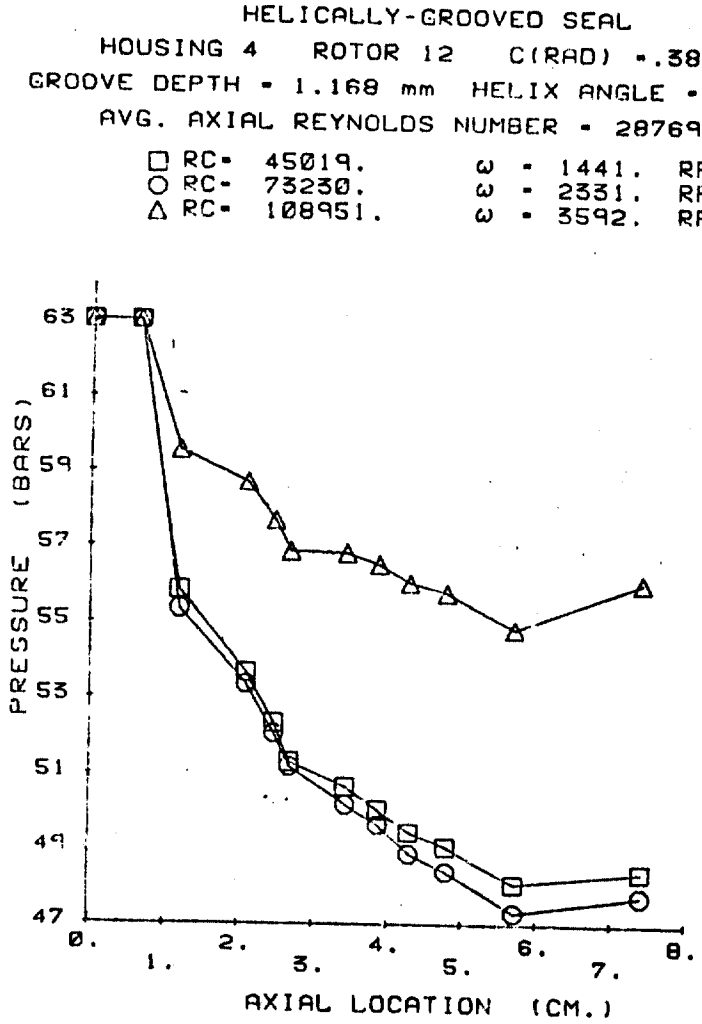

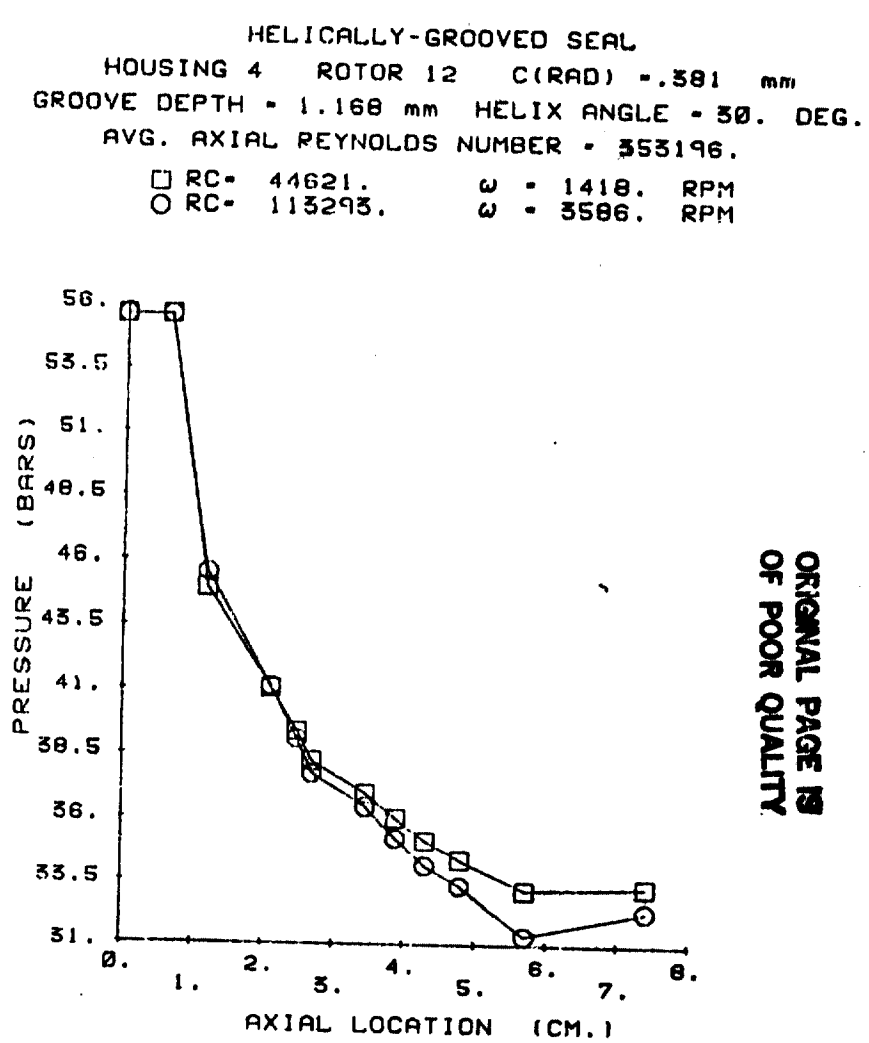

12. Static pressure distributions for seal 1 of rotor 12.

ORIGINAL PAGE IS
OF POOR QUALITY

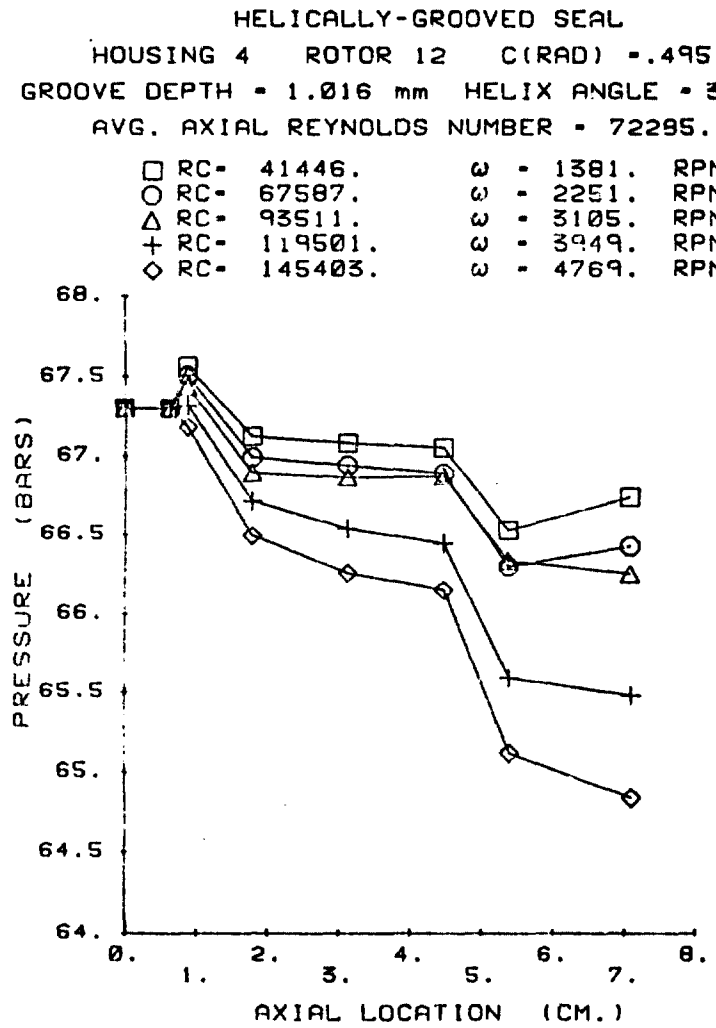

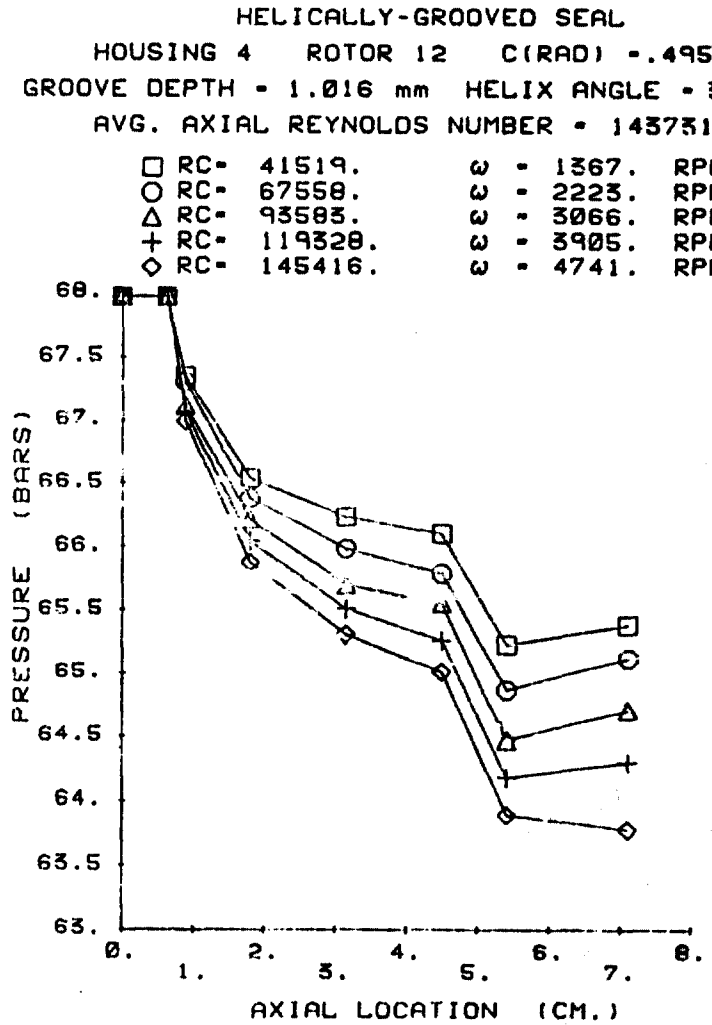

ORIGINAL PAGE IS OF POOR QUALITY

13. Static pressure distributions for seal 2 of rotor 12.

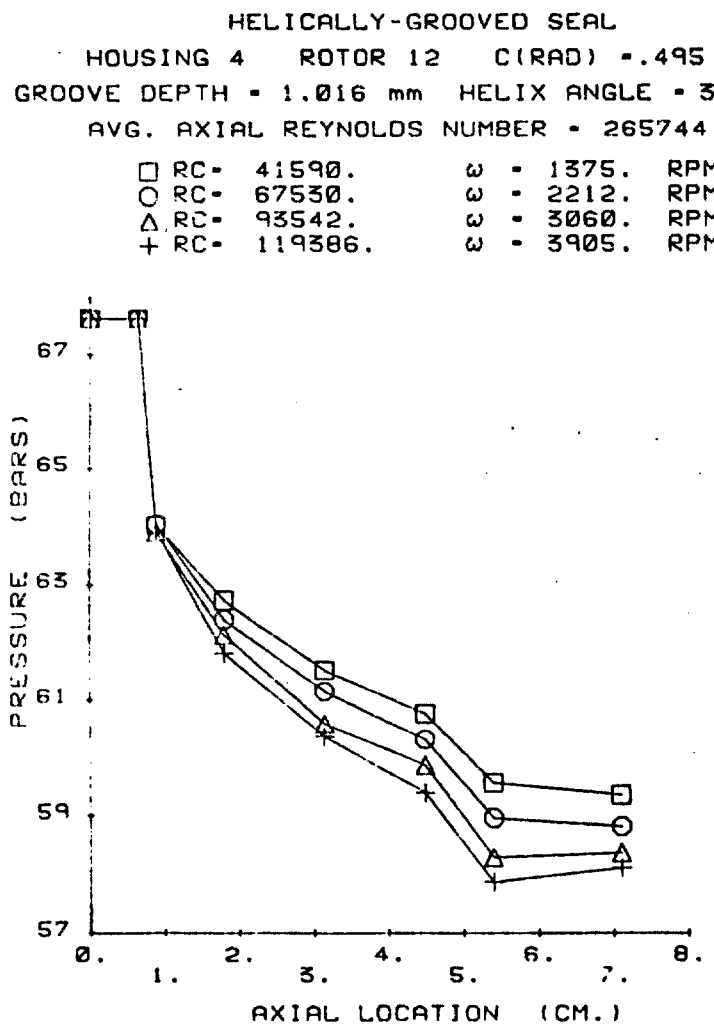

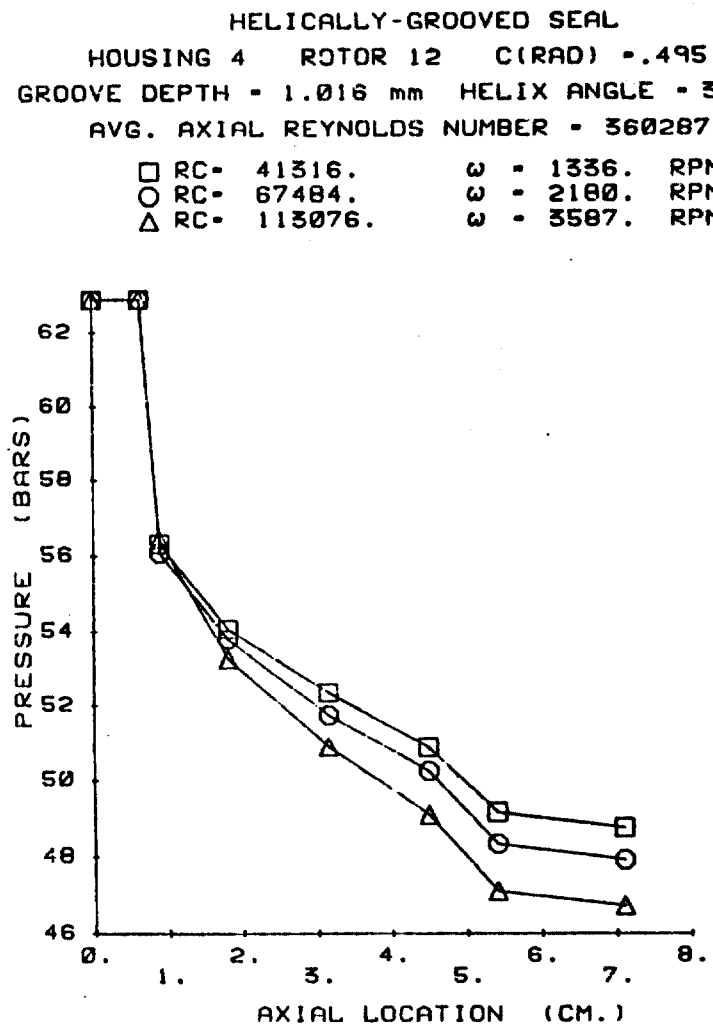

13. Static pressure distributions for seal 2 of rotor 12.

ORIGINAL PAGE IS
OF POOR QUALITY

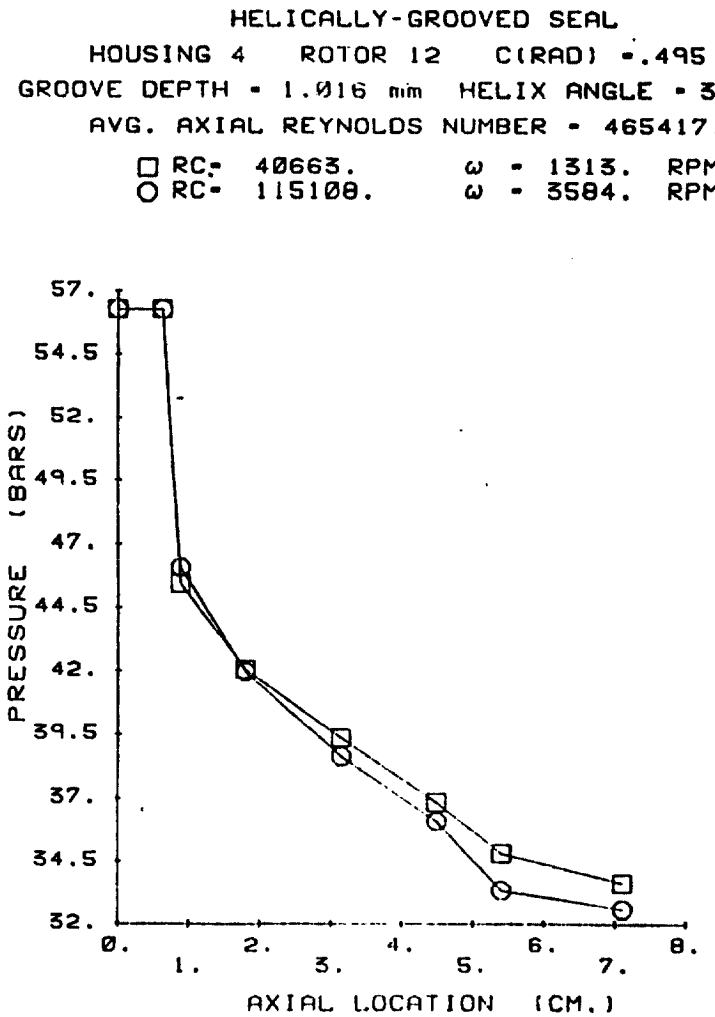

13. Static pressure distributions for seal 2 of rotor 12.

ORIGINAL PAGE IS
OF POOR QUALITY

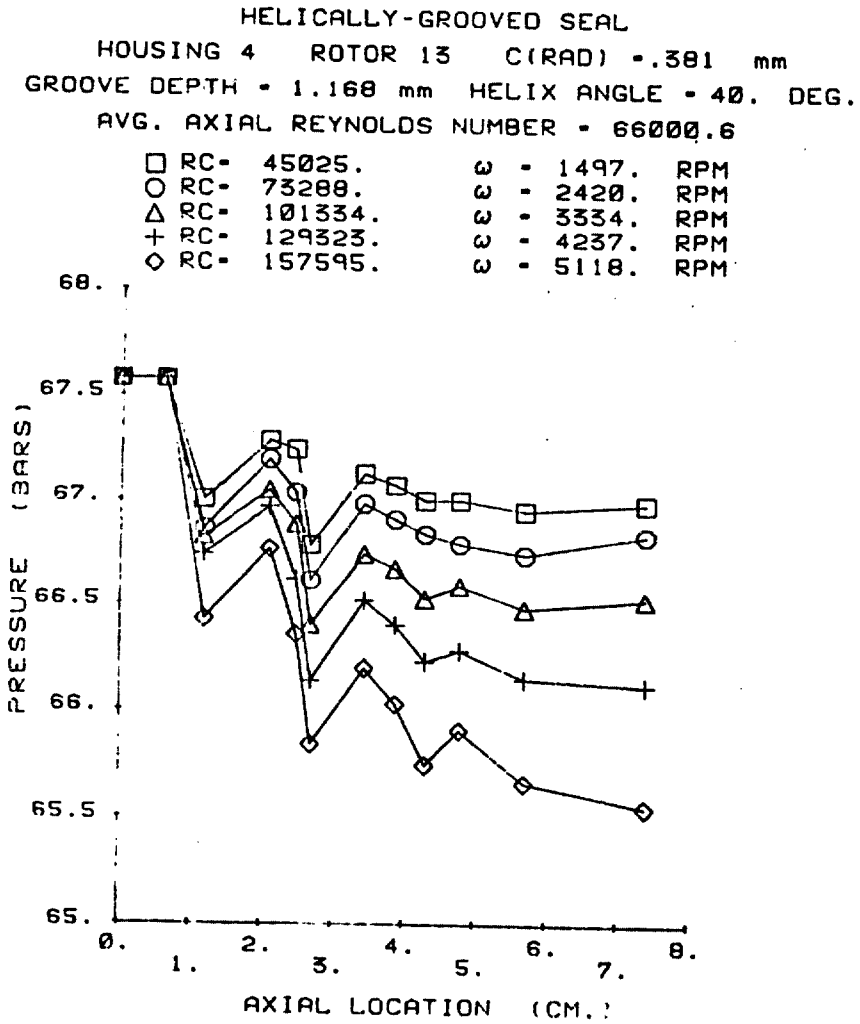

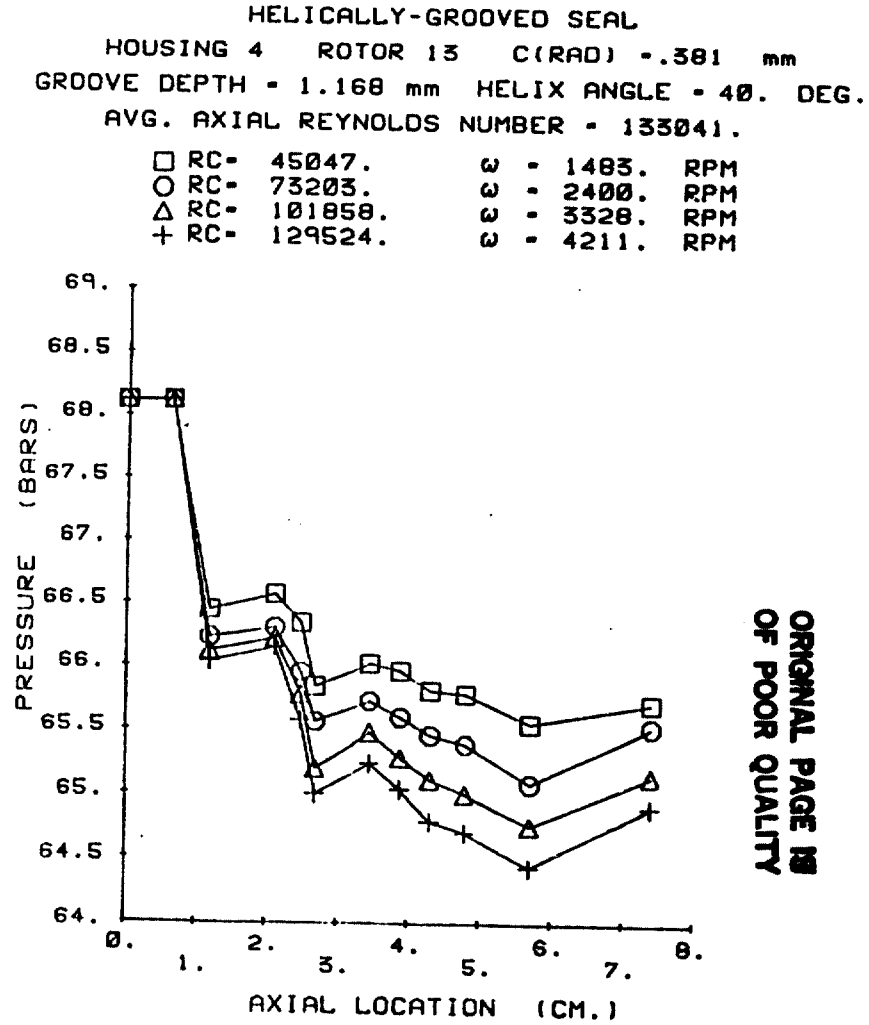

14. Static pressure distributions for seal 1 of rotor 13.

ORIGINAL PAGE IS
OF POOR QUALITY

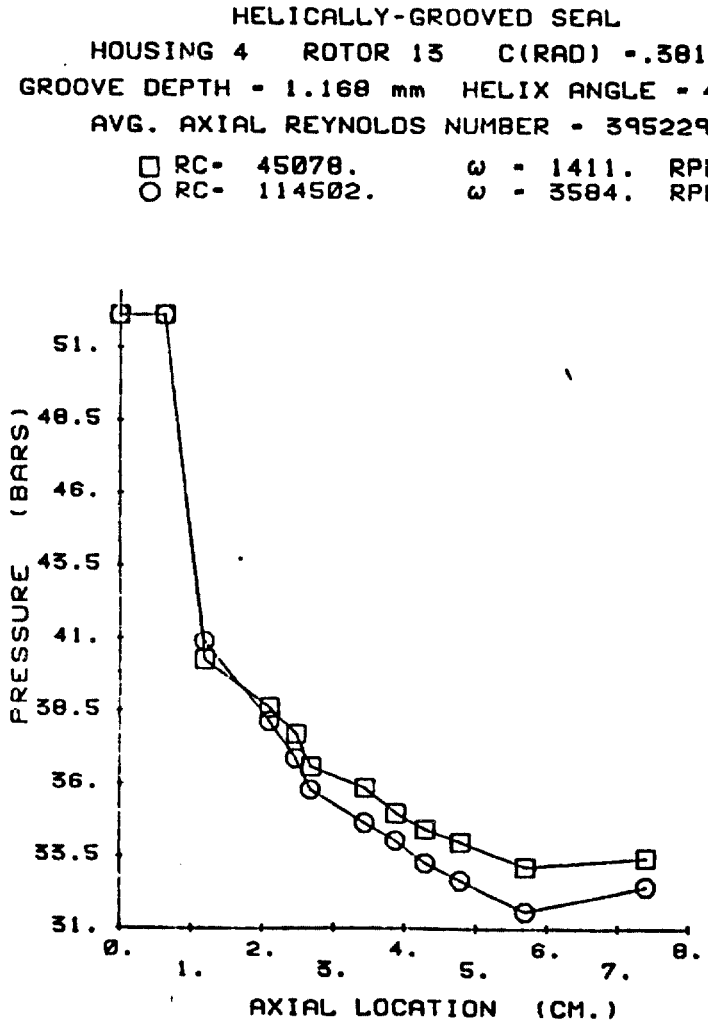

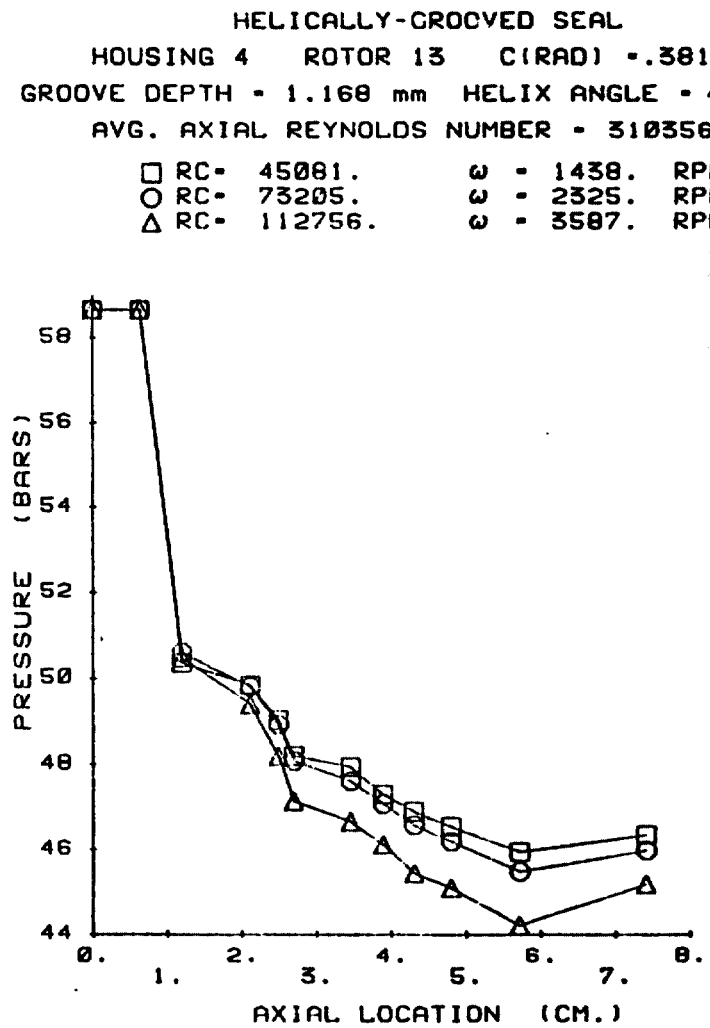

ORIGINAL PAGE IS OF POOR QUALITY

14. Static pressure distributions for seal 1 of rotor 13.

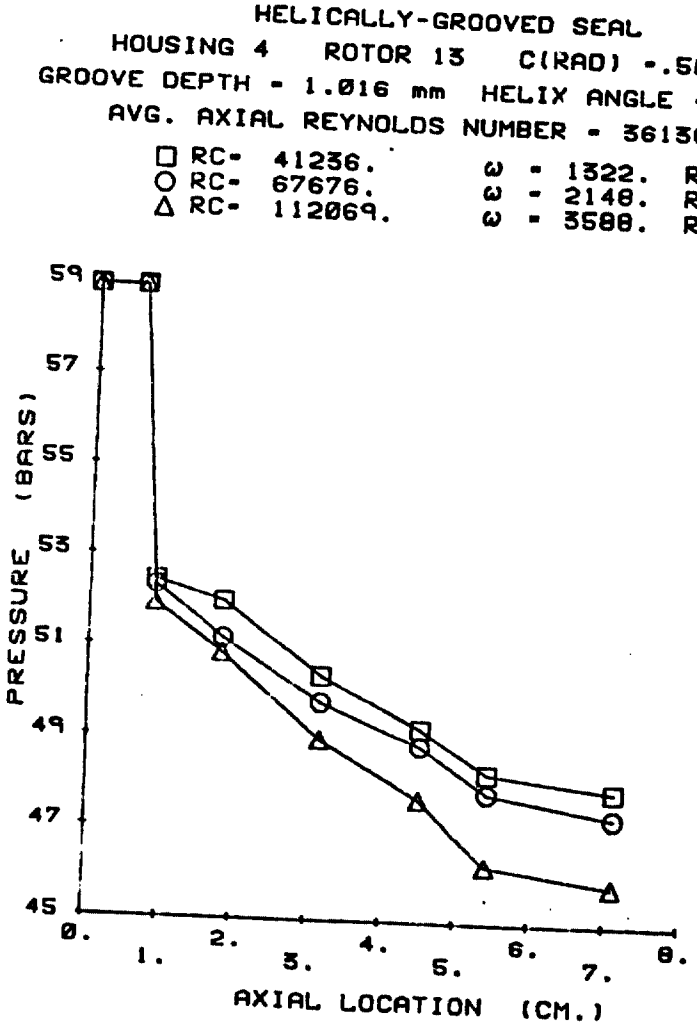

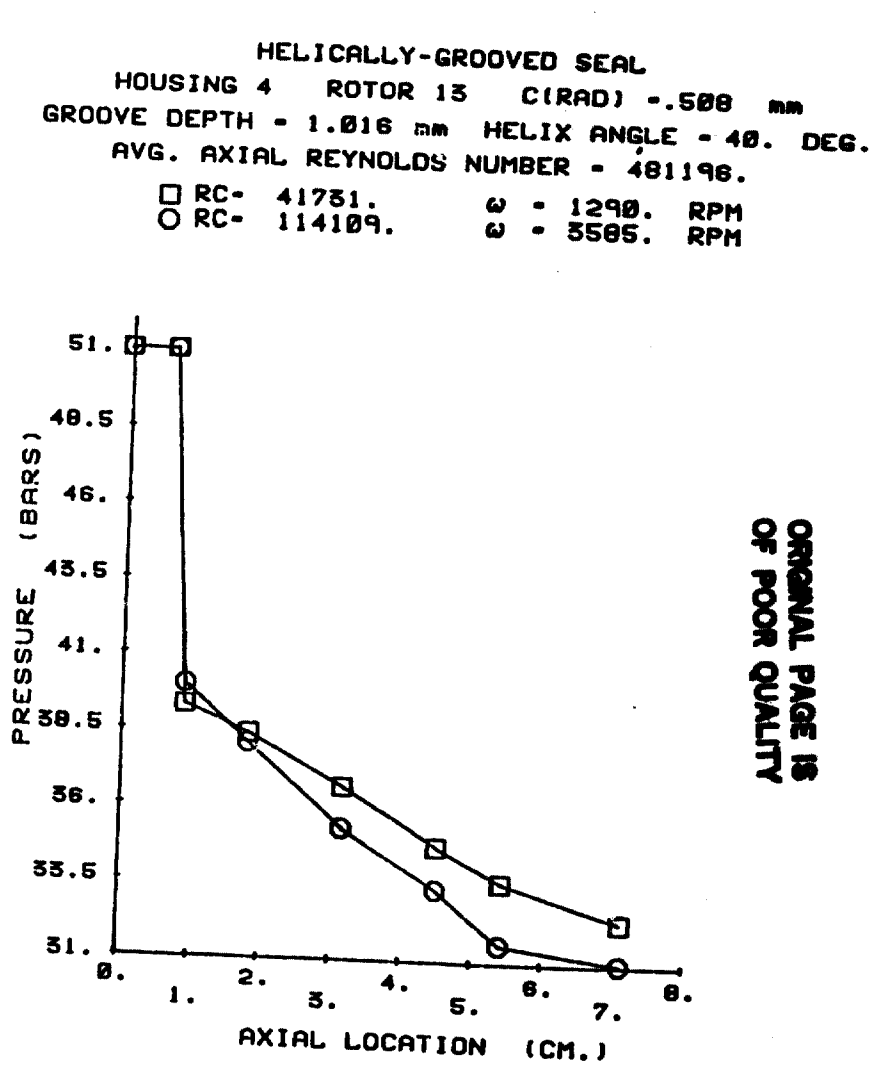

15. Static pressure distributions for seal 2 of rotor 13.

ORIGINAL PAGE IS
OF POOR QUALITY

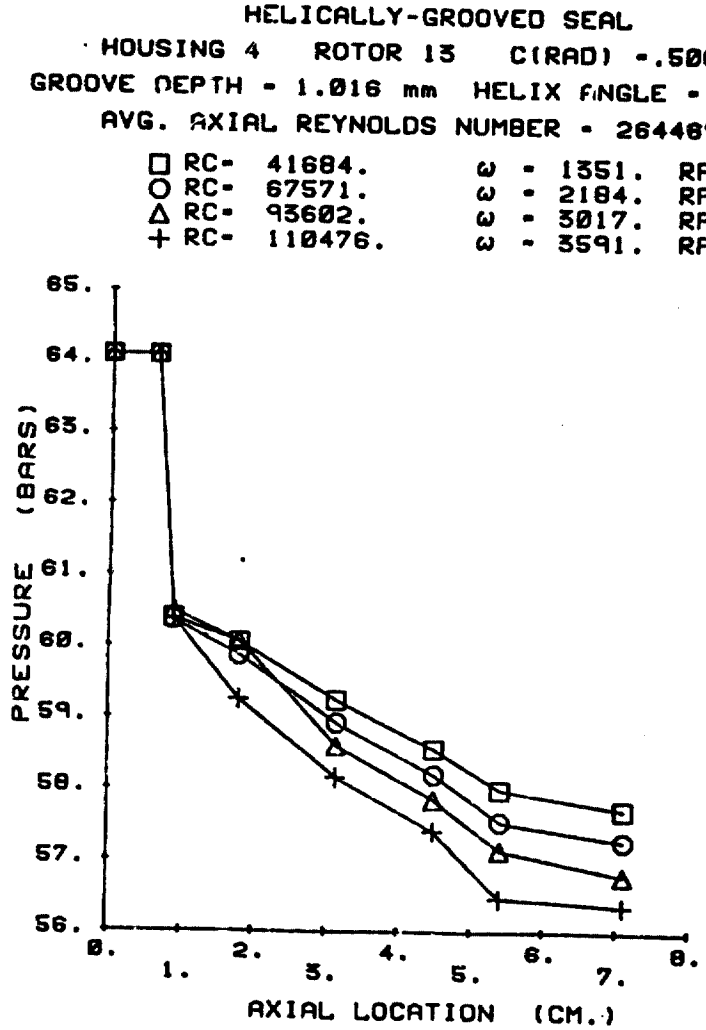

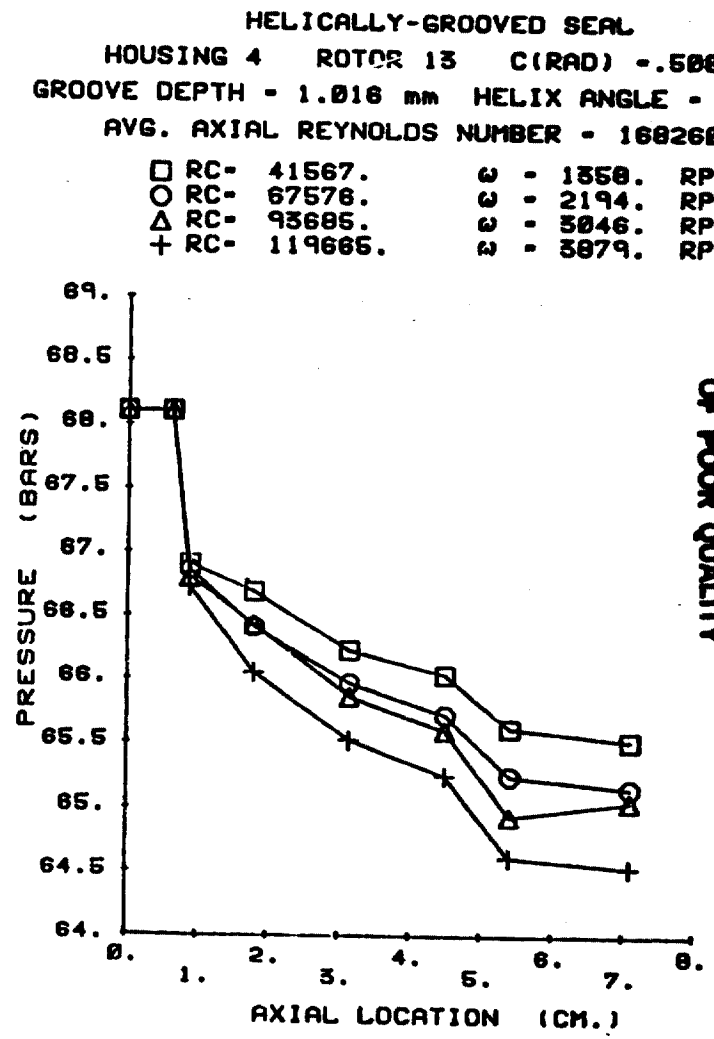

15. Static pressure distributions for seal 3 of rotor 13.

ORIGINAL PAGE IS OF POOR QUALITY

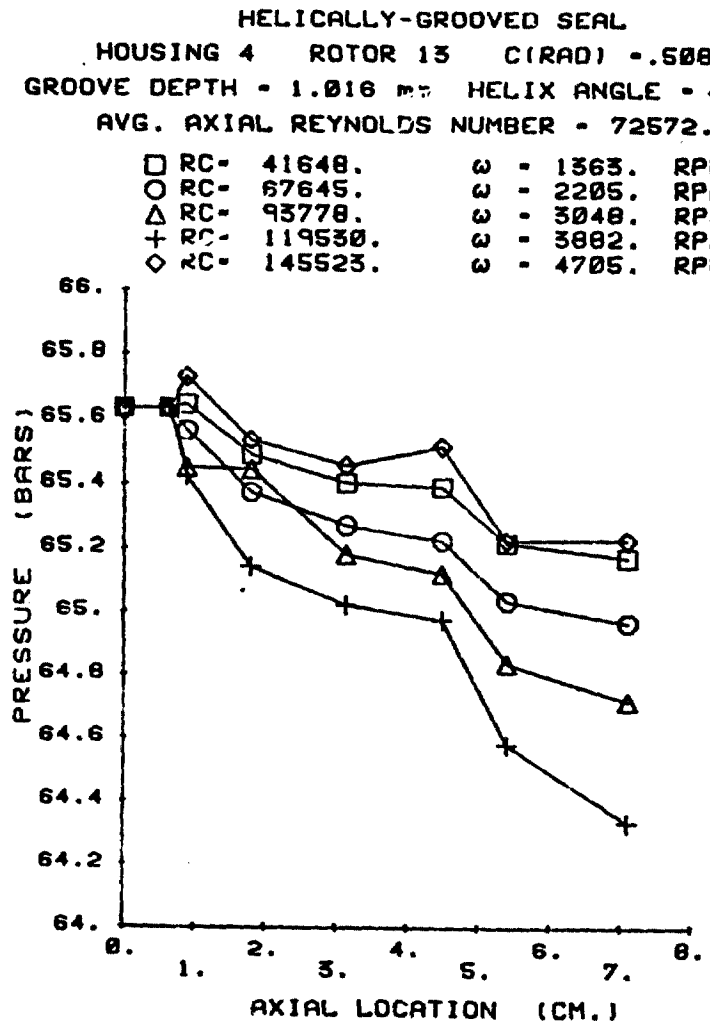

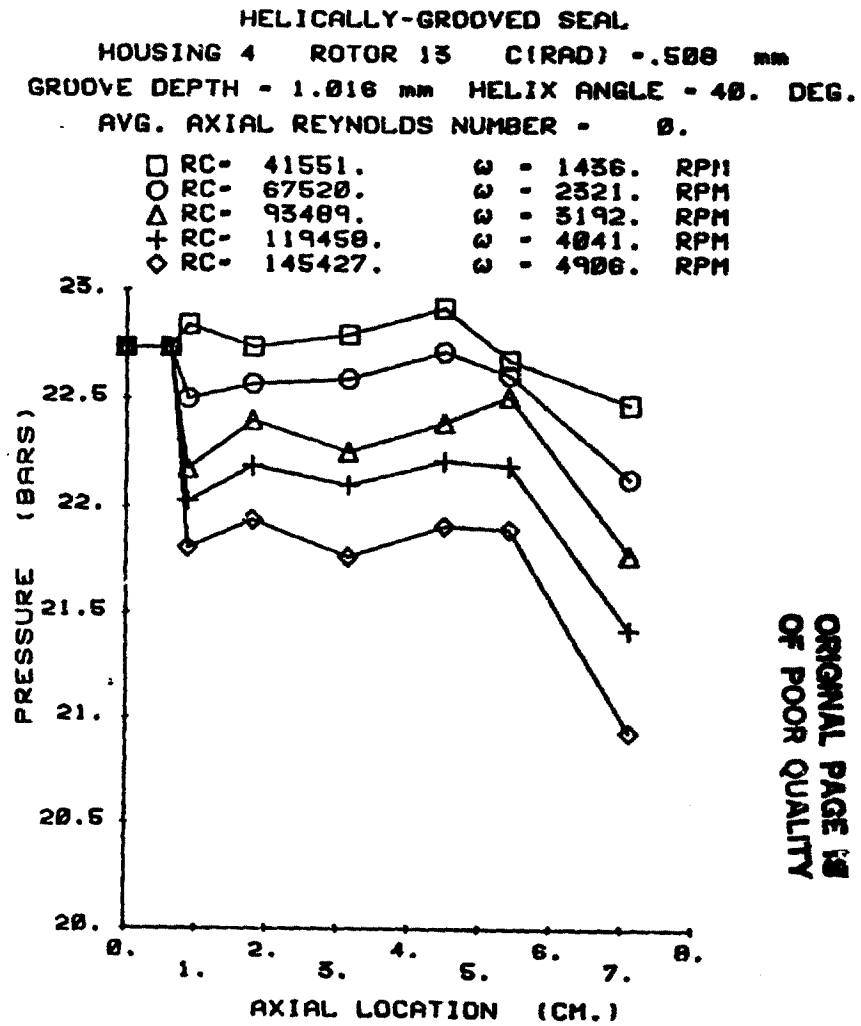

15. Static pressure distributions for seal 3 of rotor 13.

ORIGINAL PAGE IS
OF POOR QUALITY

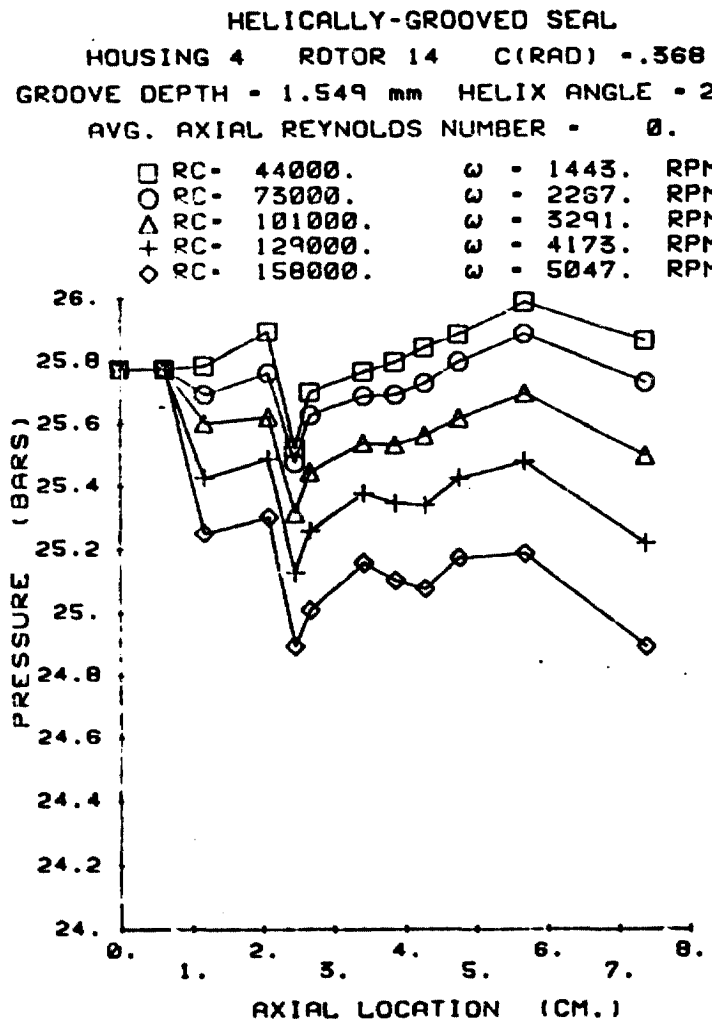

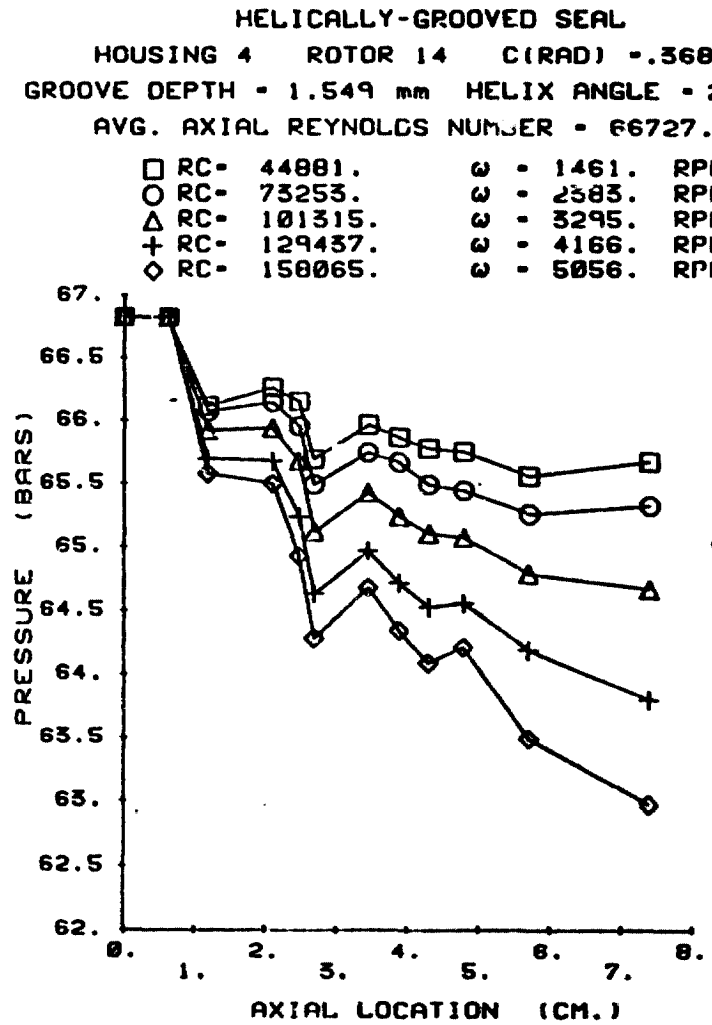

ORIGINAL PAGE IS OF POOR QUALITY

16. Static pressure distributions for seal 1 of rotor 14.

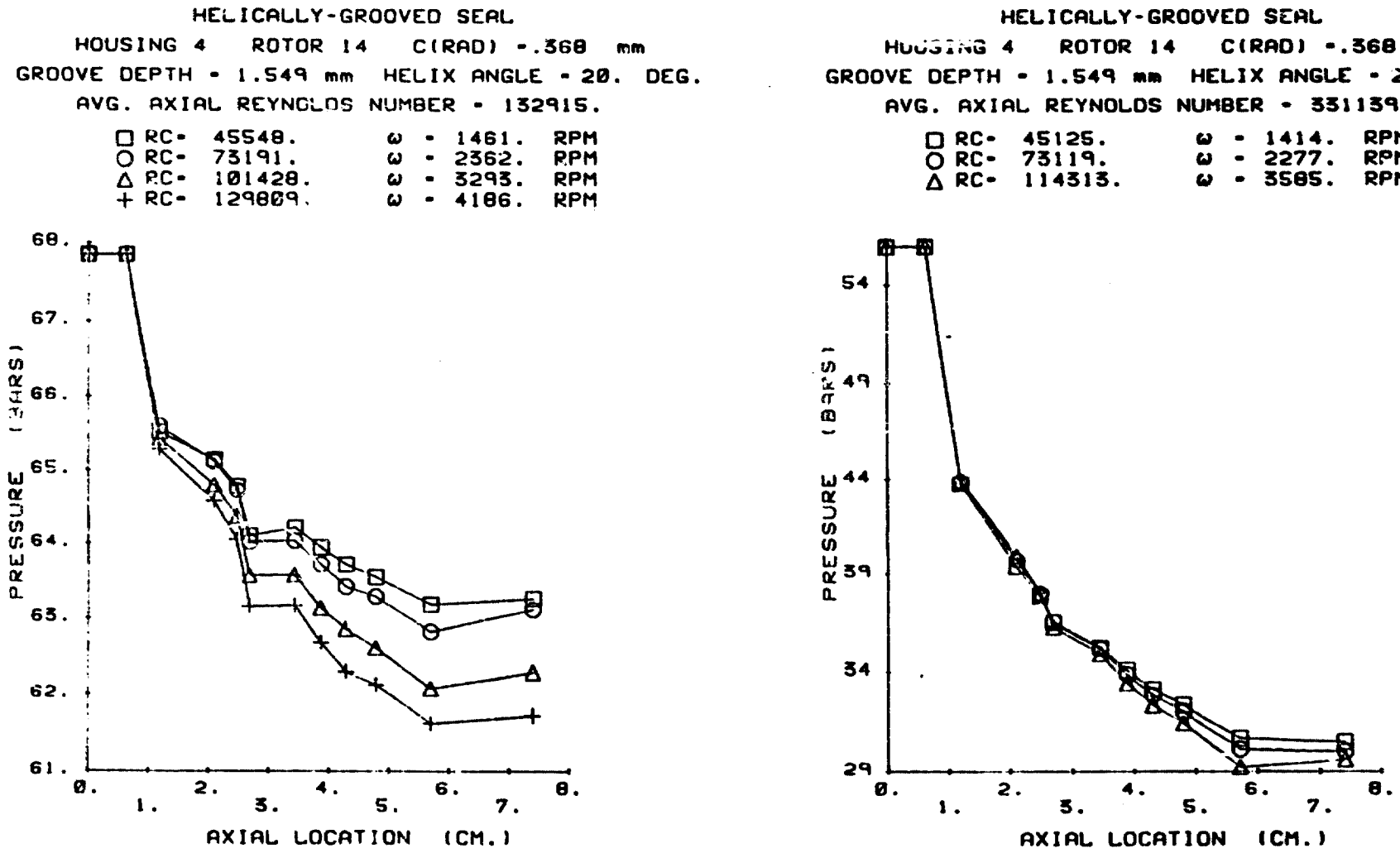

16. Static pressure distribut . or seal 1 of rotor 14.

ORIGINAL PAGE IS
OF POOR QUALITY

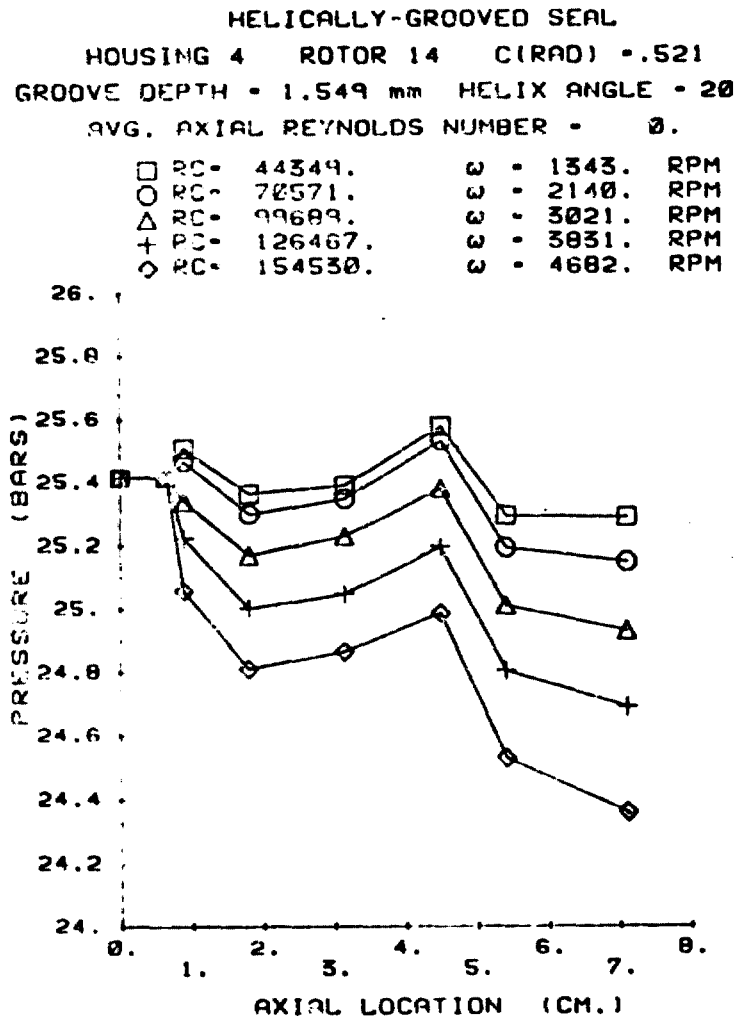

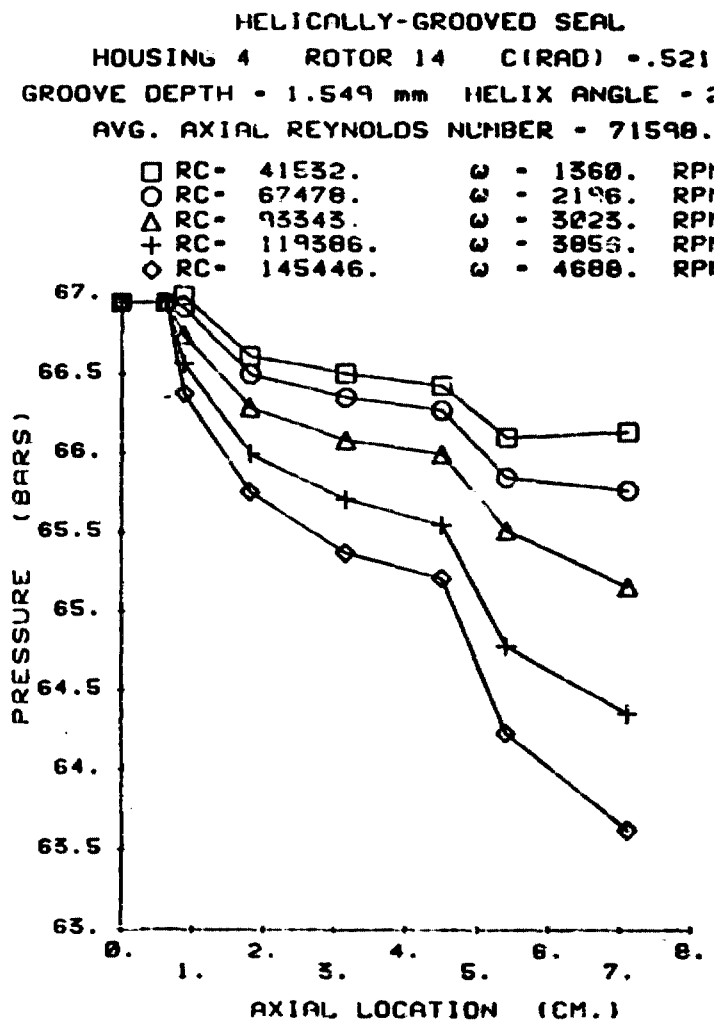

17. Static pressure distributions for seal 2 of rotor 14.

ORIGINAL PAGE IS OF POOR QUALITY

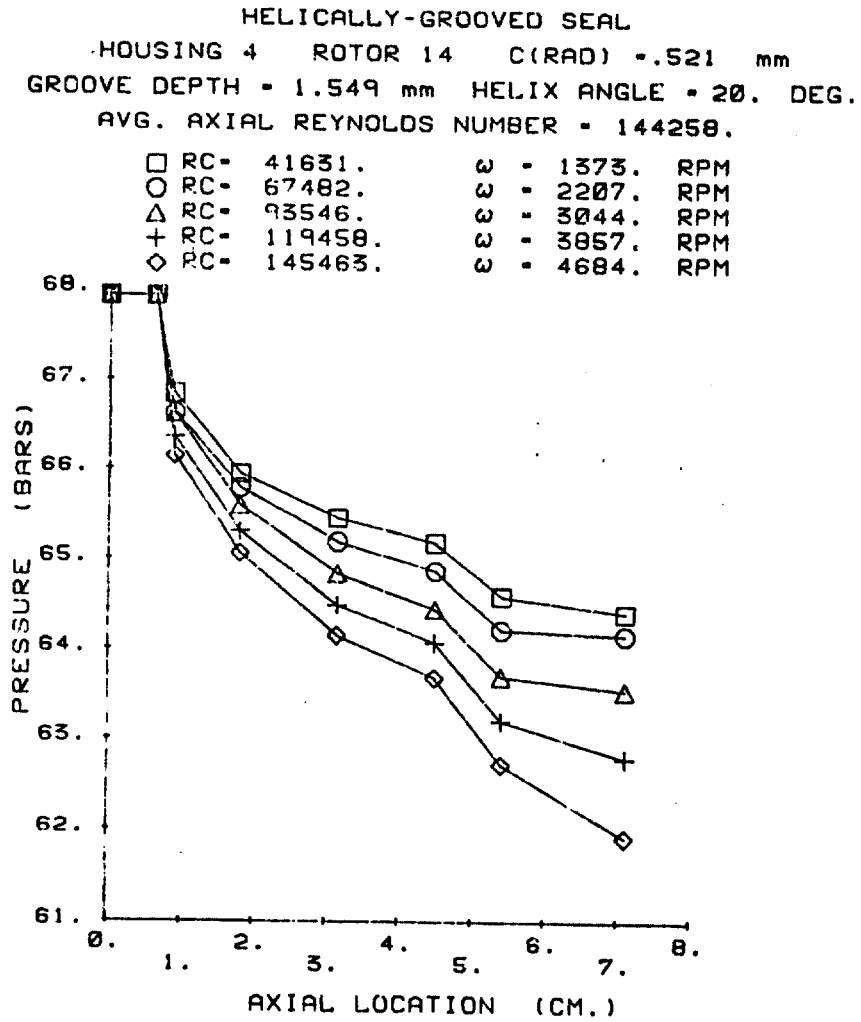

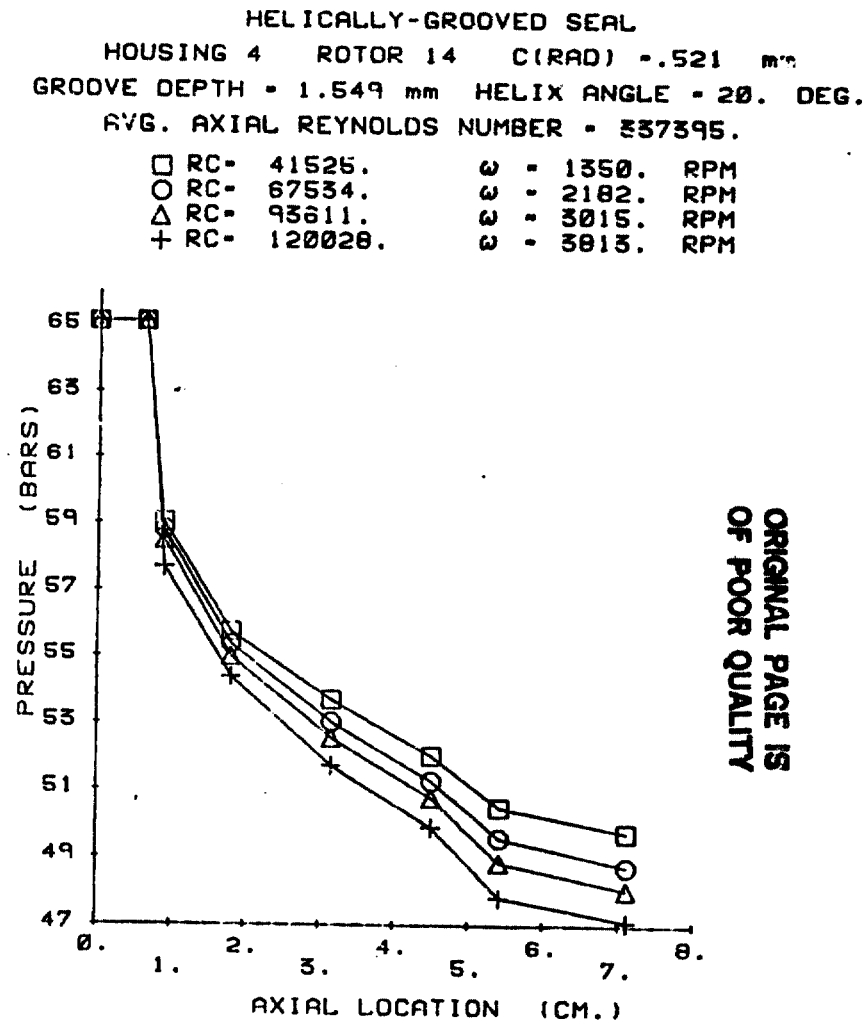

ORIGINAL PAGE IS OF POOR QUALITY

17. Static pressure distributions for seal 2 of rotor 14.

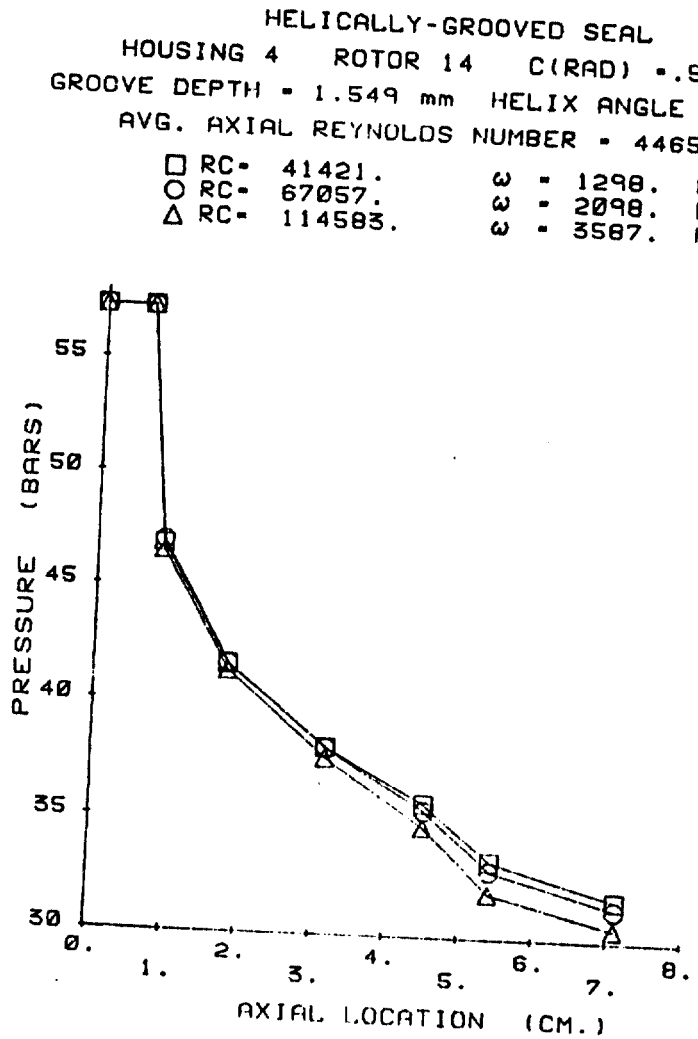

17. Static pressure distributions for seal 2 of rotor 14.

ORIGINAL PAGE IS
OF POOR QUALITY

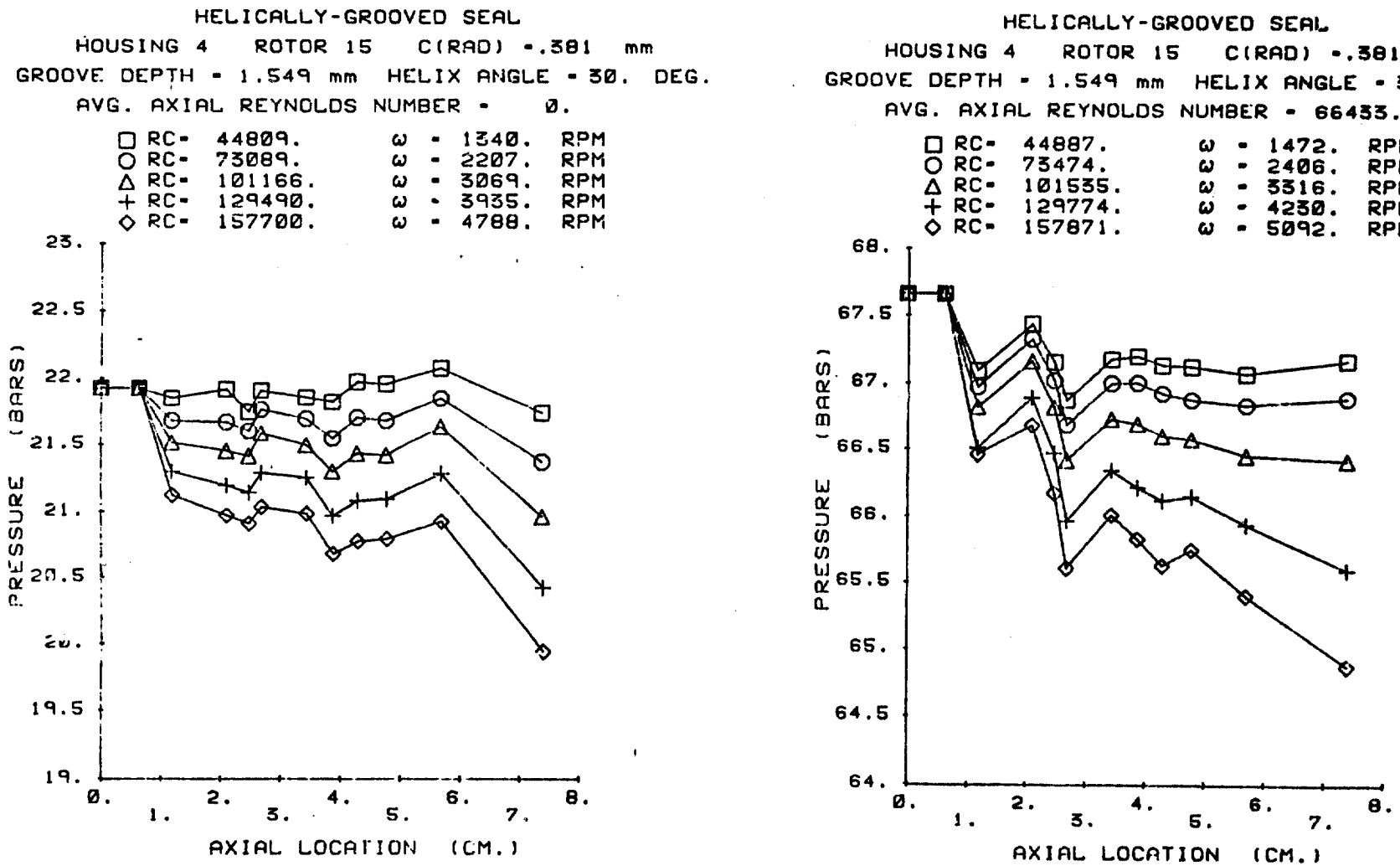

18. Static pressure distributions for seal 1 of rotor 15.

ORIGINAL PAGE IS
OF POOR QUALITY

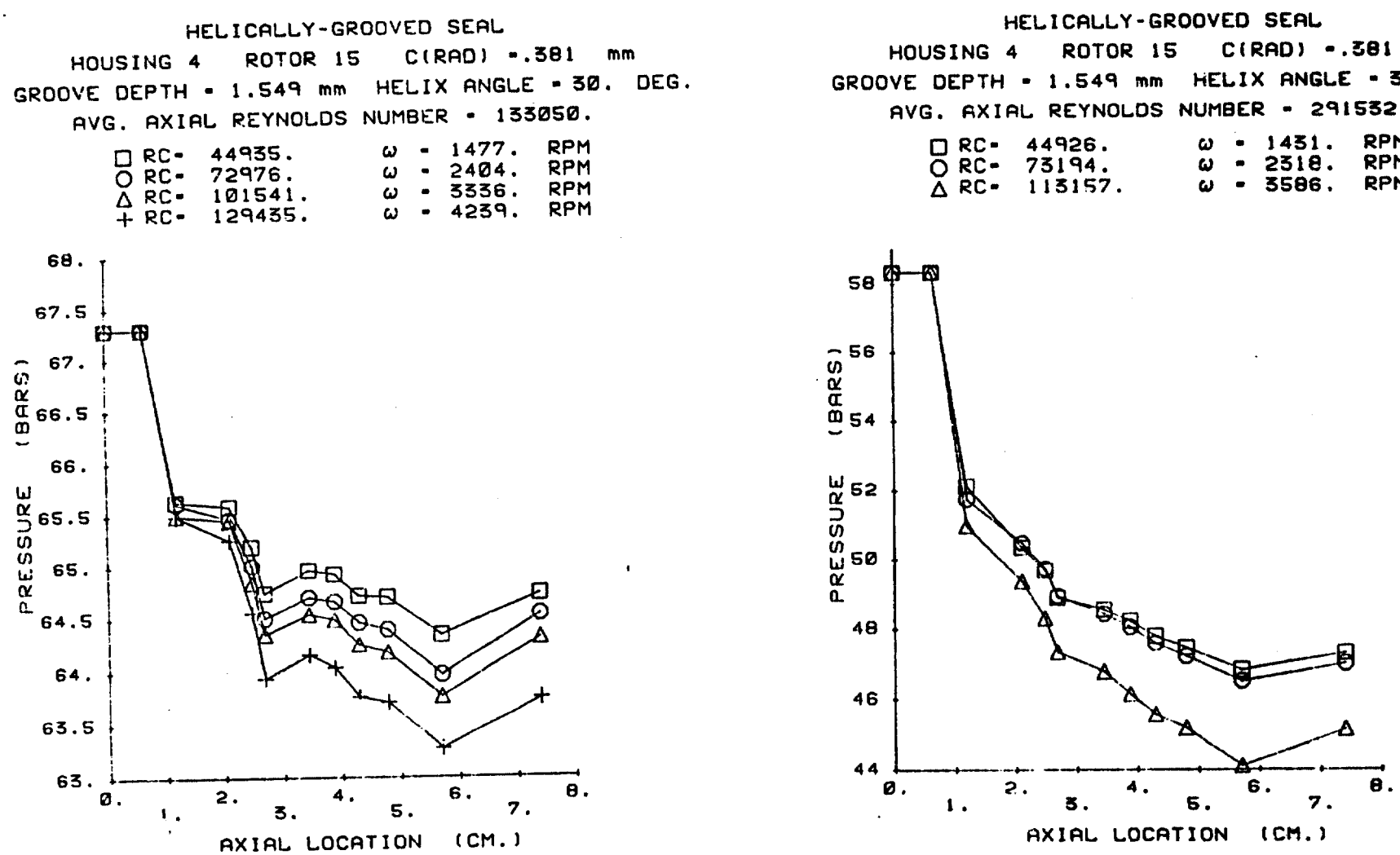

18. Static pressure distributions for seal 1 of rotor 15.

ORIGINAL PAGE IS
OF POOR QUALITY

ORIGINAL PAGE IS
OF POOR QUALITY

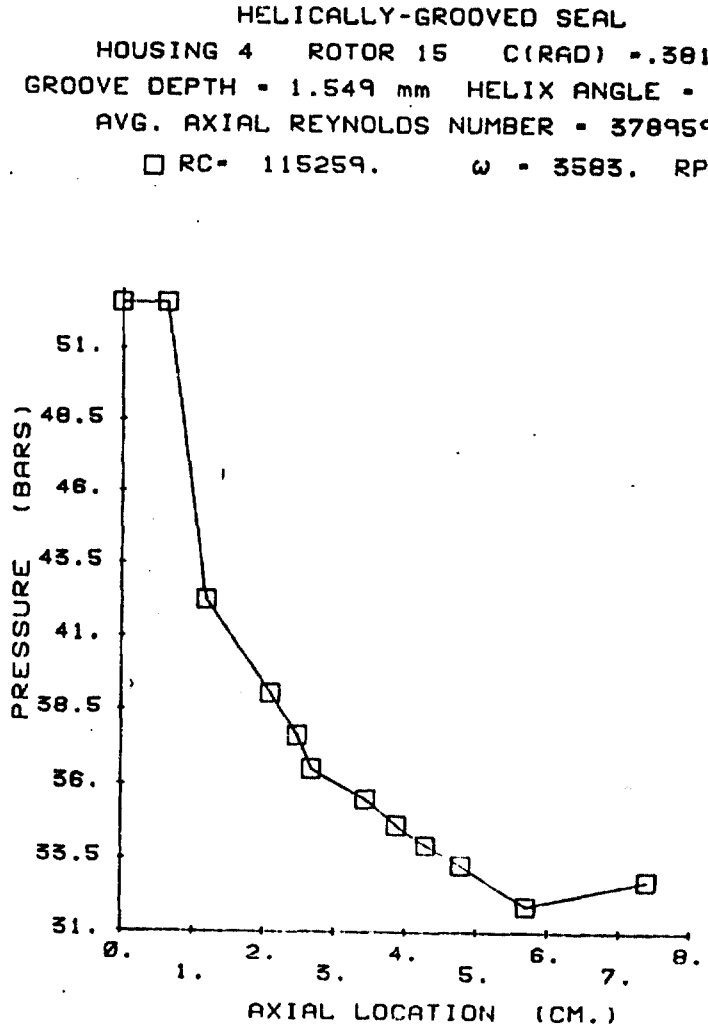

18. Static pressure distributions for seal 1 of rotor 15.

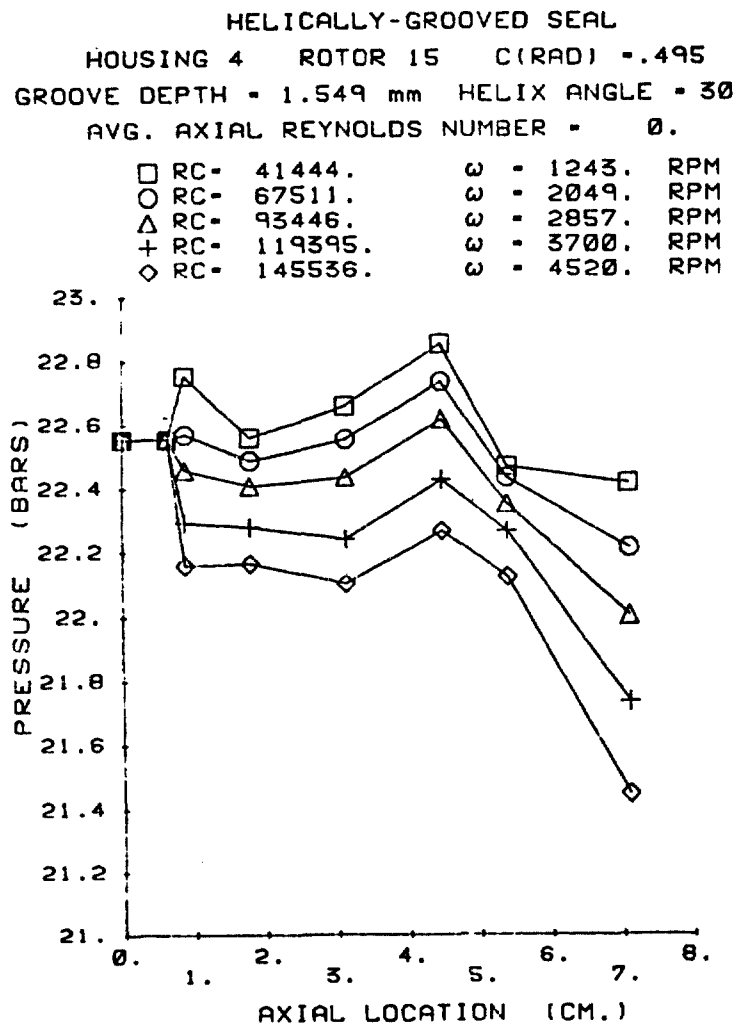

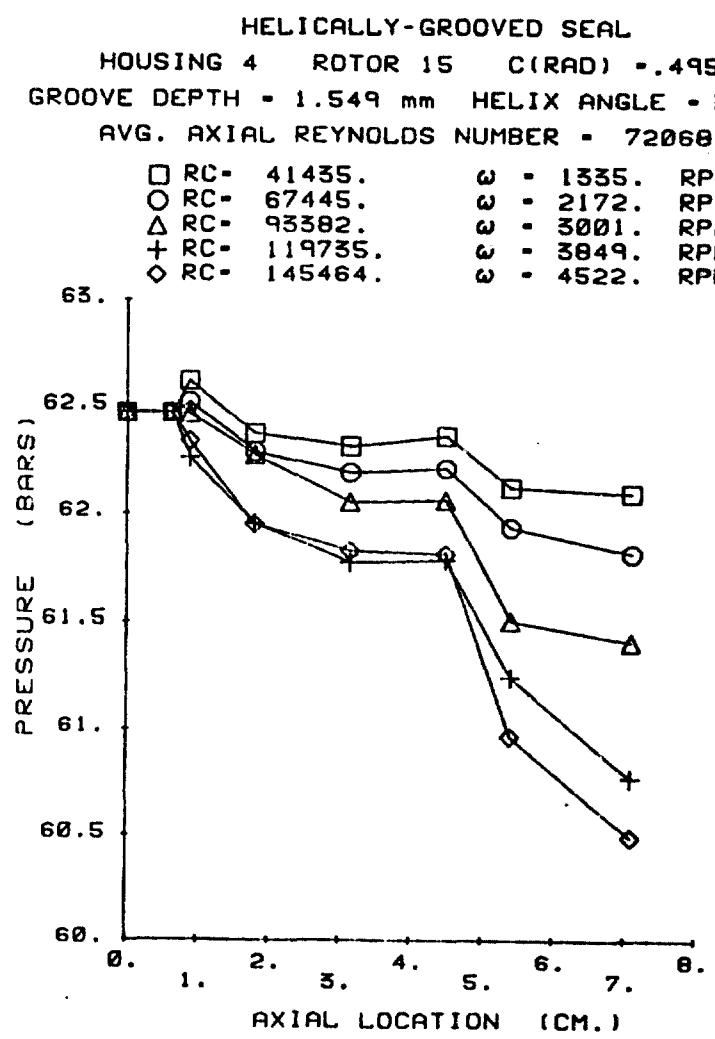

19. Static pressure distributions for seal 2 of rotor 15.

ORIGINAL PAGE IS
OF POOR QUALITY

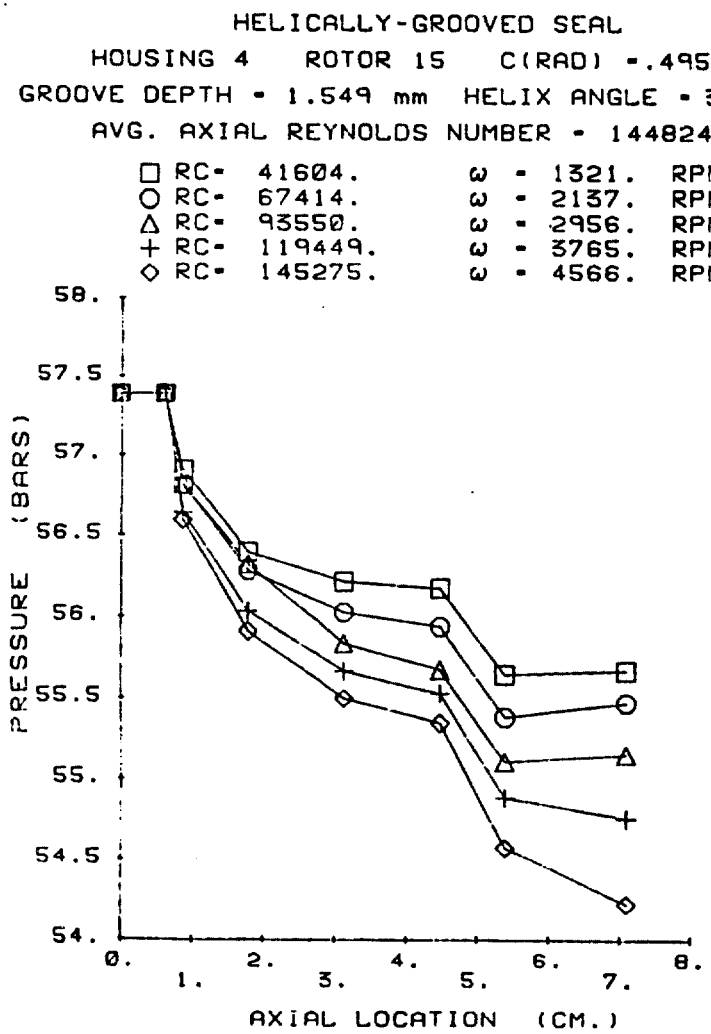

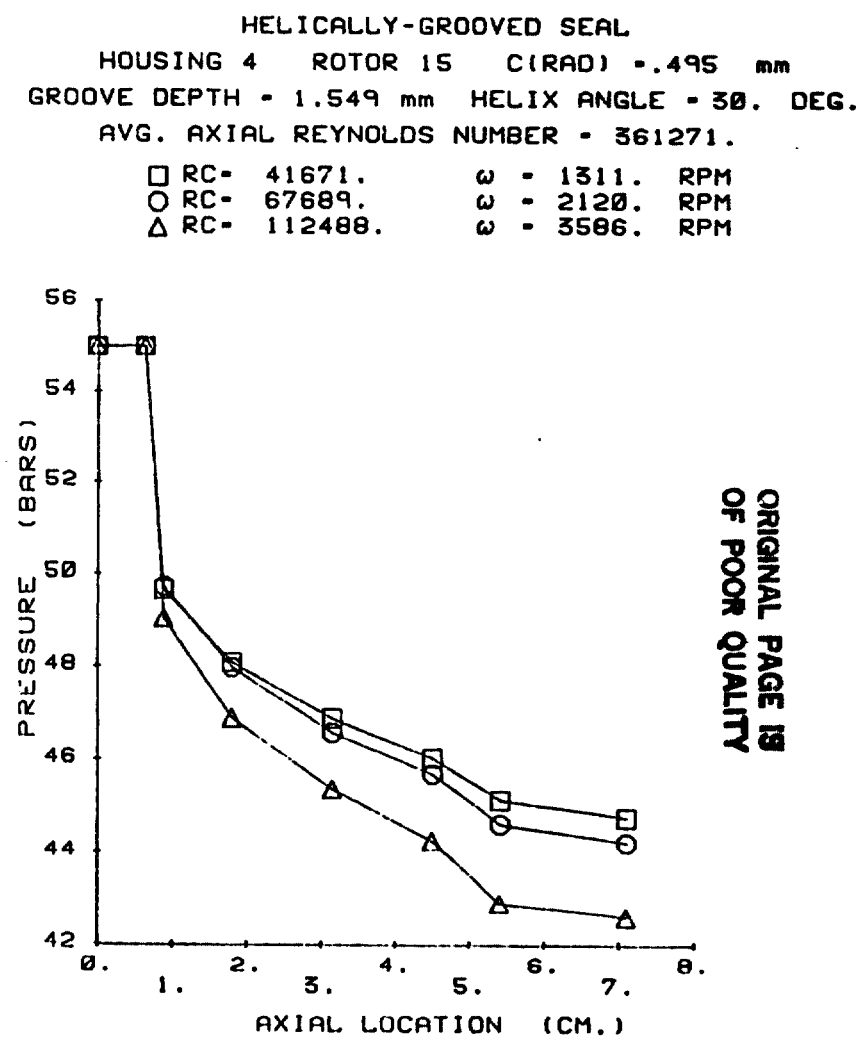

ORIGINAL PAGE IS OF POOR QUALITY

19. Static pressure distributions for seal 2 of rotor 15.

ORIGINAL PAGE IS
OF POOR QUALITY

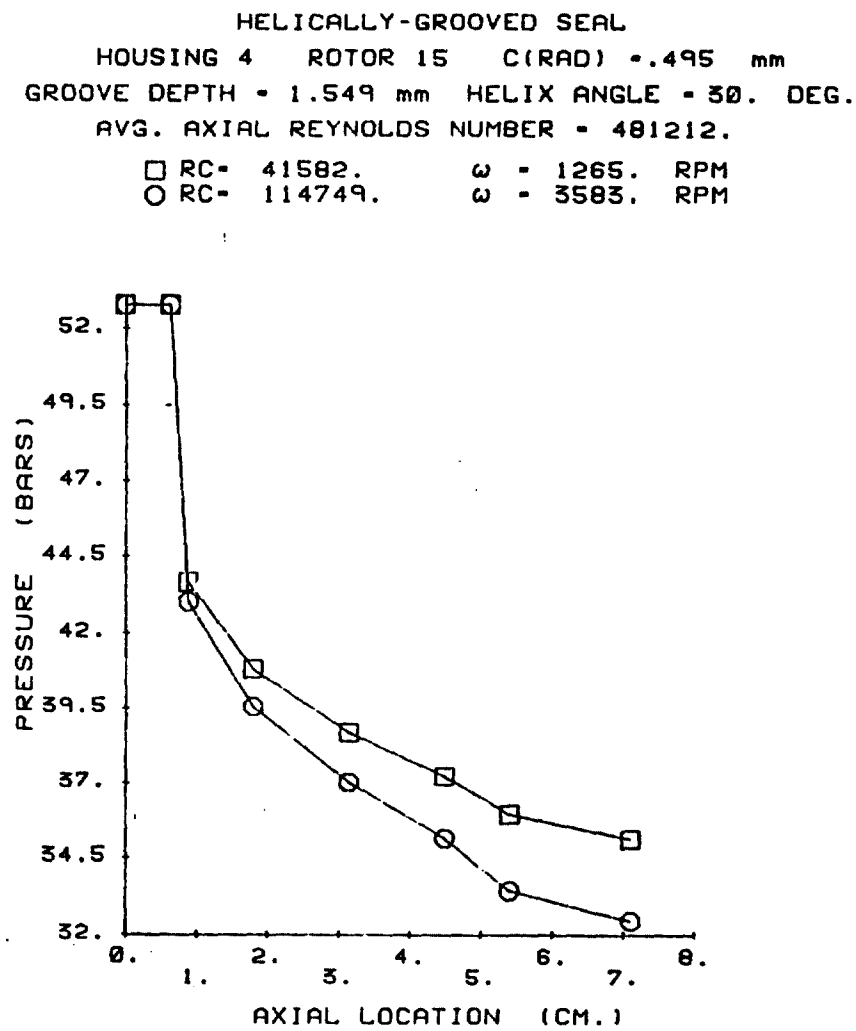

19. Static pressure distributions for seal 2 of rotor 15.

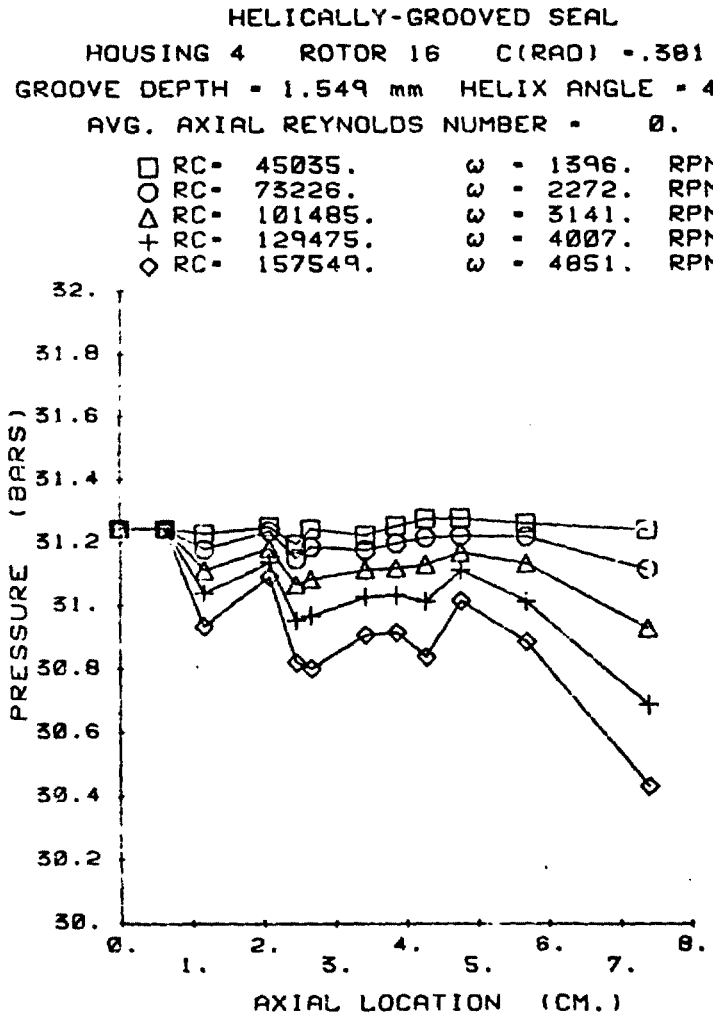

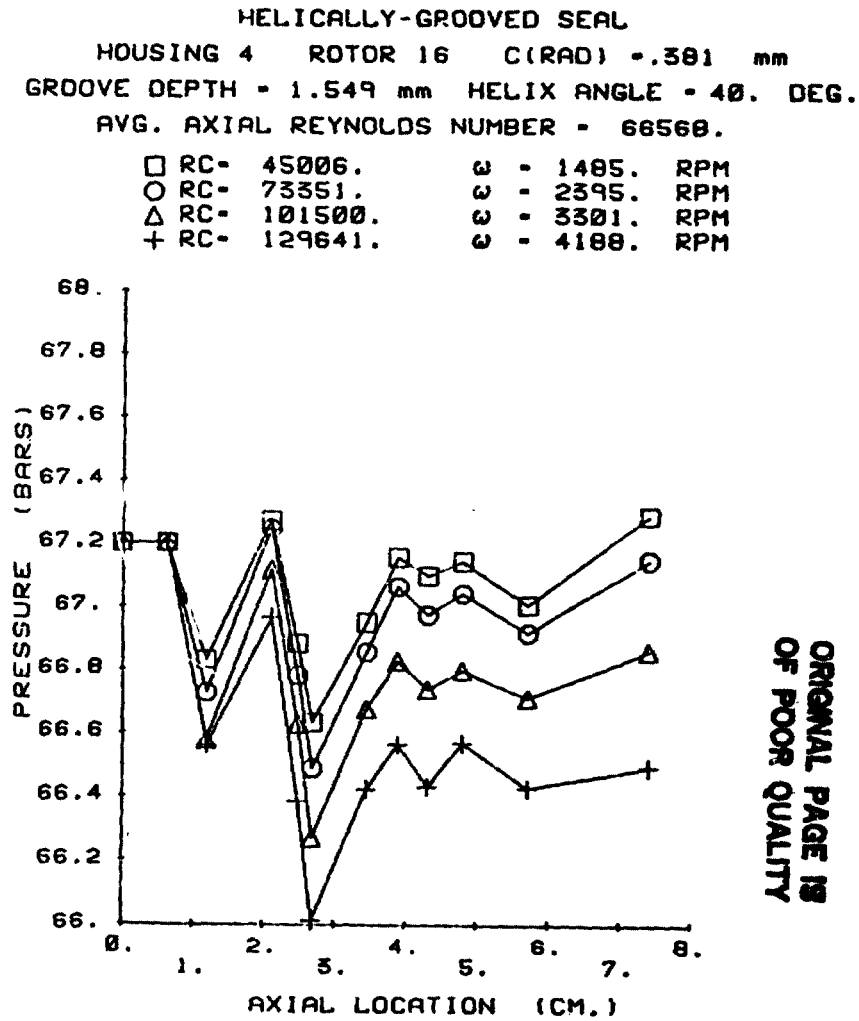

20. Static pressure distributions for seal 1 of rotor 16.

ORIGINAL PAGE IS OF POOR QUALITY

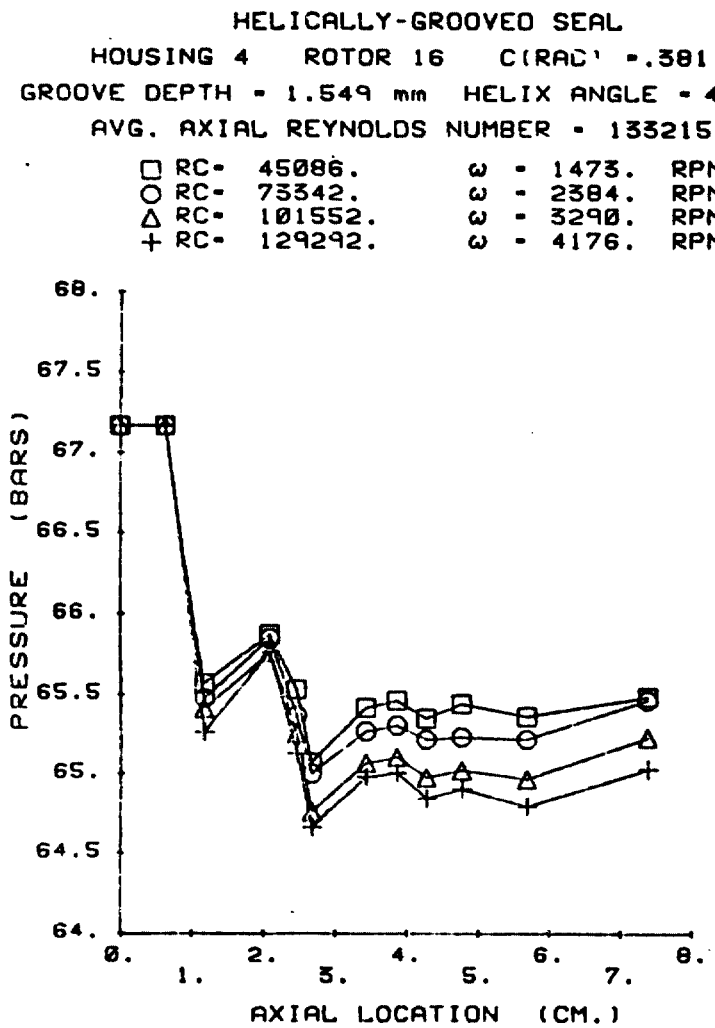

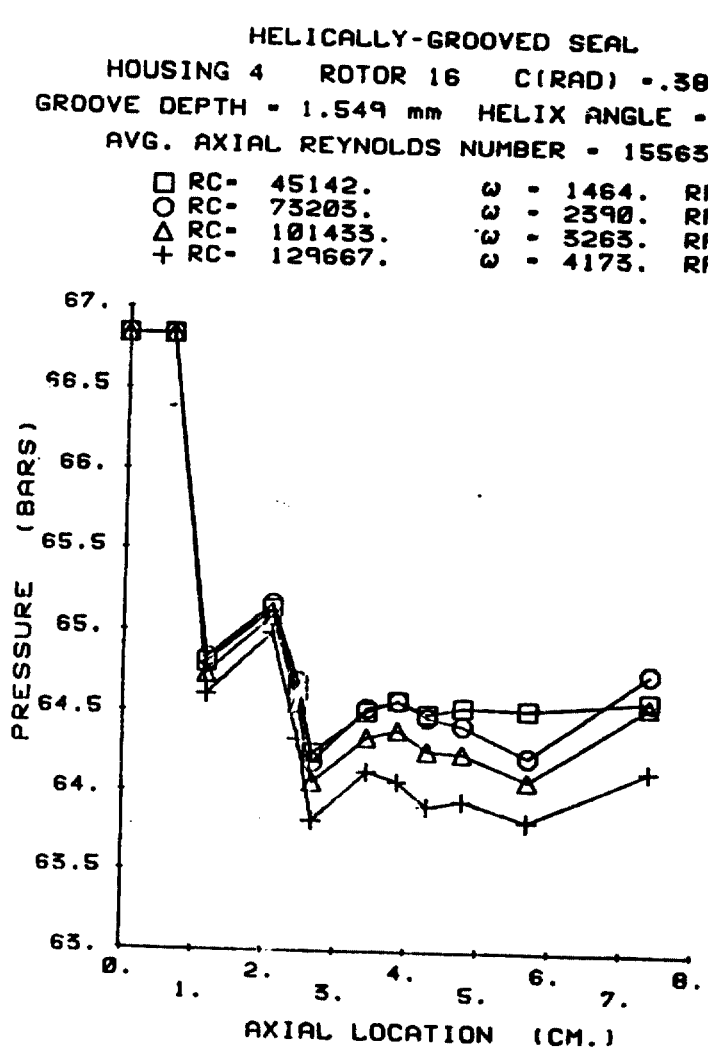

20. Static pressure distributions for seal 1 of rotor 16.

ORIGINAL PAGE IS OF POOR QUALITY

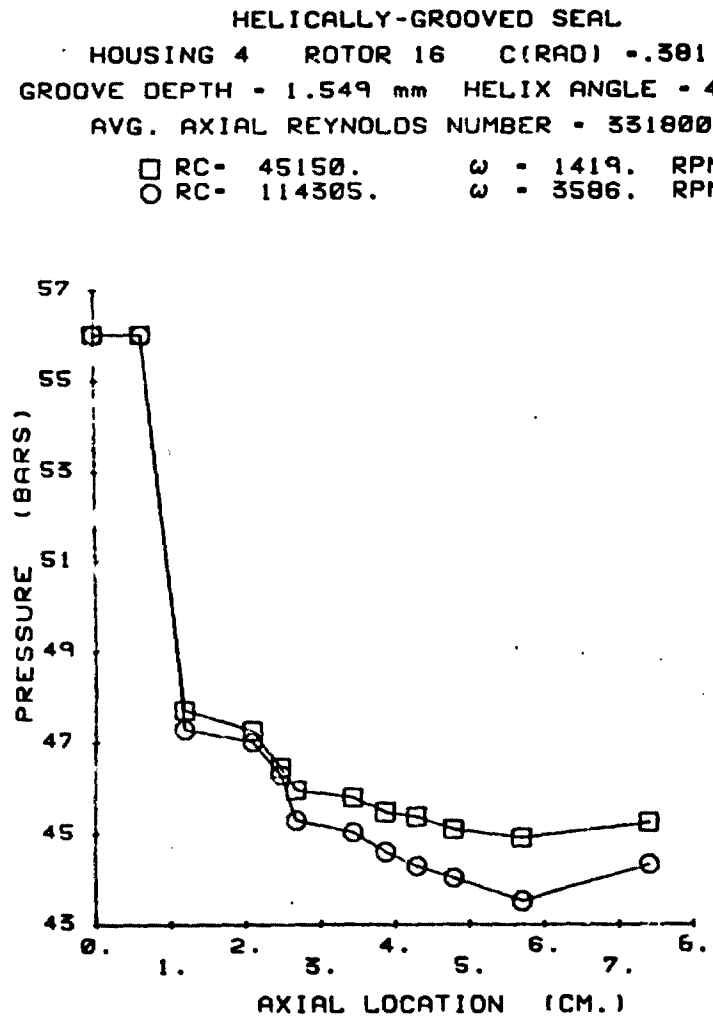

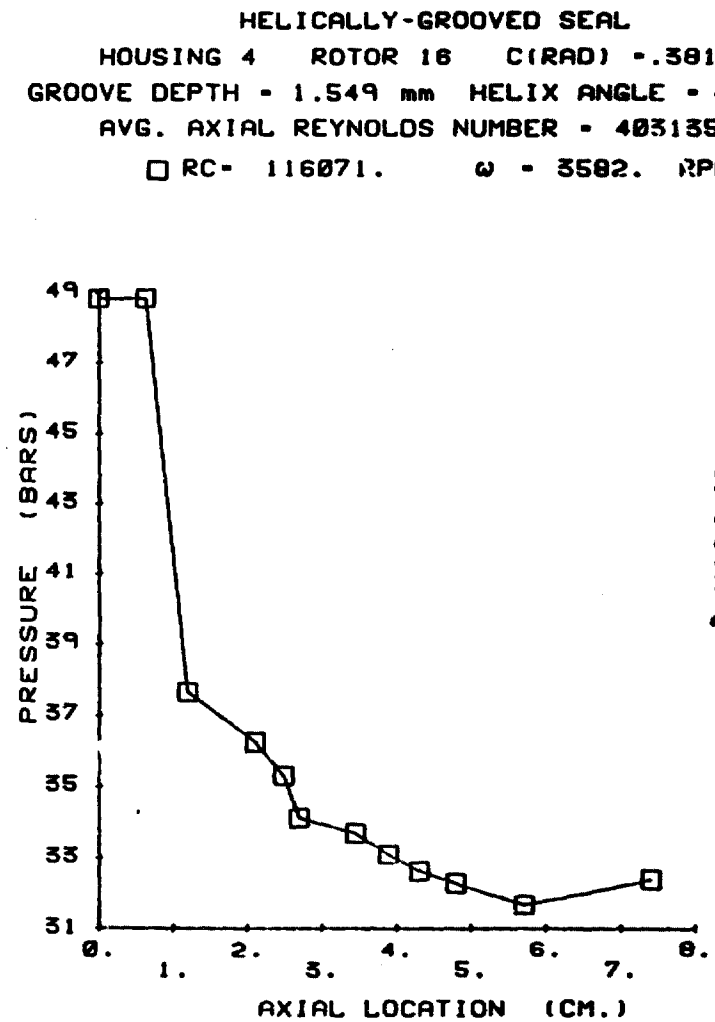

ORIGINAL PAGE IS
OF POOR QUALITY

20. Static pressure distributions for seal 1 of rotor 16.

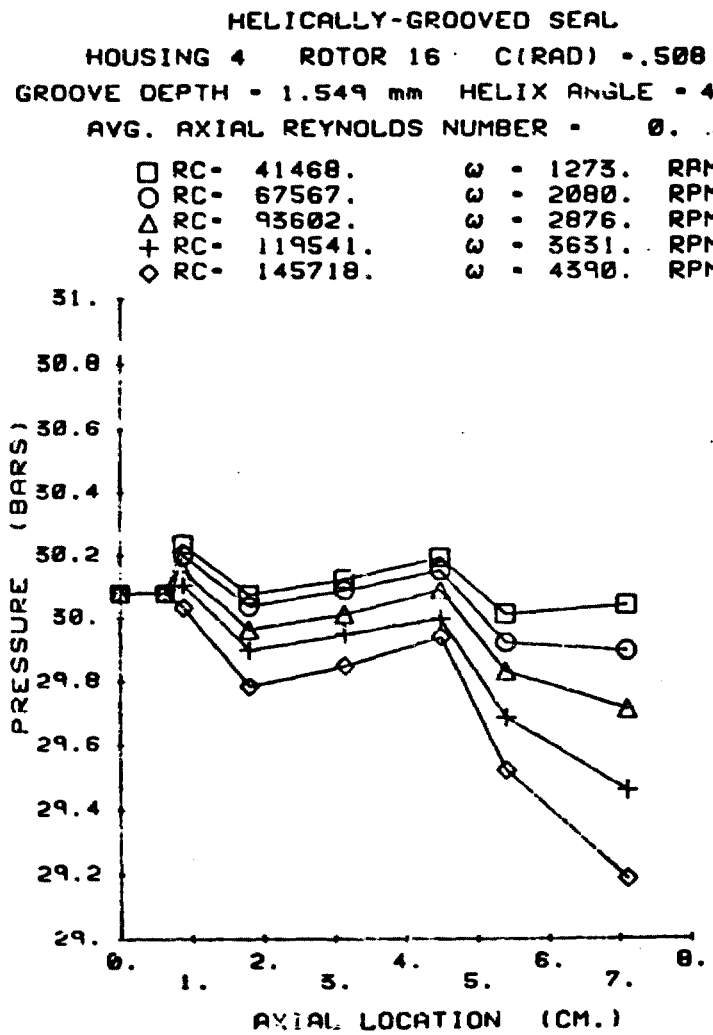

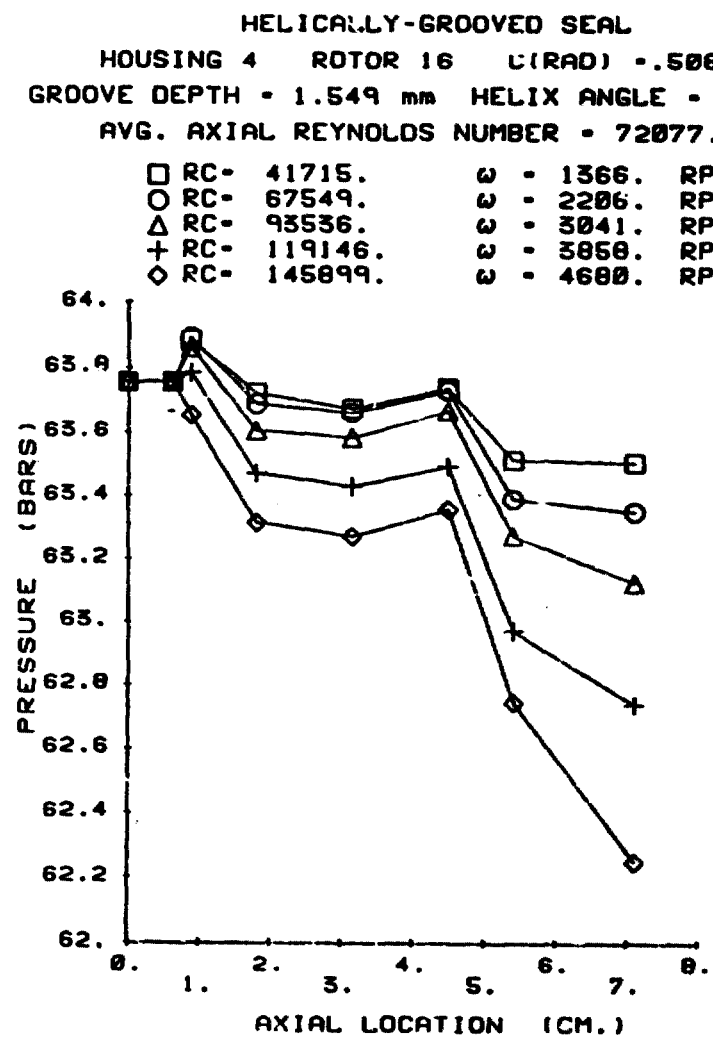

21. Static pressure distributions for seal 2 of rotor 16.

ORIGINAL PAGE IS OF POOR QUALITY

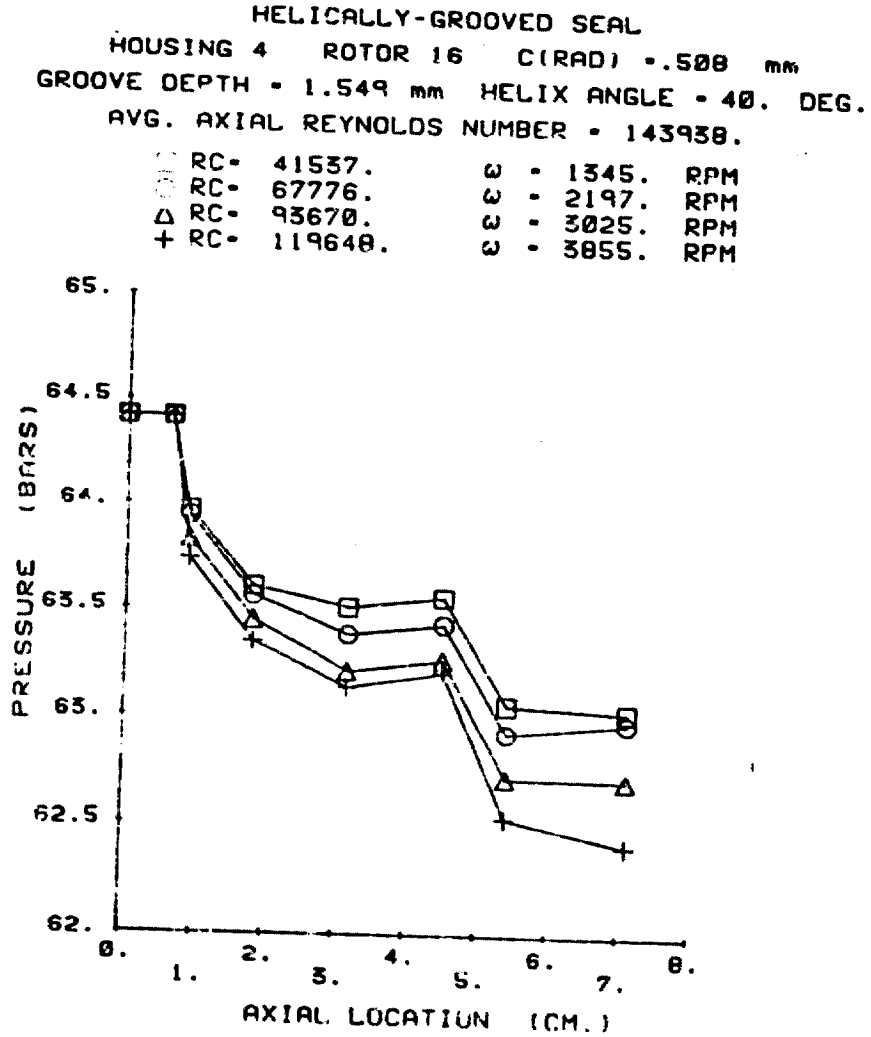

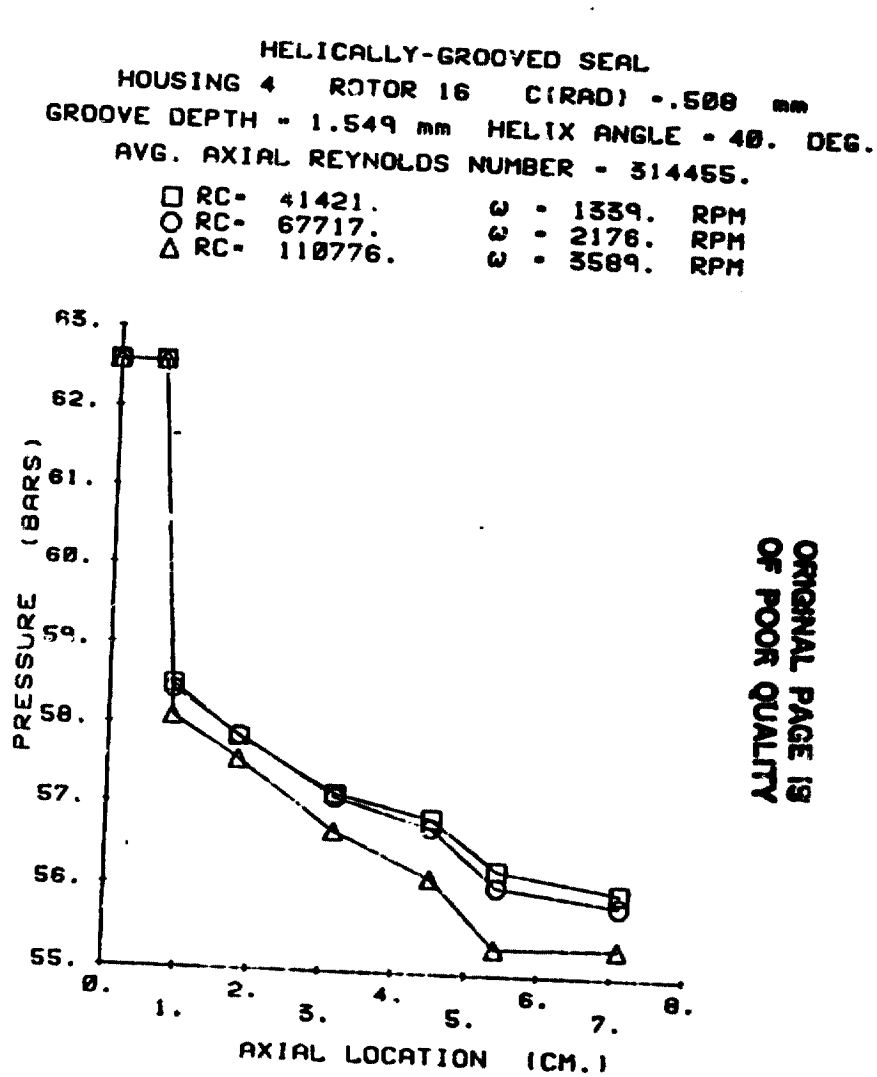

21. Static pressure distributions for seal 2 of rotor 16.

ORIGINAL PAGE IS
OF POOR QUALITY

Pressure-Gradient Coefficients.

For smooth seals, the leakage - ΔP relationship is normally written:

$$\Delta P = \frac{\rho V^2}{2} (1+\xi+2\sigma)$$

The $1+\xi$ coefficients account for entry losses, while σ accounts for the pressure gradient due to wall friction. For plain seals σ is a fairly weak function of the running speed, particularly at high flowrates. The idea of helically-grooved seal is that "pumping action" will increase with increasing running speed. Figures 22 through 30 generally illustrate this characteristic of the helically-grooved seals which were tested. An examination of these figures supports the following conclusions:

(a) σ decreases with increasing taper angles.

(b) For the same axial Reynolds number, σ decreases with increasing groove depth.

(c) The $\frac{d\sigma}{d\omega}$ gradient decreases with increasing values of R_a.

ORIGINAL PAGE IS
OF POOR QUALITY

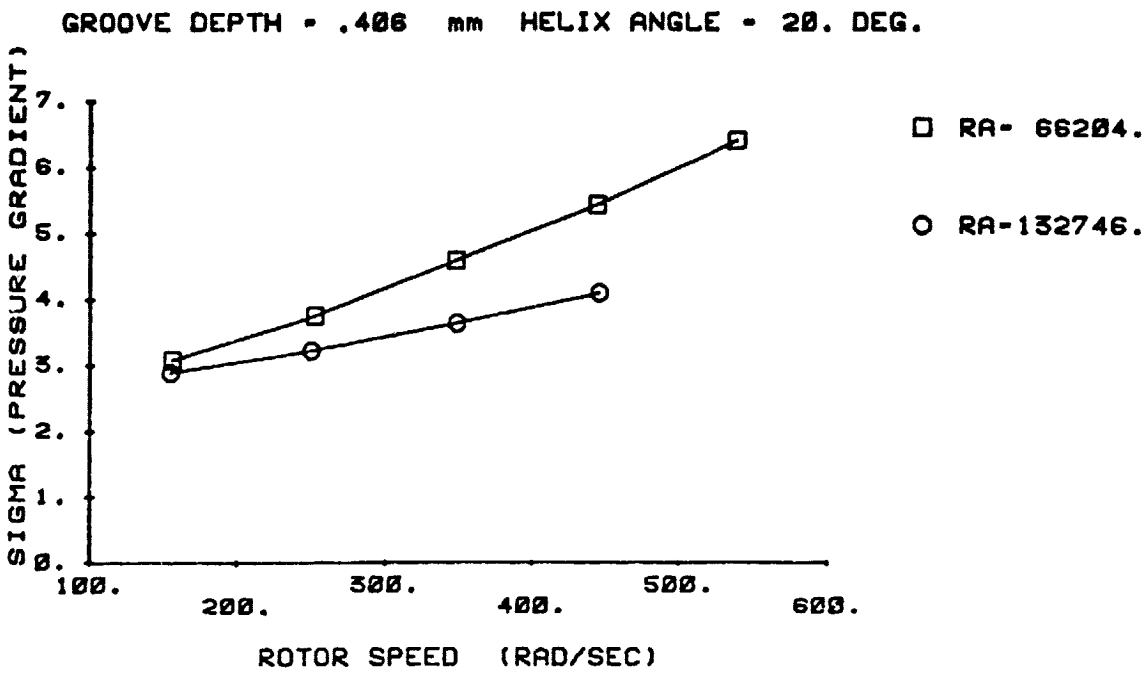

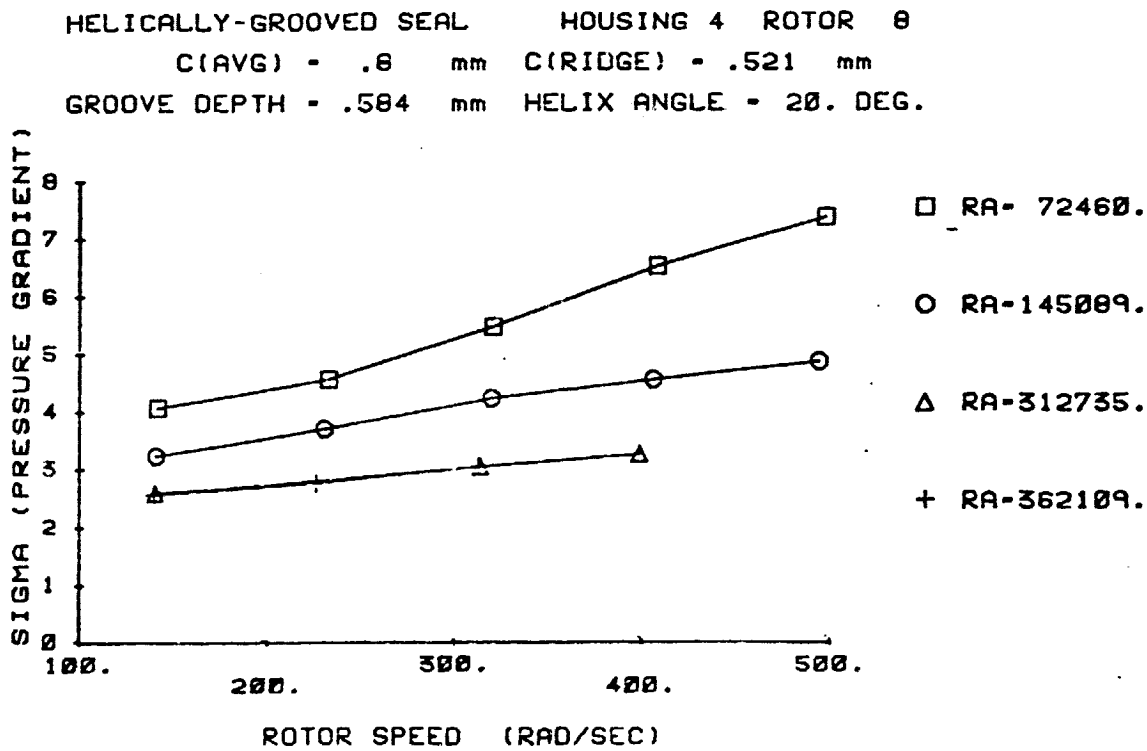

22. Pressure gradient coefficients for seals 1 and 2 of rotor 8.

ORIGINAL PAGE IS
OF POOR QUALITY

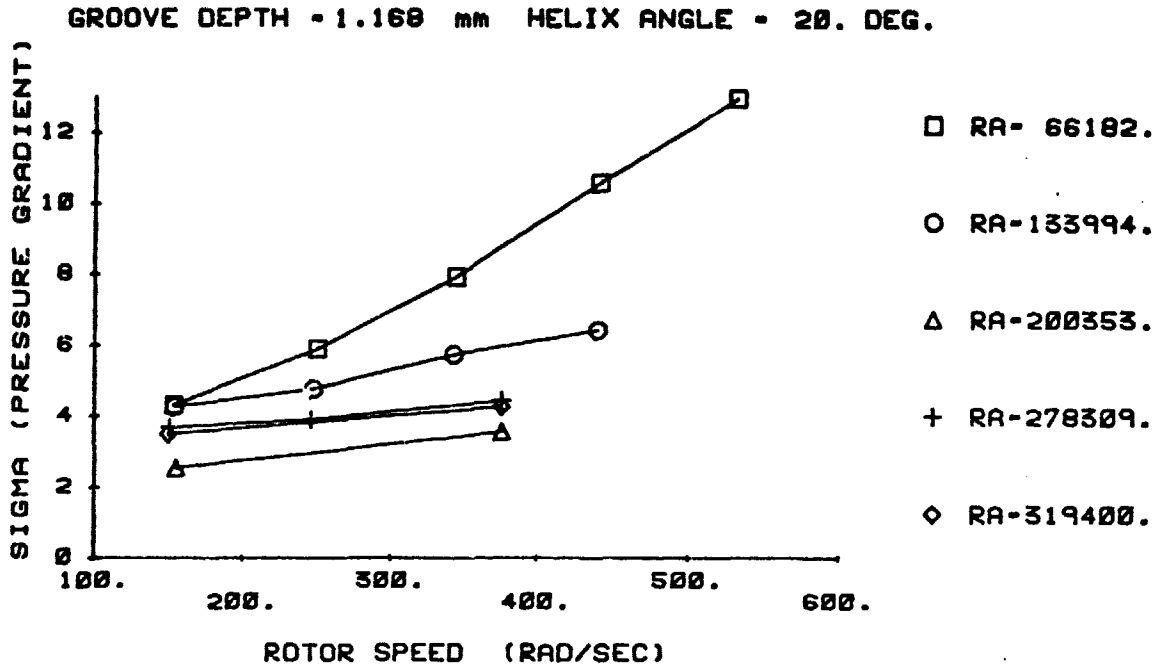

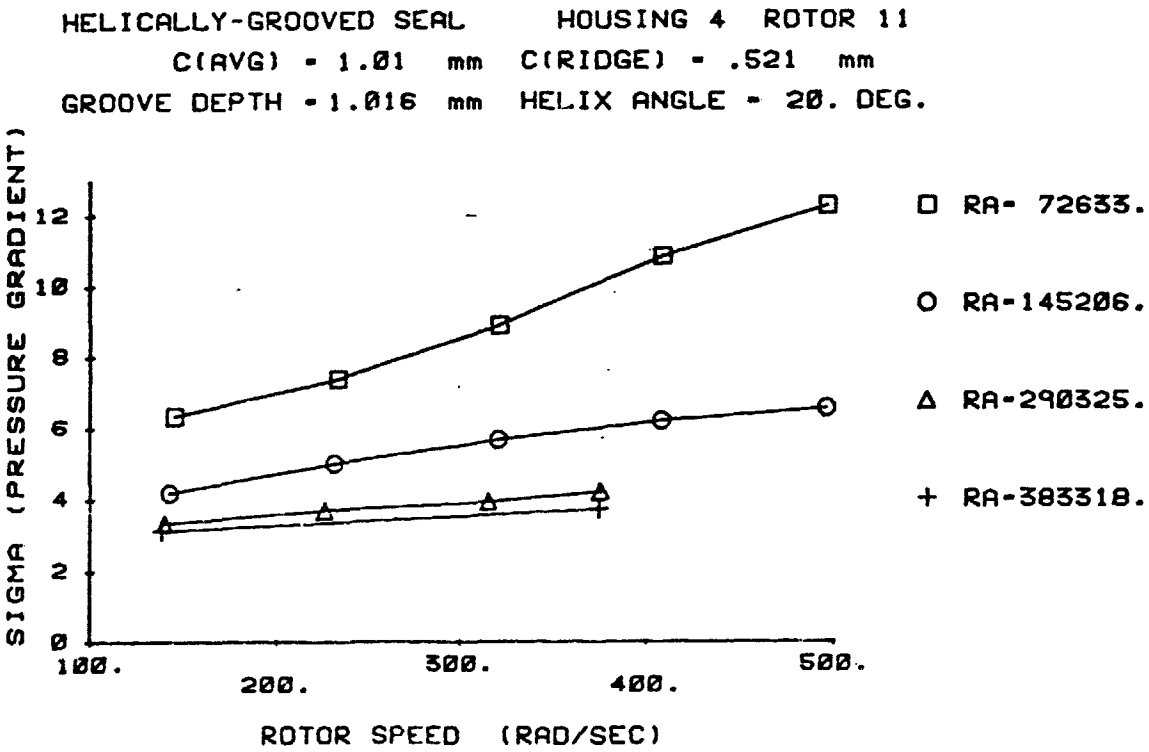

23. Pressure gradient coefficients for seals 1 and 2 of rotor 11.

ORIGINAL PAGE IS
OF POOR QUALITY

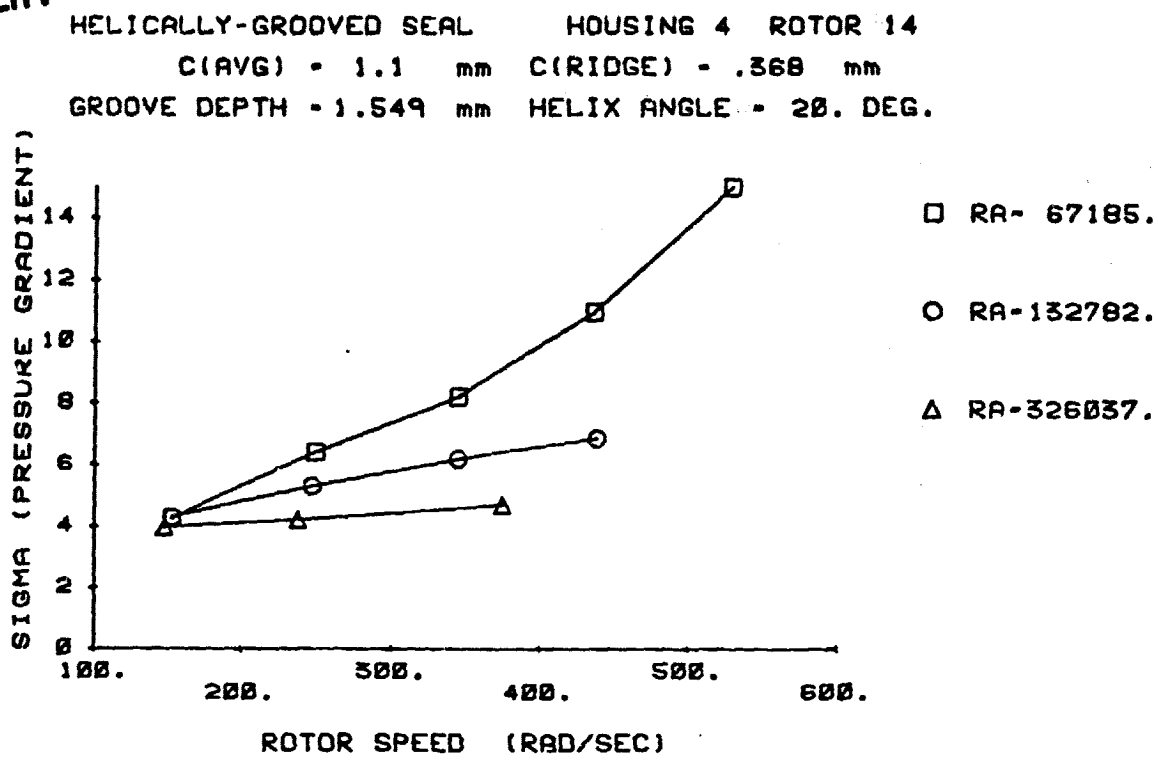

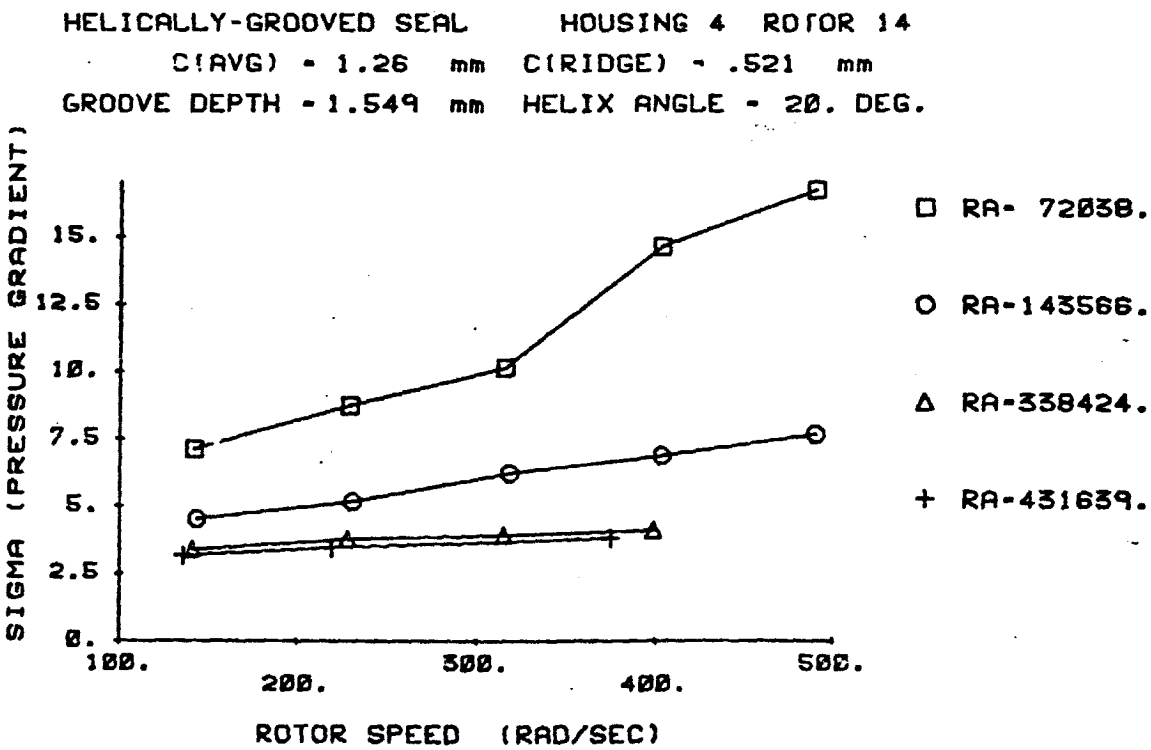

24. Pressure gradient coefficients for seals 1 and 2 of rotor 14.

ORIGINAL PAGE IS
OF POOR QUALITY

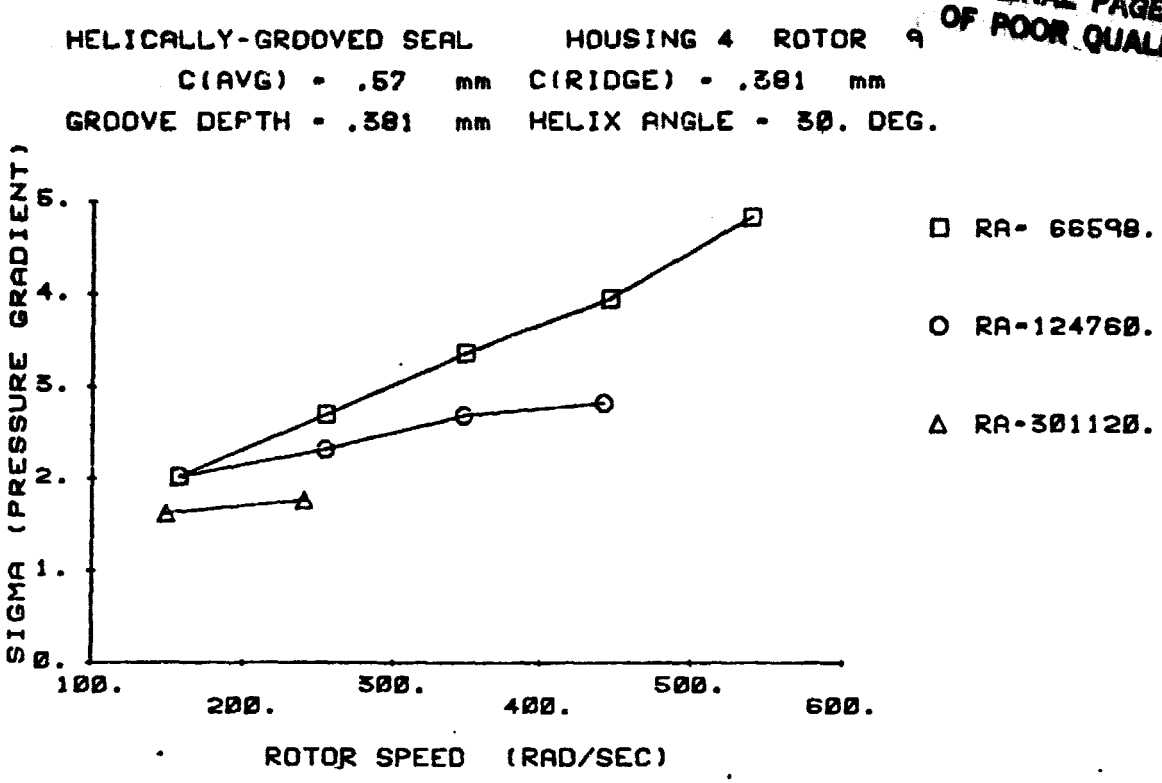

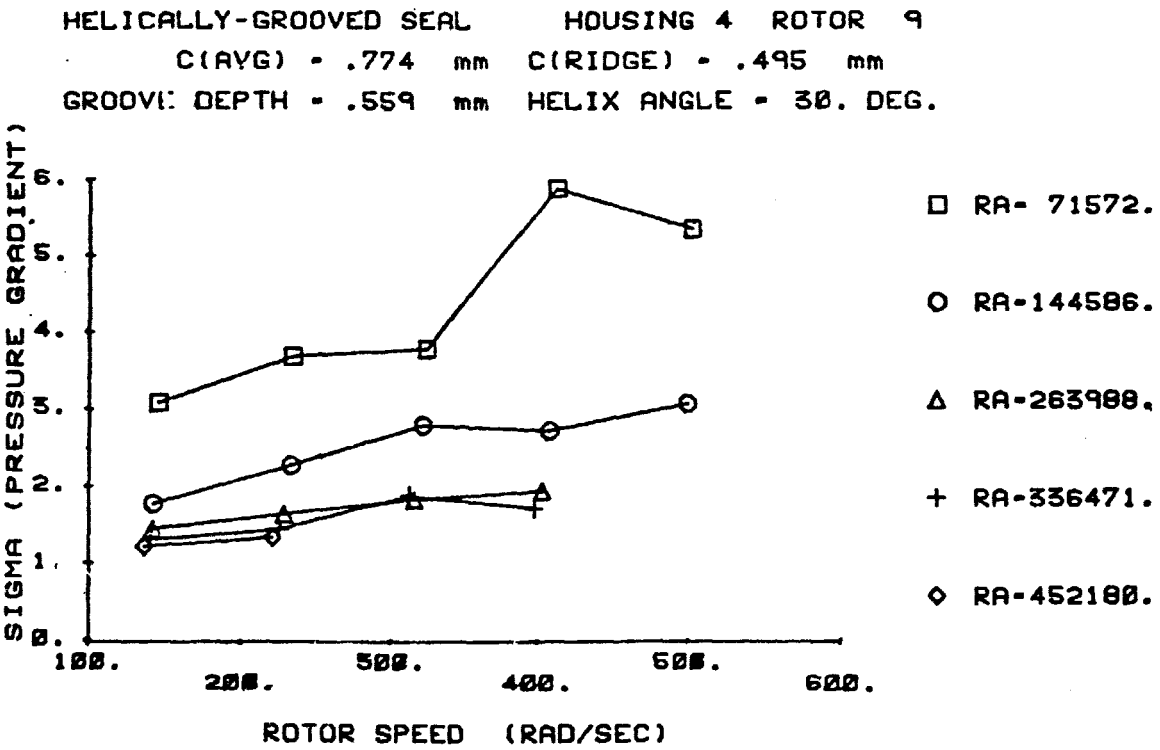

25. Pressure gradient coefficients for seals 1 and 2 of rotor 9.

ORIGINAL PAGE IS
OF POOR QUALITY

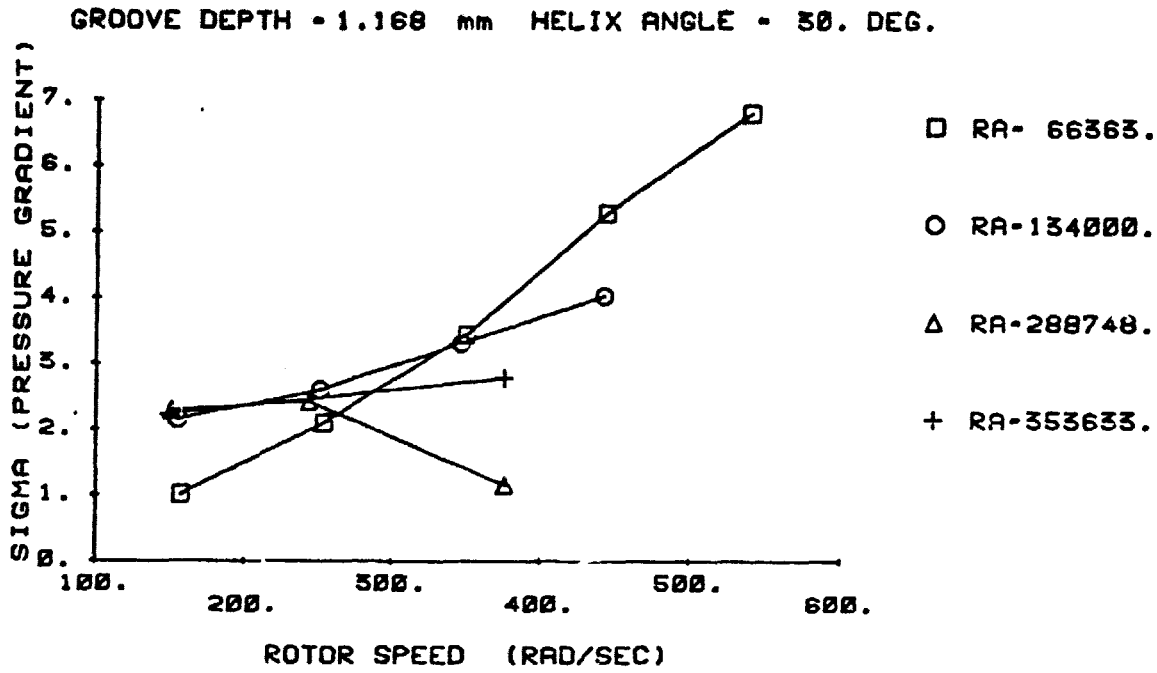

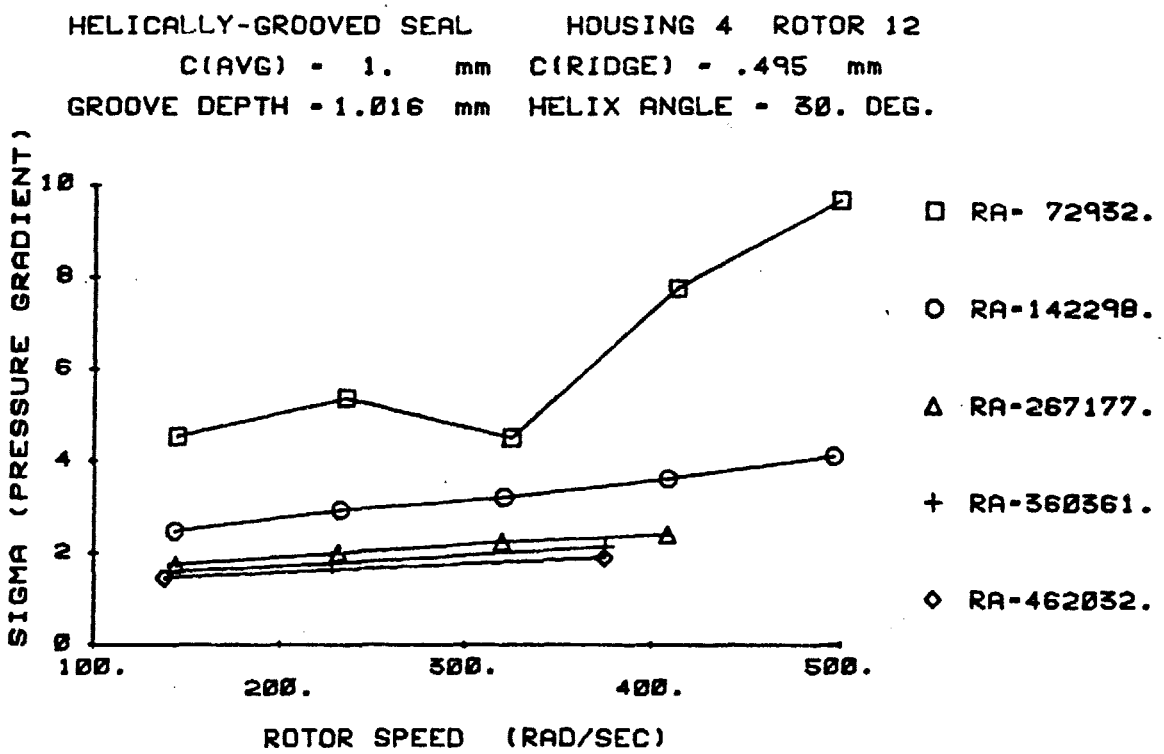

26. Pressure gradient coefficients for seals 1 and 2 of rotor 12.

ORIGINAL PAGE IS
OF POOR QUALITY

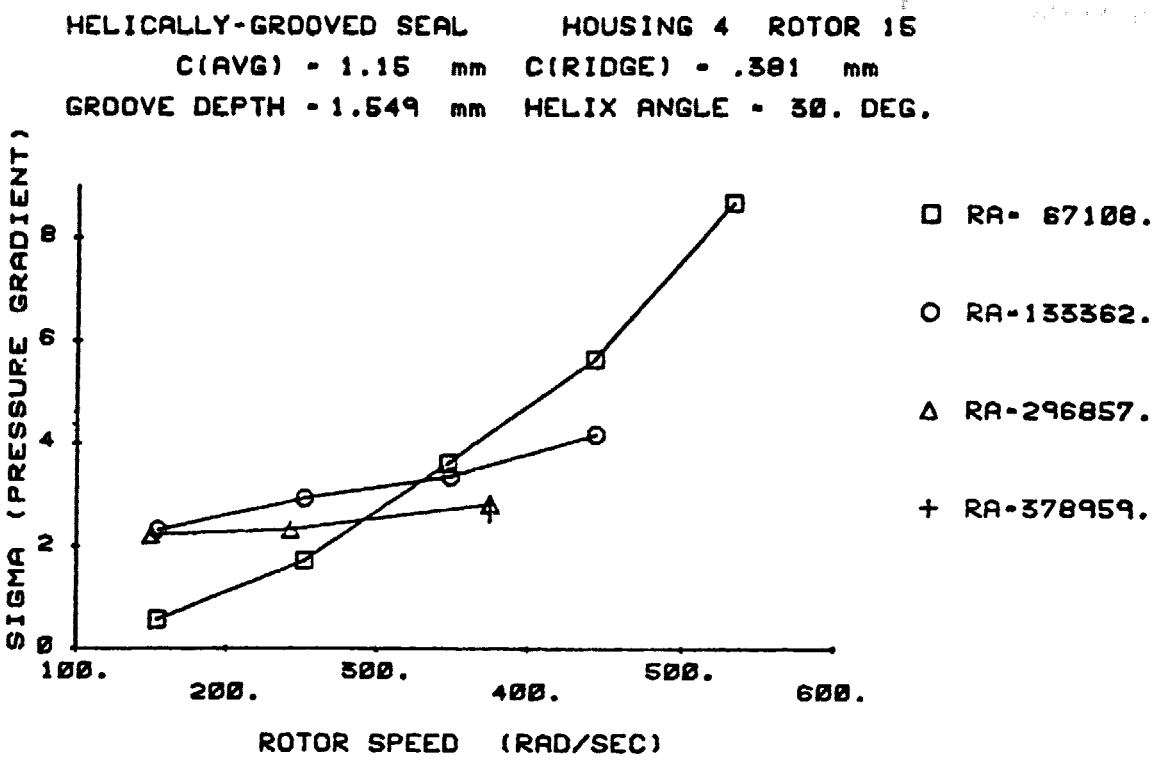

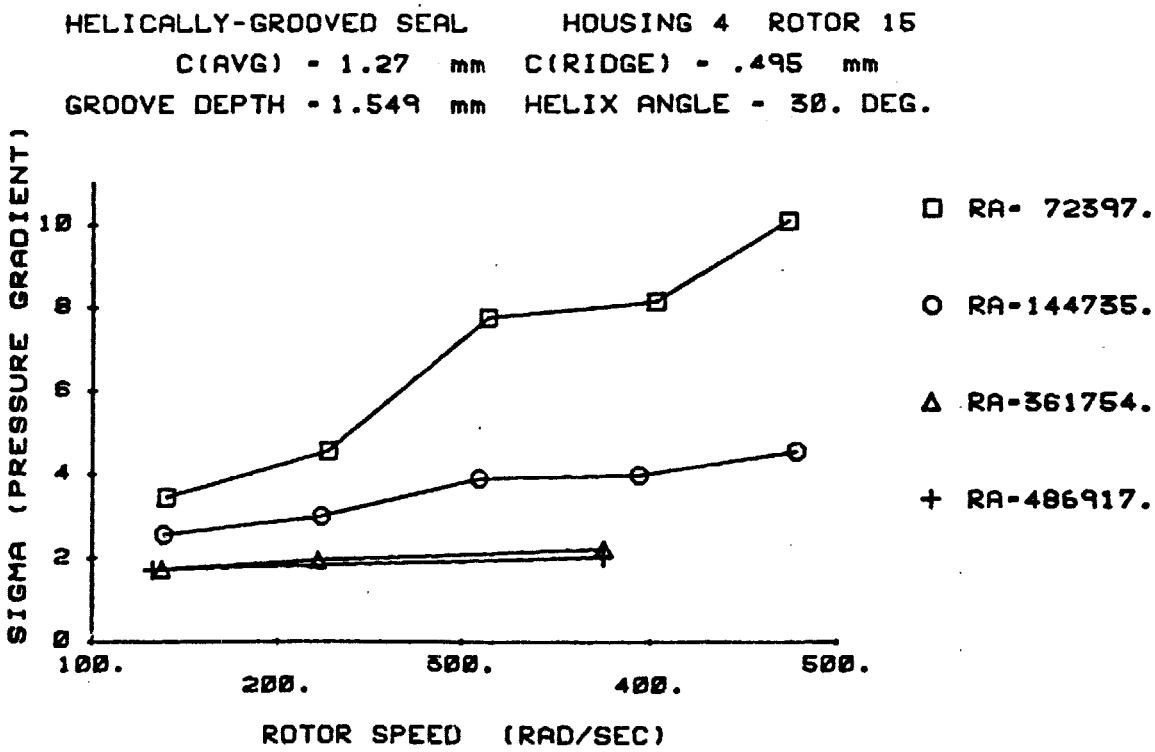

27. Pressure gradient coefficients for seals 1 and 2 of rotor 15.

ORIGINAL PAGE IS
OF POOR QUALITY

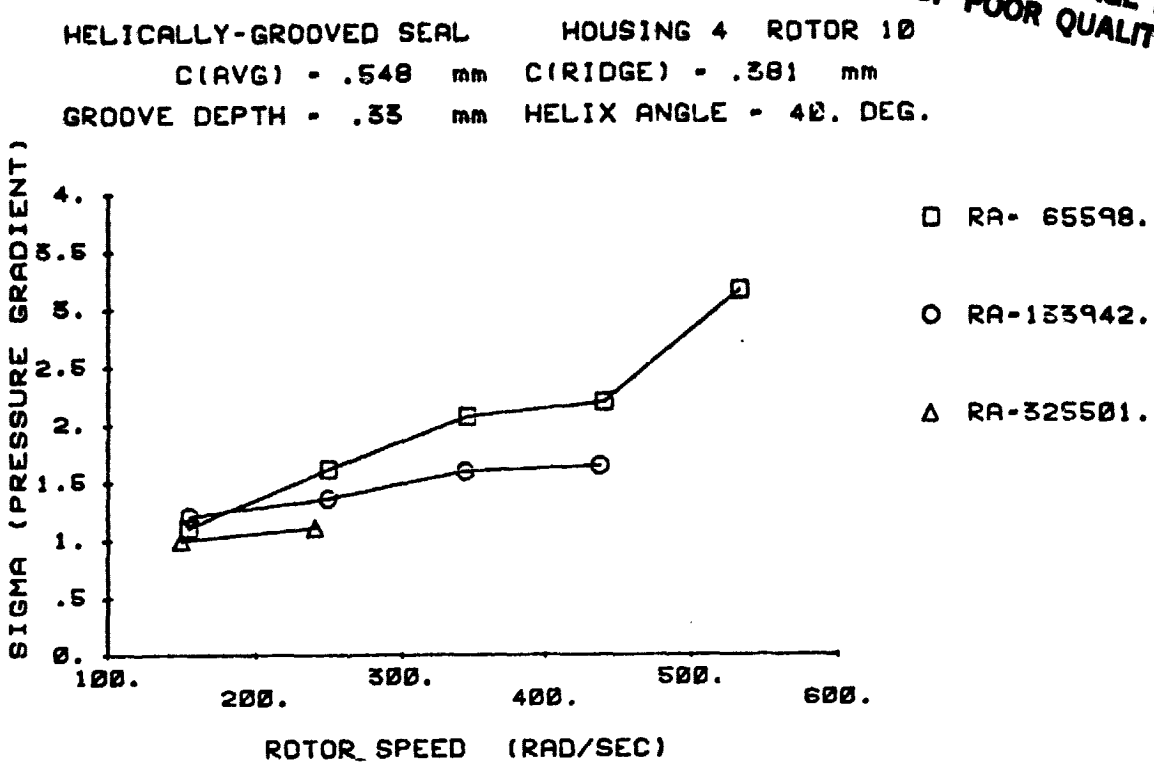

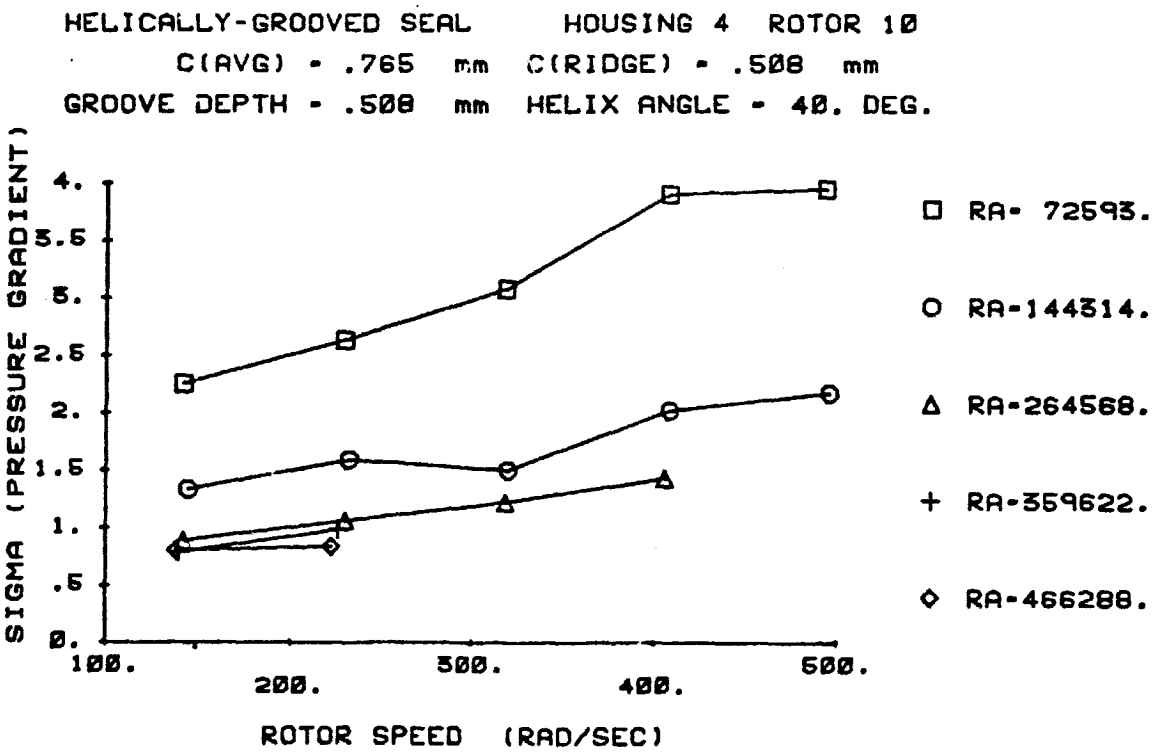

28. Pressure gradient coefficients for seals 1 and 2 of rotor 10.

ORIGINAL PAGE IS
OF POOR QUALITY

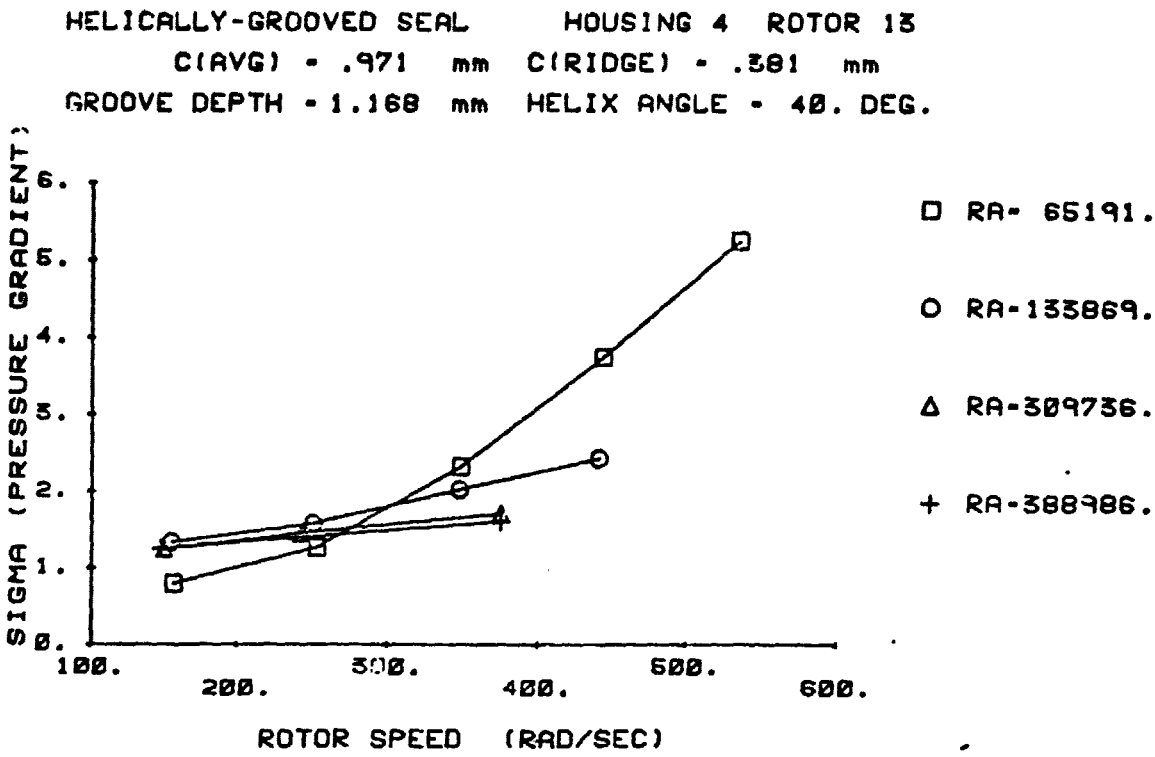

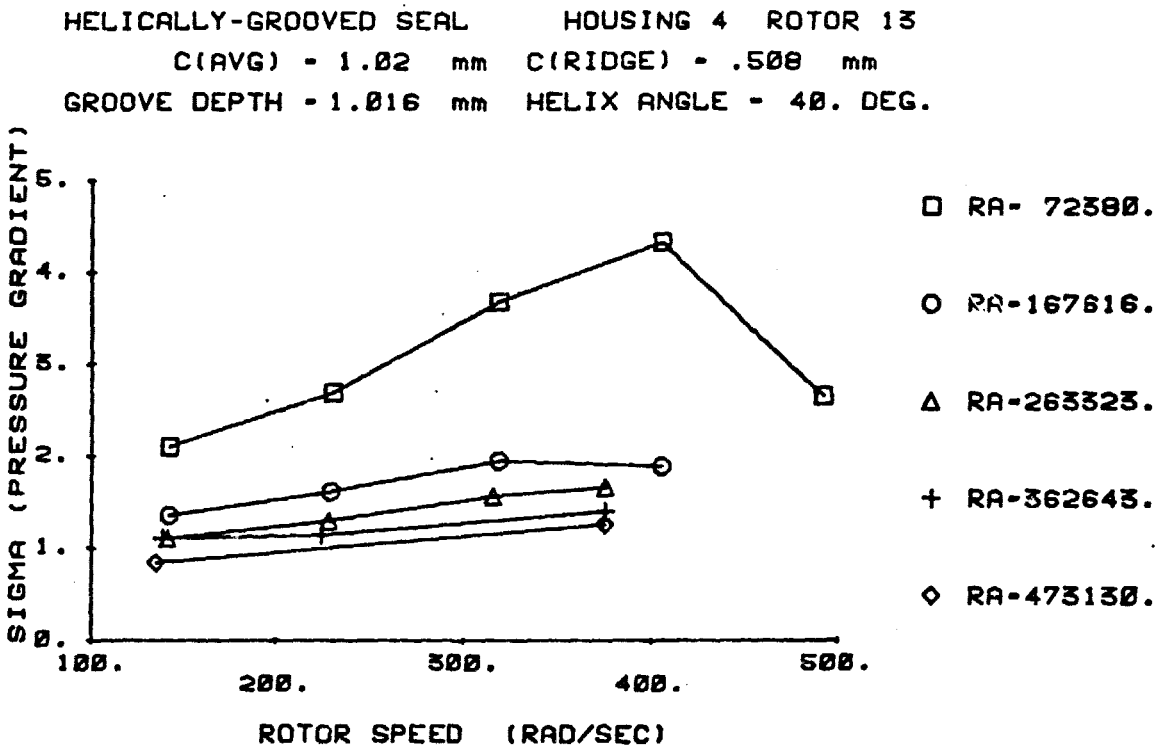

29. Pressure gradient coefficients for seals 1 and 2 of rotor 13.

ORIGINAL PAGE IS
OF POOR QUALITY

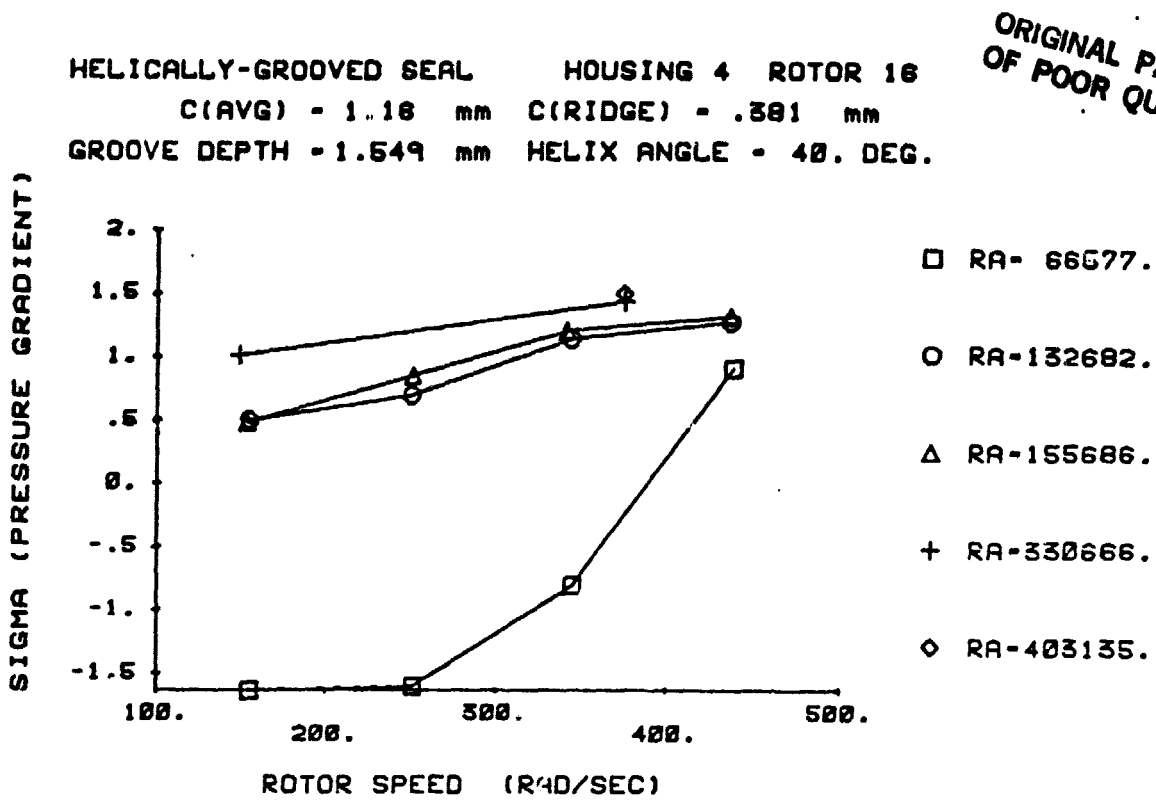

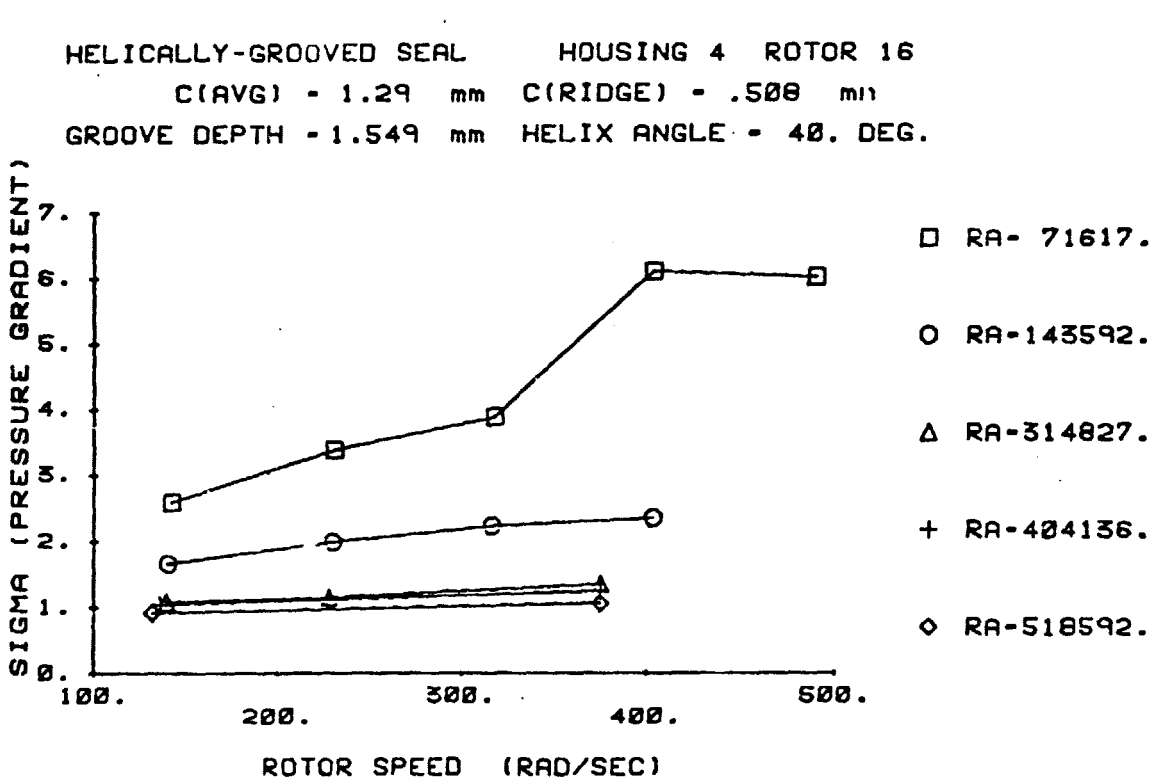

30. Pressure gradient coefficients for seals 1 and 2 of rotor 16.

ORIGINAL PAGE IS
OF POOR QUALITY

Leakage Performance

Generally speaking, leakage characteristics of seals are given in terms of a discharge coefficient C_d defined by

$$\Delta P = C_d \frac{\rho V^2}{2} \tag{1}$$

Hence the volumetric leakage rate is

$$\begin{aligned} Q = VA &= C_d^{-1/2}\left(\frac{2\Delta P}{\rho}\right)^{1/2} (2\pi RC) \\ &= C_d^{-1/2}\left(\frac{C}{R}\right) \cdot 2\pi R \left(\frac{2\Delta P}{\rho}\right)^{1/2} \end{aligned} \tag{2}$$

Where C is the average clearance and V is the average resultant velocity. The "leakage coefficient" C_L defined by

$$C_L = C_d^{1/2} \left(\frac{C}{R}\right) \tag{3}$$

is a measure of the leakage to be expected in a seal if the radius is held constant and the clearance is varied. For a plain seal, the leakage coefficient is relatively insensitive to changes in running speed. However, the pumping action provided by helically-grooved seals should yield an increase in resistance with running speed, i.e., a decrease in leakage. Figures 31 through 39 illustrate C_L for all seal configurations which were tested. The upper and lower frames of these figures correspond, respectively, to seal 1 (C_r = .368 mm = 15 mils) and seal 2 (C_r = .521 mm = 20 mils). The average clearance used in calculating the average velocity, axial Reynolds numbers, etc. are given in the figure heading.

Figure 31 is representative of the test results and demonstrates the following results:

(a) Leakage decreases with increasing running speed.

(b) Leakage reduction due to increasing running speed is greater at lower values for R_a.

(c) An asymptote for leakage is indicated with increasing running speed.

(d) Leakage is reduced by reducing the ridge (minimum) and average clearances.

The following additional conclusions are supported by an examiniation and comparison of all the results of figures 31 through 39:

(a) Leakage increases with increasing pitch angles.

(b) Leakage increases with increasing groove depth.

The best leakage performance is provided by seal 1 (C_r = .368 mm) with a 20° pitch angle and a .406 mm groove depth.

The seal 2 ridge clearance of .521 mm (20 mils) is the same as the clearances used earlier in plain seals; hence, its leakage performance may be compared directly to prior seal tests. From [6], the results of earlier tests at maximum flow conditions are repeated in table 3, and show a range of $C_L x10^3$ from 4 to 6.86, depending upon rotor and stator surface roughnesses. By comparison, the higher Reynolds number results for seal 2 (C_r = .521 mm) yield $C_L x10^3 \cong 4.8$. This value is comparable to the smooth-rotor/rough-housing results of table 3. Based on these results, one would conclude that the leakage performance of a 20°-pitch-angle helically-grooved seal, with approximately equal ridge clearance and groove depths, is comparable to a plain seal with either a roughened rotor or stator. Plain seals with smooth rotors and stators will leak more than a properly designed helically-grooved seals. Plain seals with roughened rotors and stators will have less leakage than a properly designed helically-grooved seal.

ORIGINAL PAGE IS
OF POOR QUALITY

Housing (μm) Roughness	Rotor (μm) Roughness	$C_L \times 10^3$
.81*	.66*	6.75
	1.1*	6.86
	---	6.66
	15.9	4.83
	16.5	5.36
9.53	.66*	4.67
	15.9	3.58
	16.5	3.86
10.9	.66*	4.94
	15.9	3.82
	16.5	4.13
	12.2	4.00

Table 3. Leakage coefficients for plain seals with various measured surface roughness values on the rotor and stator. Almost circumferentially-grooved patterns are used for intentional surface roughness.

*Nominally smooth rotor or housing.

ORIGINAL PAGE IS
OF POOR QUALITY

HELICALLY-GROOVED SEAL HOUSING 4 ROTOR 8
C(AVG) = .581 mm C(RIDGE) = .560 mm
GROOVE DEPTH = .406 mm HELIX ANGLE = 20. DEG.

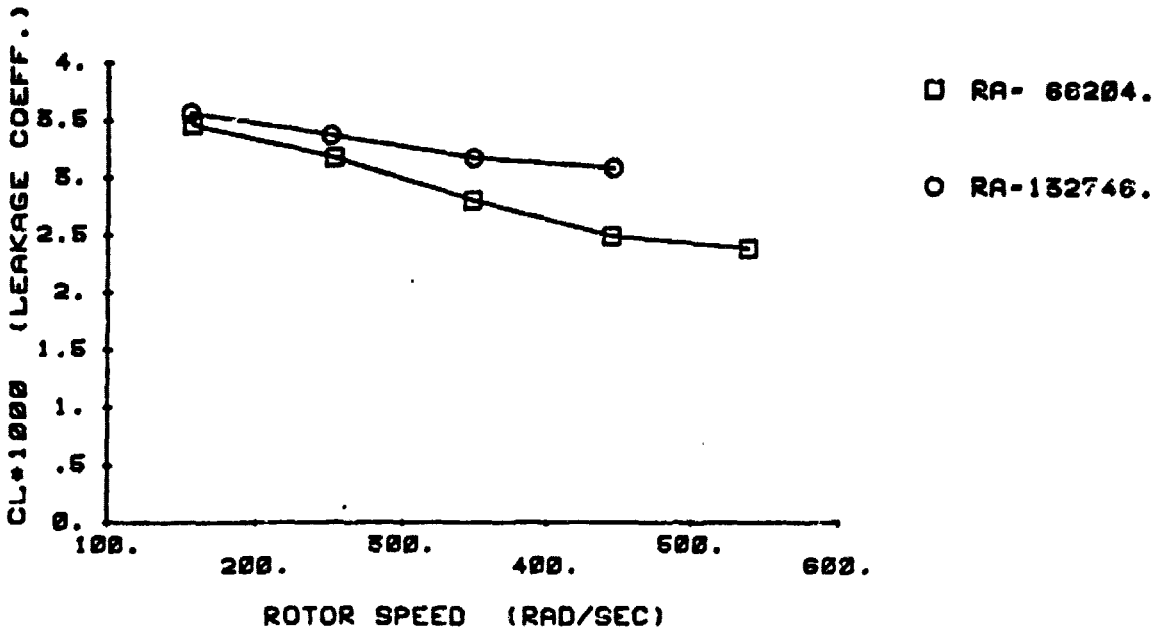

HELICALLY-GROOVED SEAL HOUSING 4 ROTOR 8
C(AVG) = .8 mm C(RIDGE) = .521 mm
GROOVE DEPTH = .584 mm HELIX ANGLE = 20. DEG.

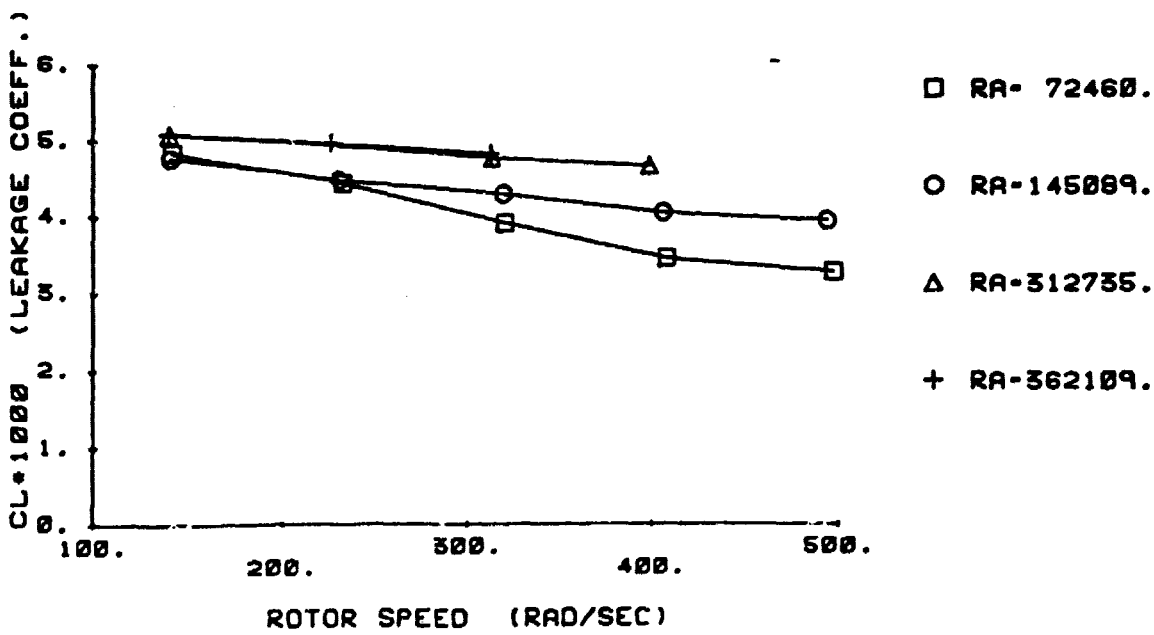

31. Leakage coefficients for seals 1 and 2 of rotor 8.

ORIGINAL PAGE IS
OF POOR QUALITY

HELICALLY-GROOVED SEAL HOUSING 4 ROTOR 11
C(AVG) = .924 mm C(RIDGE) = .560 mm
GROOVE DEPTH = 1.160 mm HELIX ANGLE = 20. DEG.

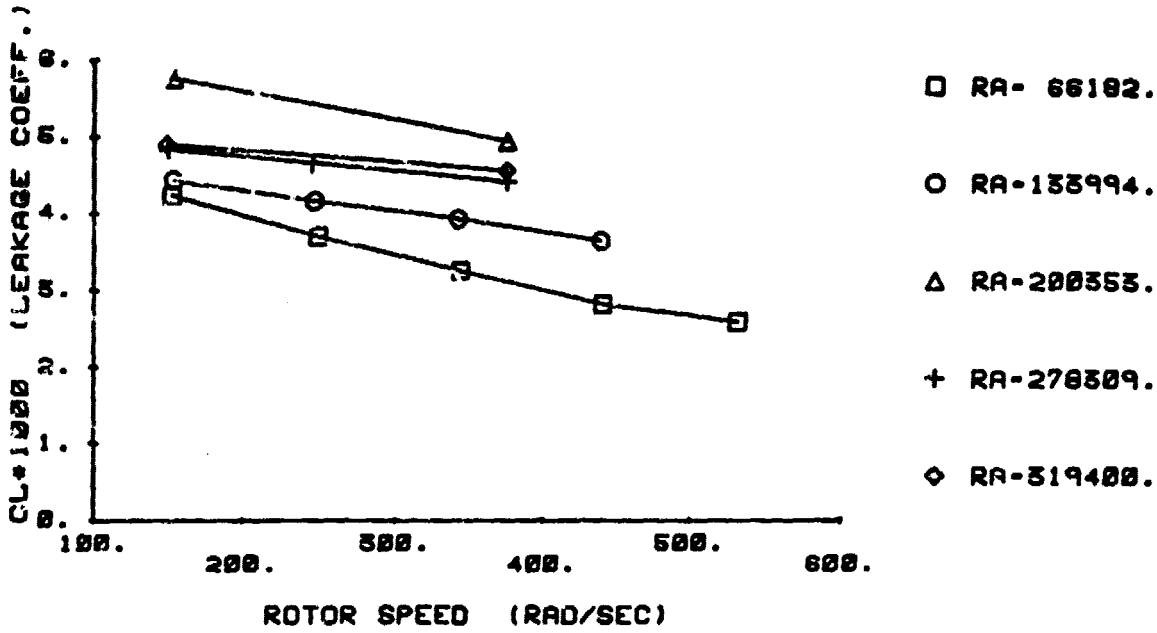

HELICALLY-GROOVED SEAL HOUSING 4 ROTOR 11
C(AVG) = 1.01 mm C(RIDGE) = .521 mm
GROOVE DEPTH = 1.016 mm HELIX ANGLE = 20. DEG.

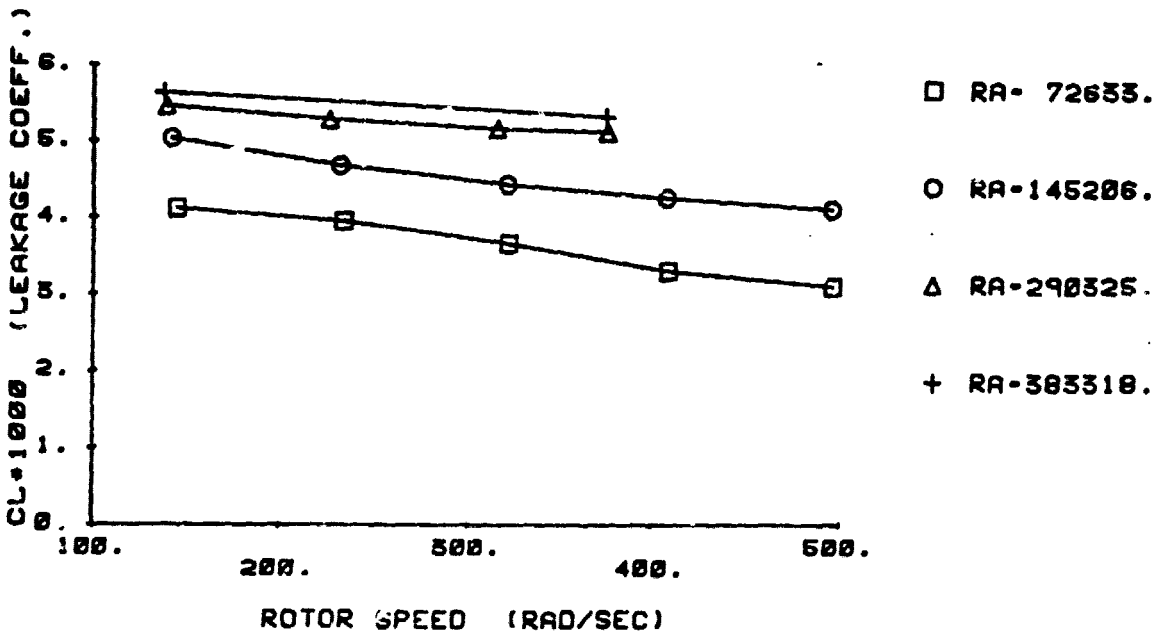

32. Leakage coefficients for seals 1 and 2 of rotor 11.

ORIGINAL PAGE IS
OF POOR QUALITY

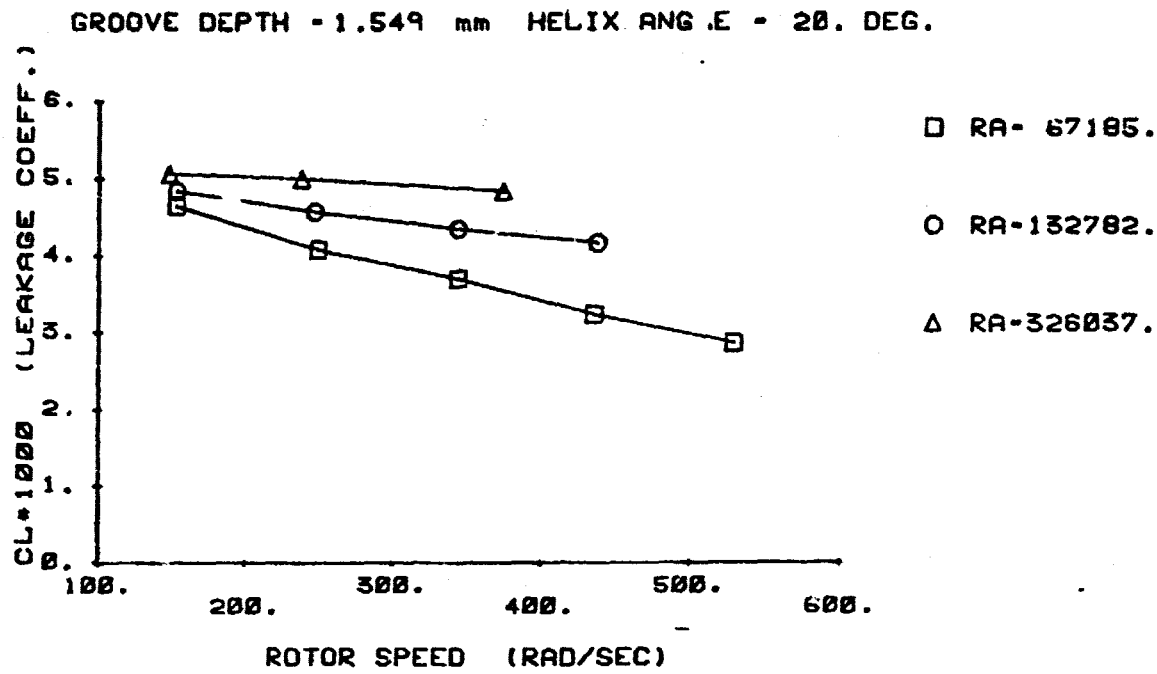

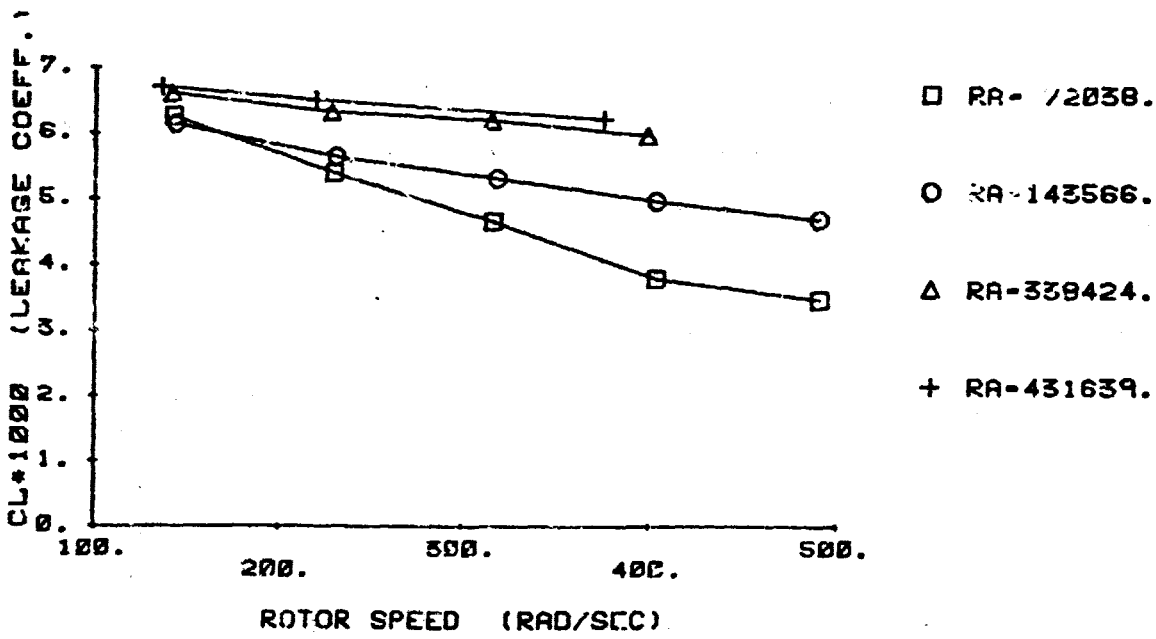

33. Leakage coefficients for seals 1 and 2 of rotor 14.

ORIGINAL PAGE IS
OF POOR QUALITY

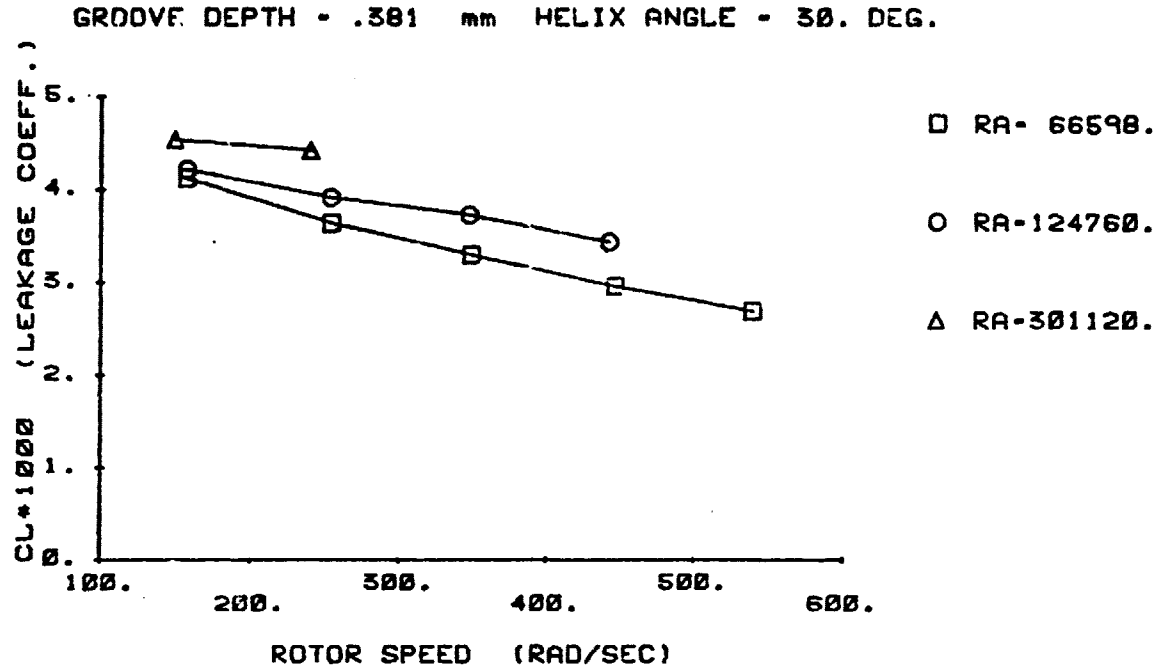

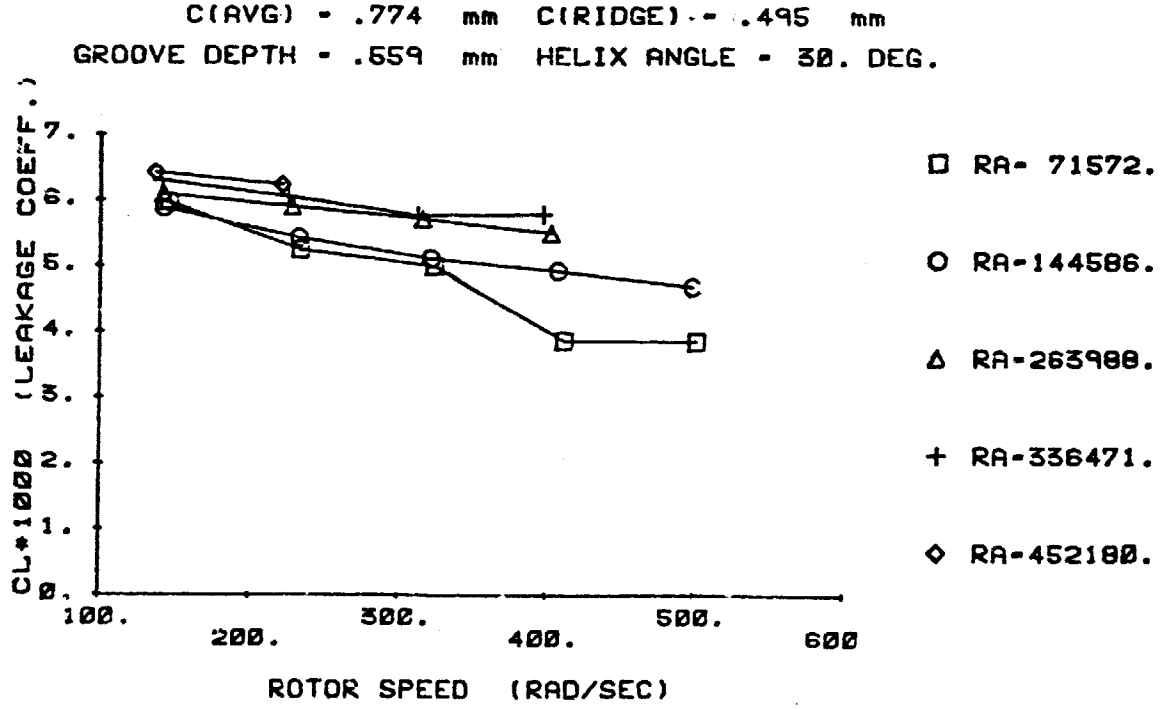

34. Leakage coefficients for seals 1 and 2 of rotor 9

ORIGINAL PAGE IS
OF POOR QUALITY

HELICALLY-GROOVED SEAL HOUSING 4 ROTOR 12
C(AVG) = .96 mm C(RIDGE) = .381 mm
GROOVE DEPTH = 1.168 mm HELIX ANGLE = 30. DEG.

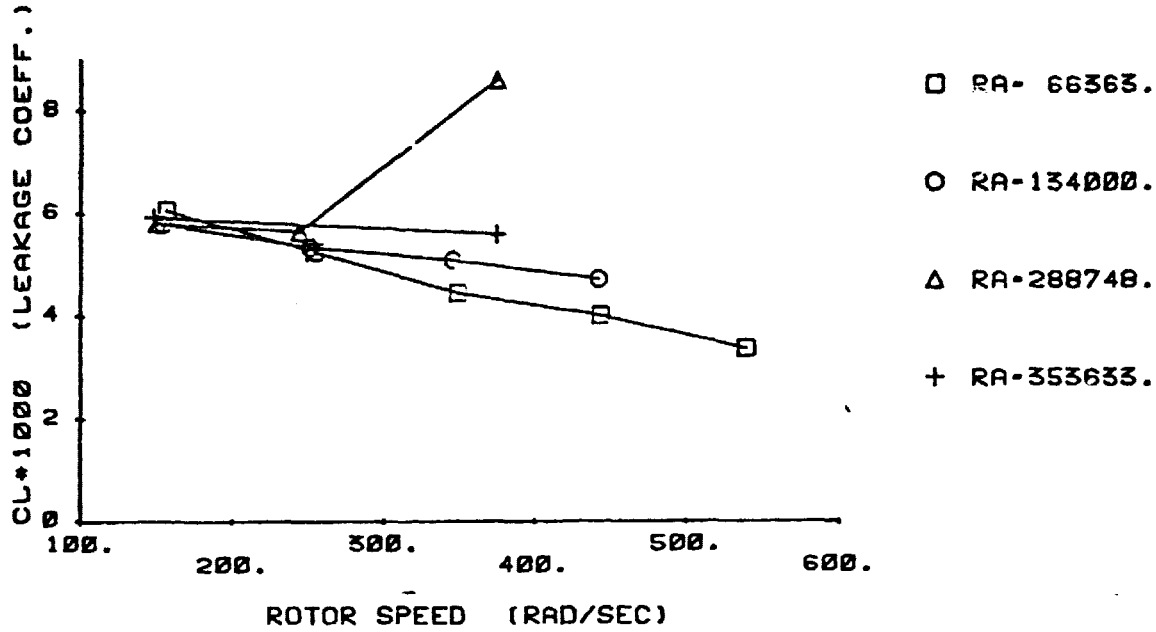

HELICALLY-GROOVED SEAL HOUSING 4 ROTOR 12
C(AVG) = 1. mm C(RIDGE) = .495 mm
GROOVE DEPTH = 1.016 mm HELIX ANGLE = 30. DEG.

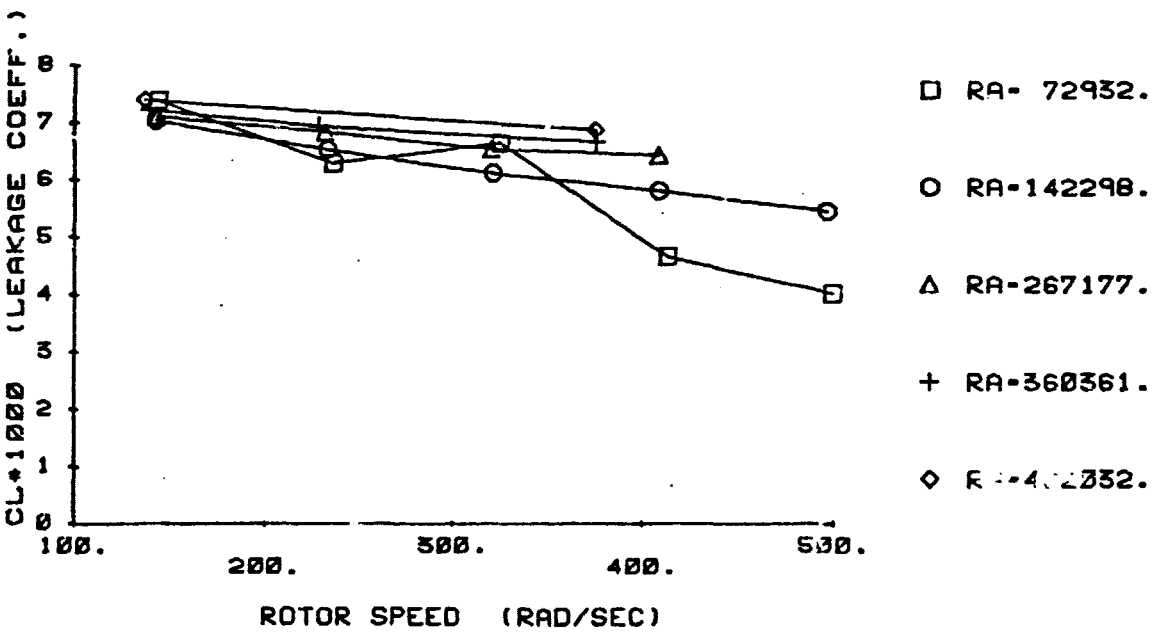

35. Leakage coefficients for seals 1 and 2 of rotor 12.

ORIGINAL PAGE IS
OF POOR QUALITY

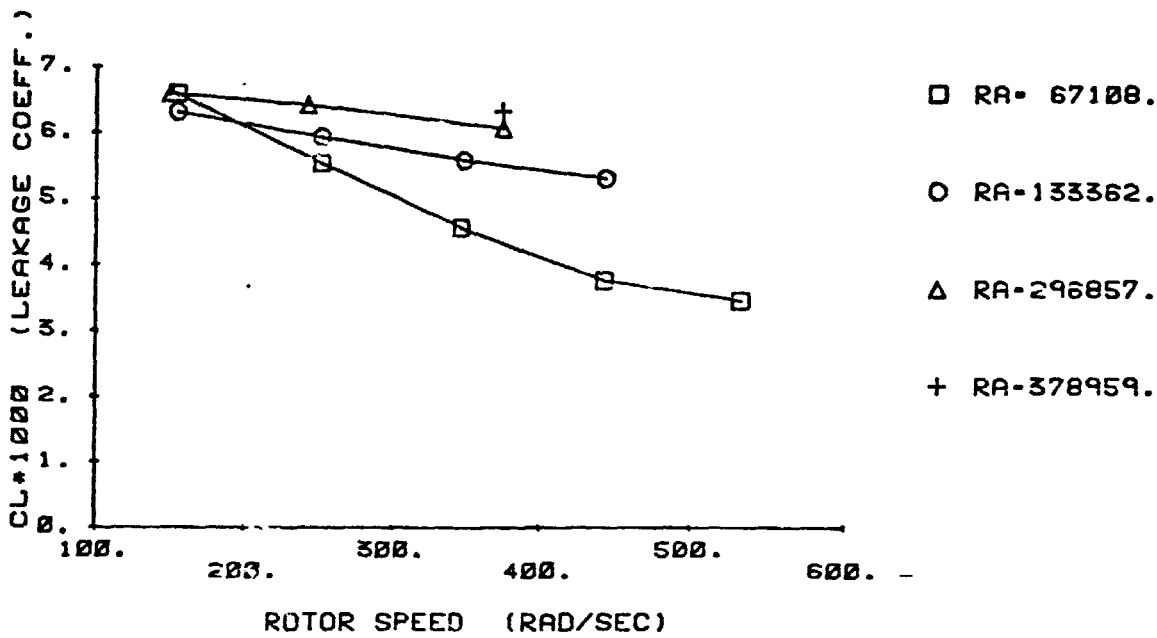

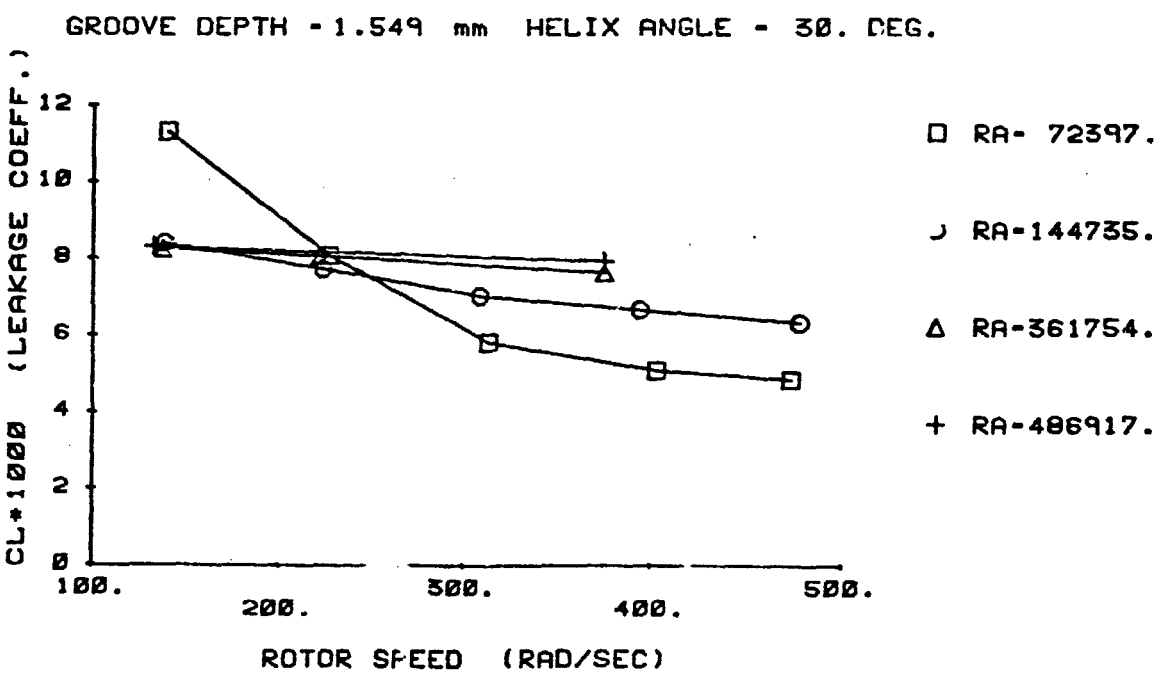

36. Leakage coefficients for seals 1 and 2 of rotor 15.

ORIGINAL PAGE IS
OF POOR QUALITY

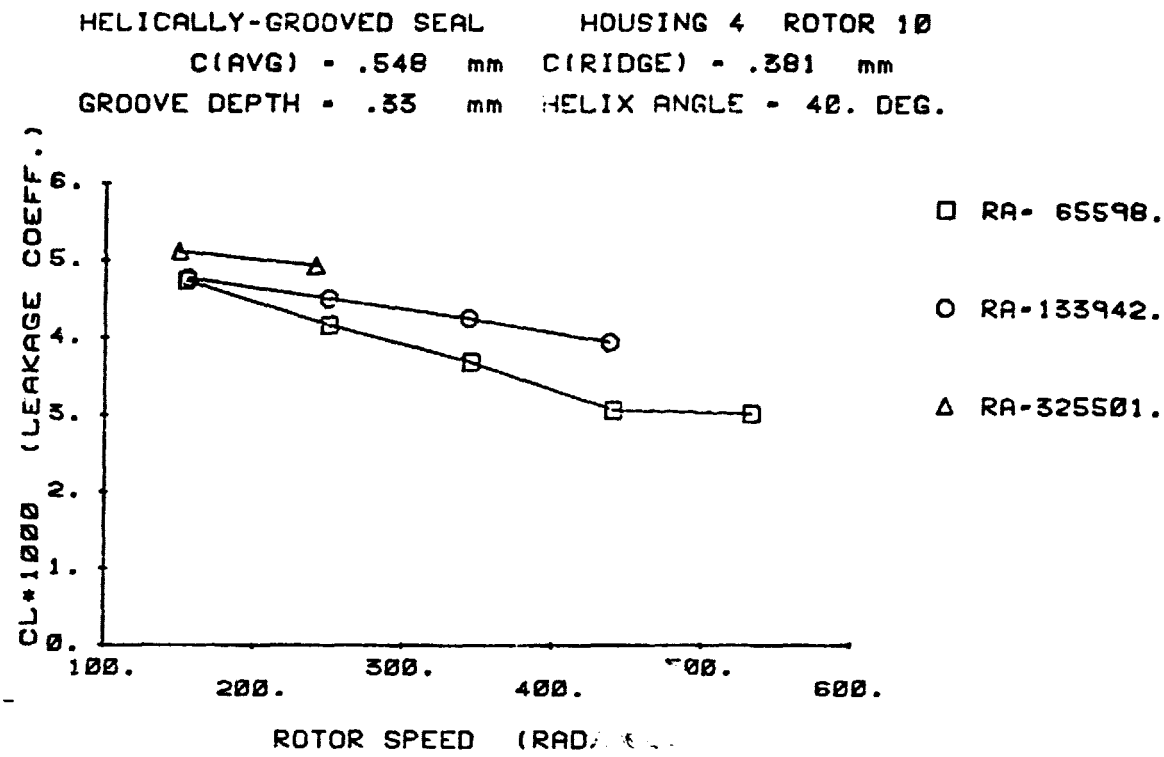

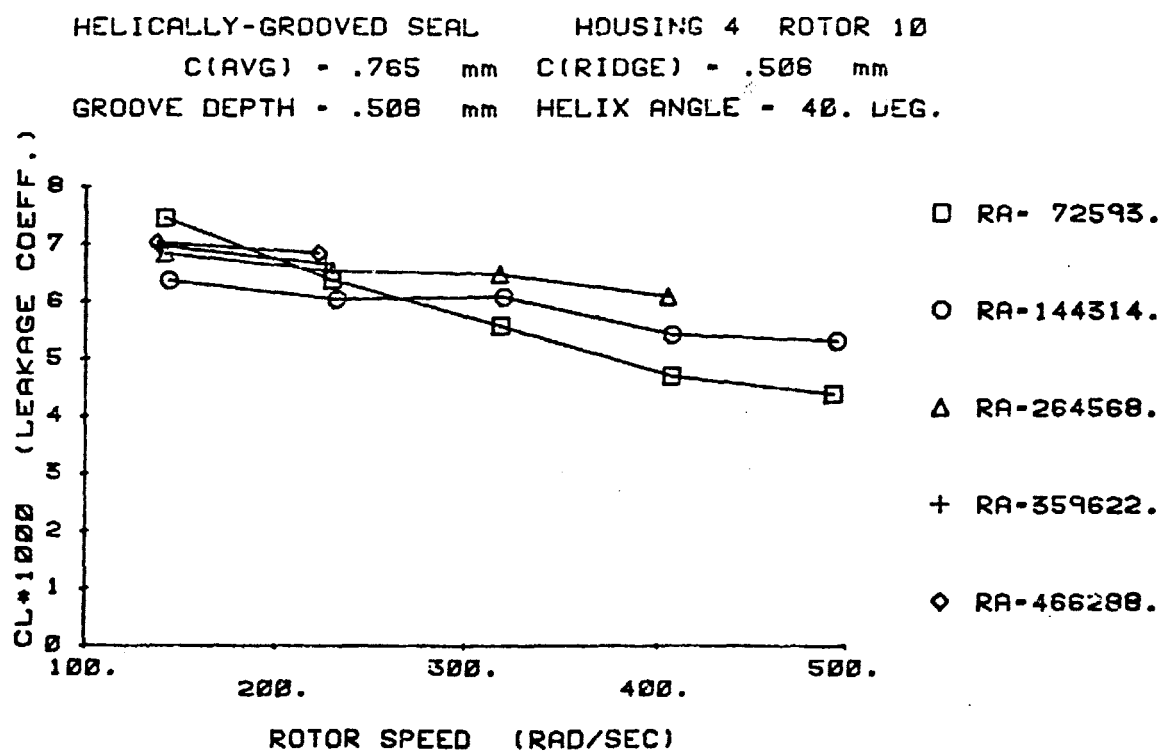

37. Leakage coefficients for seals 1 and 2 of rotor 10.

ORIGINAL PAGE IS
OF POOR QUALITY

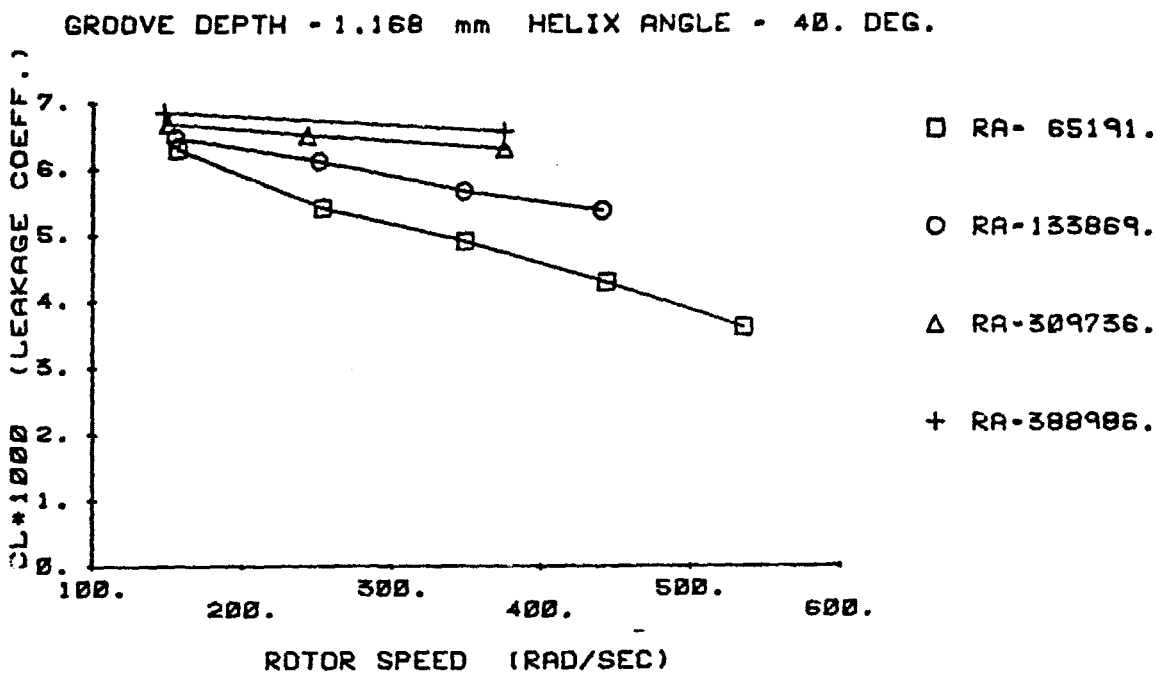

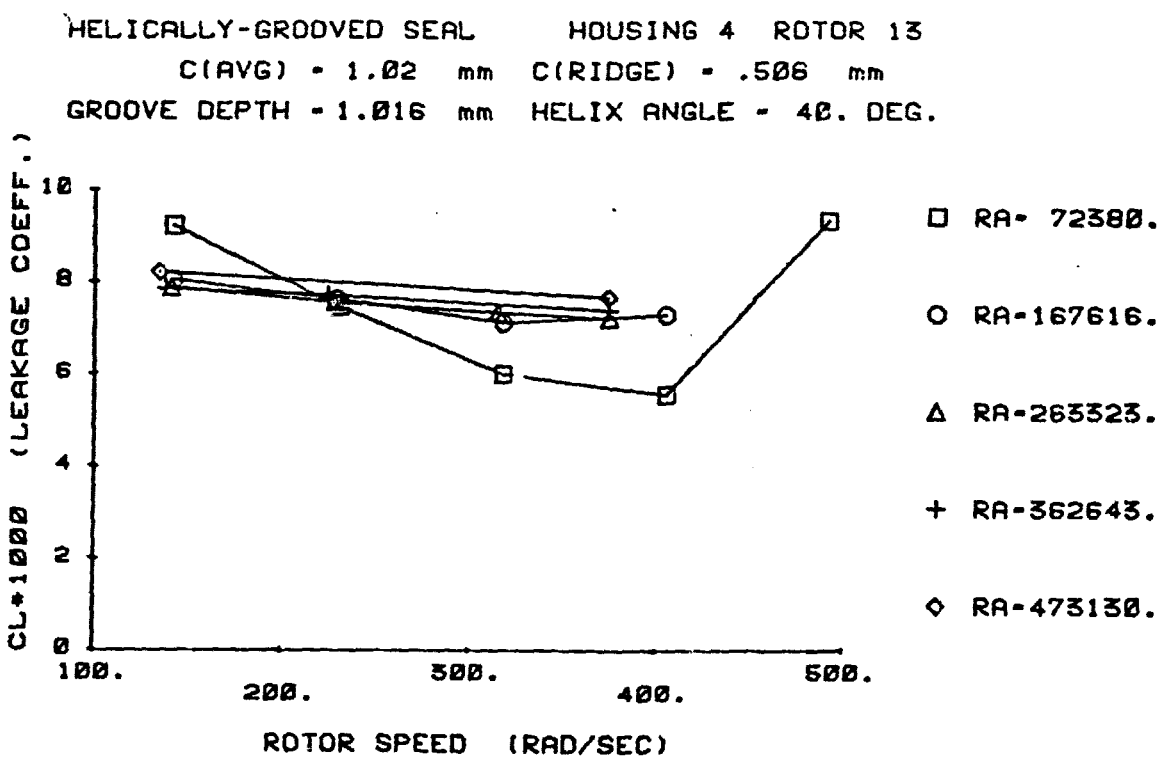

38. Leakage coefficients for seals 1 and 2 of rotor 13.

ORIGINAL PAGE IS
OF POOR QUALITY

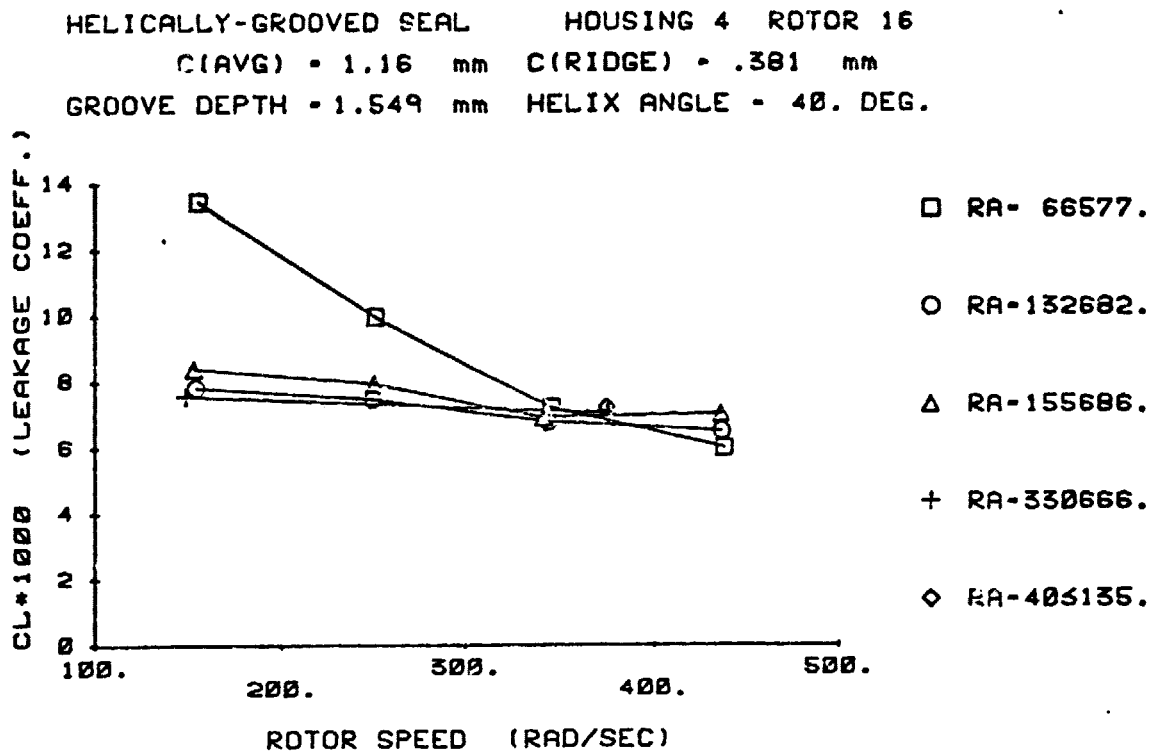

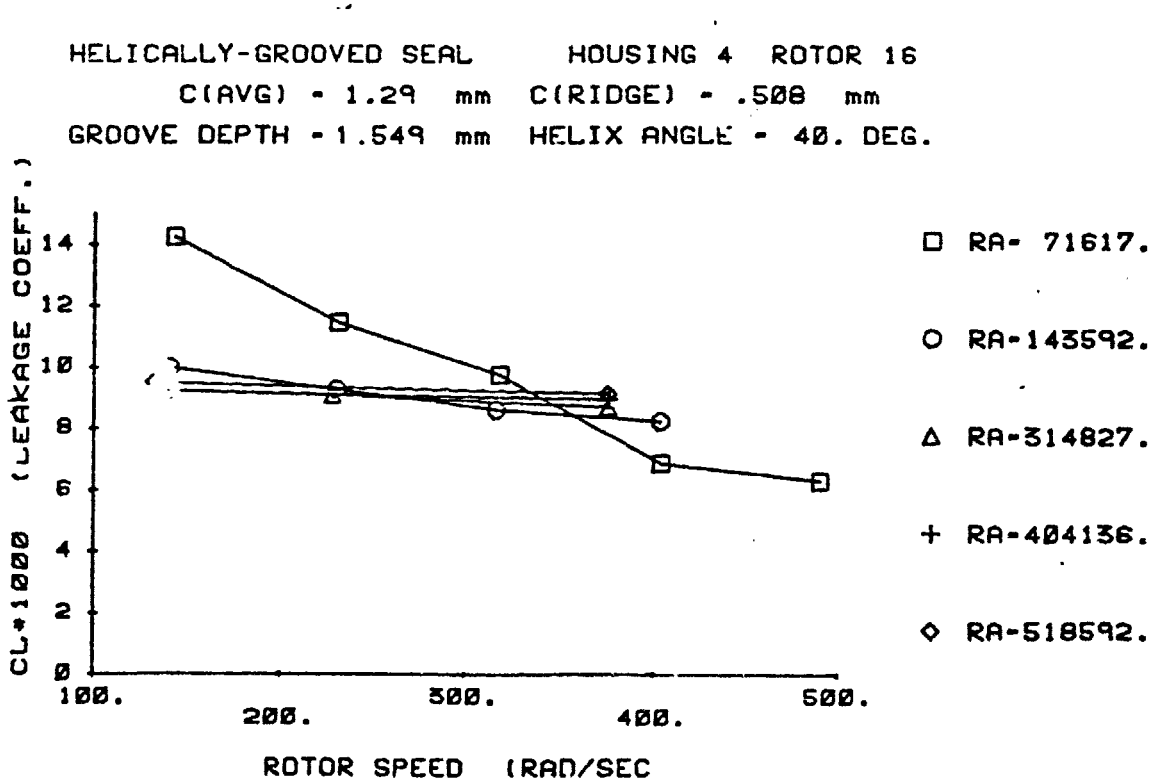

39. Leakage coefficients for seals 1 and 2 of rotor 16.

ORIGINAL PAGE IS
OF POOR QUALITY

Power Consumption

Test experience with the helically-grooved rotors clearly demonstrates that they require more power than the plain annular seals which have been tested previously. A direct measurement of the power consumption of smooth and helically grooved seals would obviously be very helpful; however, the present apparatus does not permit measurement of the resistance torque. Amperage consumption at the drive motor is the only direct measurement of power consumption which is possible in the present test apparatus.

Amperage measurement (or torque measurement) at the drive motor measures the total resistance load of the apparatus including the significant drag due to the hollow roller bearings and the mechanical seals. Our circumstances only allow a comparison of amperage measurements between rotors mounting helically-grooved seals and rotors mounting more conventional annular seals. Given that our helically-grooved seals have diameters of 11.1 cm (4.37 in) verus the 10.2 cm (4 in) diameters of seals in plain seals which have been tested, some additional normalization is required to make this comparison more meaningful.

The theoretical power consumption of a plain seal with the fluid prerotated to an inlet tangential velocity of $\frac{R\omega}{2}$ is

$$P\omega r = \lambda \pi R^3 L \rho V \omega^2 / 2$$

Hence, for the present purposes, the values plotted are AMP/R^3. Representative helically-grooved seal results are presented in figures 40 through 42. Figure 43 provides comparable results for a recently-tested configuration consisting of a smooth rotor with one smooth stator and one roughened stator. A review of these figures supports the following conclusions:

(a) Power consumption increases with groove depth

(b) At high flowrates, the power consumption of the minimum-leakage hellically grooved rotor (rotor 18) is approximately twice the corresponding power consumption of the rotor with smooth seals.

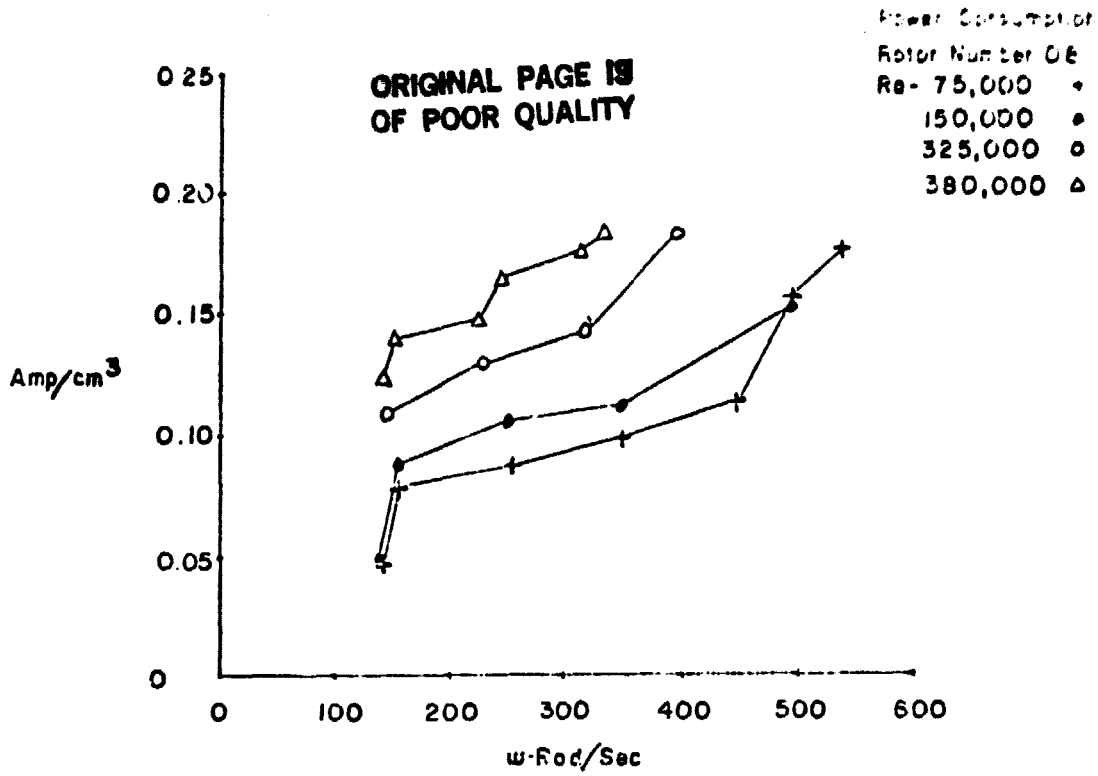

Figure 40. $P\omega r/I^3$ (Normalized amperage consumption) for rotor 8.

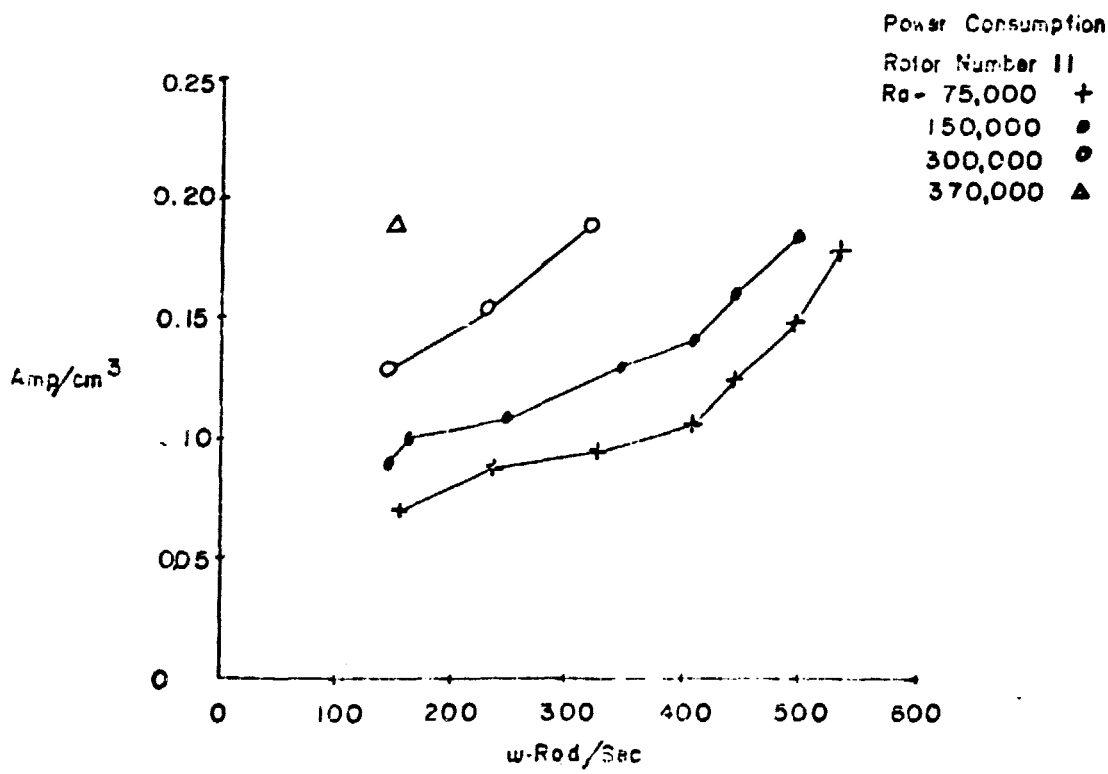

Figure 41. $P\omega r/I^3$ (Normalized amperage consumption) for rotor 11.

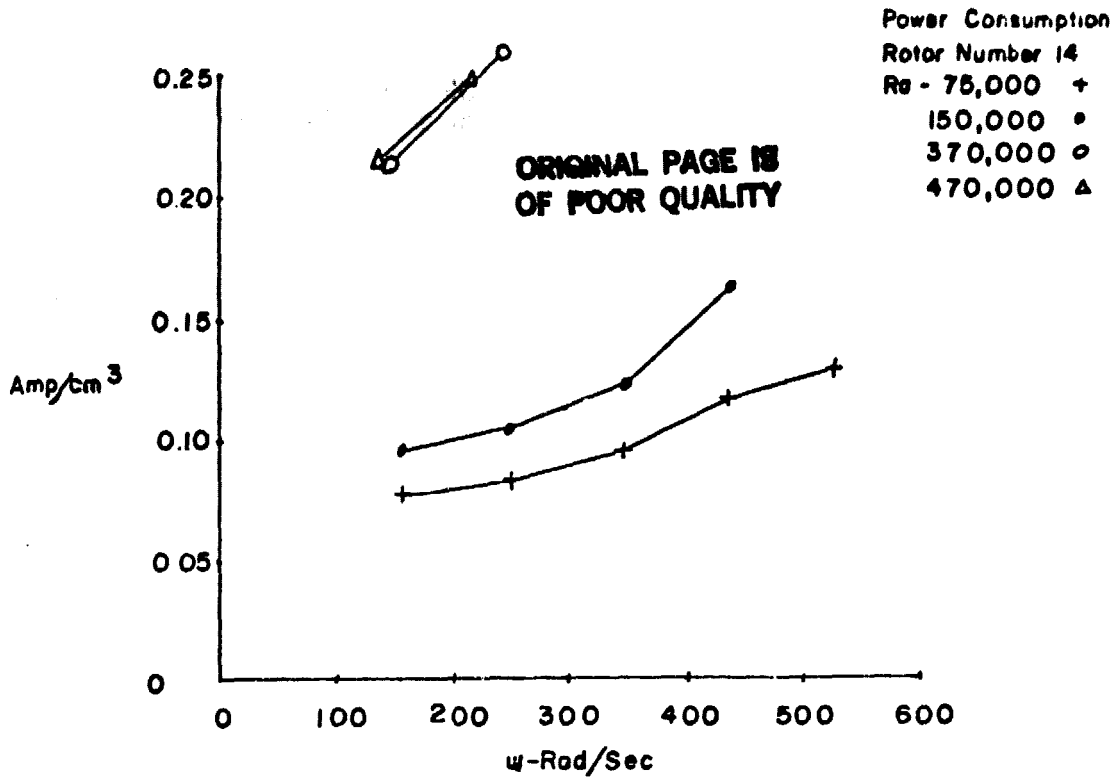

Figure 42. $P\omega r/I^3$ (Normalized amperage consumption) for rotor 14.

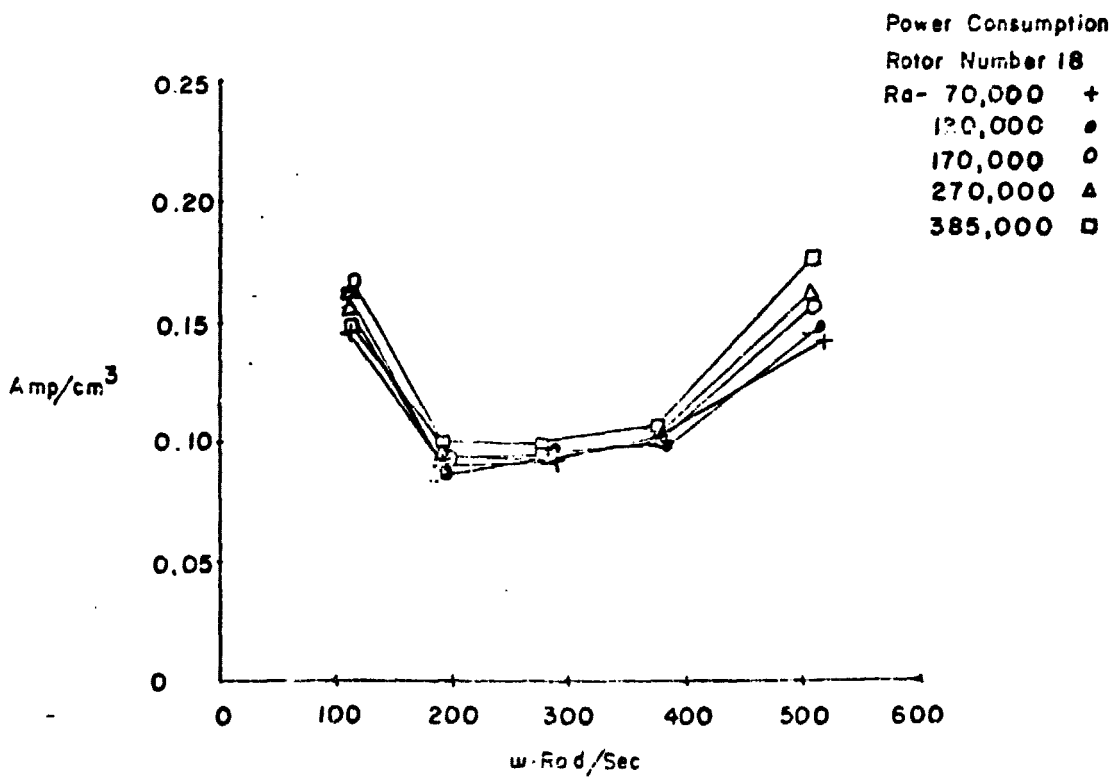

Figure 43. $P\omega r/I^3$ (Normalized amperage consumption) for a smooth rotor.

CONCLUSIONS

The following conclusions are supported by the test results:

(a) Leakage of helically-grooved seals decreases with running speed.

(b) Leakage reduction due to increasing running speed is greater at lower values of R_a.

(c) An asymptote for leakage reduction is indicated with increasing running speed.

(d) Leakage is reduced by reducing the ridge (minimum) and average clearances.

(e) Leakage increases with increasing pitch angles.

(f) Leakage increases with increasing groove depth.

In comparison to more conventional seal designs, the following conclusions are supported:

(a) Plain seals with smooth rotors and stators will leak more than a helically-grooved seal.

(b) Plain seals with either a smooth rotor and a rough stator or a rough rotor and smooth stator will have comparable leakage rates to a properly-designed helically-grooved seal.

(c) Plain seals with a rough rotor and a rough stator will leak less than a properly-designed helically-grooved seal.

(d) A properly-designed helically-grooved seal will consume at least twice as much power as a conventional annular seal.

REFERENCES

1. J. Bootsma, "Liquid-Lubricated Spiral-Groove Bearings," Ph.D. Thesis, Technological University Delft, 19 November 1975, also Philips Research Laboratories Report No. 7, 1975.

2. C. Y. Chow and J. H. Vohr, "Helical-Grooved Journal Bearing Operated in Turbulent Regime, "ASME Trans. J. of Lubrication Technology, Vol. 92, 1970, pp. 346-358.

3. W. L. Bowen, and R. Bhateje, "The Hollow Roller Bearing," ASME Paper No. 79-Lub-15, ASME/ASLE Lubrication Conference, Dayton, Ohio, 16-18 October 1979.

4. Anon., T-1301, Thermodynamic Properties, Dupont Fire Extinguisher Properties E. I. Dupont DeMemour & Co., Wilmington, Delaware, 1966.

5. H. Stephen and K. Lucas, Viscosity of Dense Fluids, p. 59, Plenum Press, New York-London.

6. Dara W. Childs, "SSME HPFTP Interstage Seals: Analysis and Experiments for Leakage and Reaction-Force Coefficients," Progress Report, NAS8-33716, 15 February 1983.